



**Idaho
National
Engineering
Laboratory**

INEL-96/0223

July 1996

Volatilization and Redox Testing in a DC Arc Melter: FY-93 and FY-94


RECEIVED

OCT 07 1996

OSTI

**J. D. Grandy
J. W. Sears
N. R. Soelberg
G. A. Reimann
M. E. McIlwain**

MASTER

DISTRIBUTION OF THIS DOCUMENT IS UNLIMITED 

LOCKHEED MARTIN 

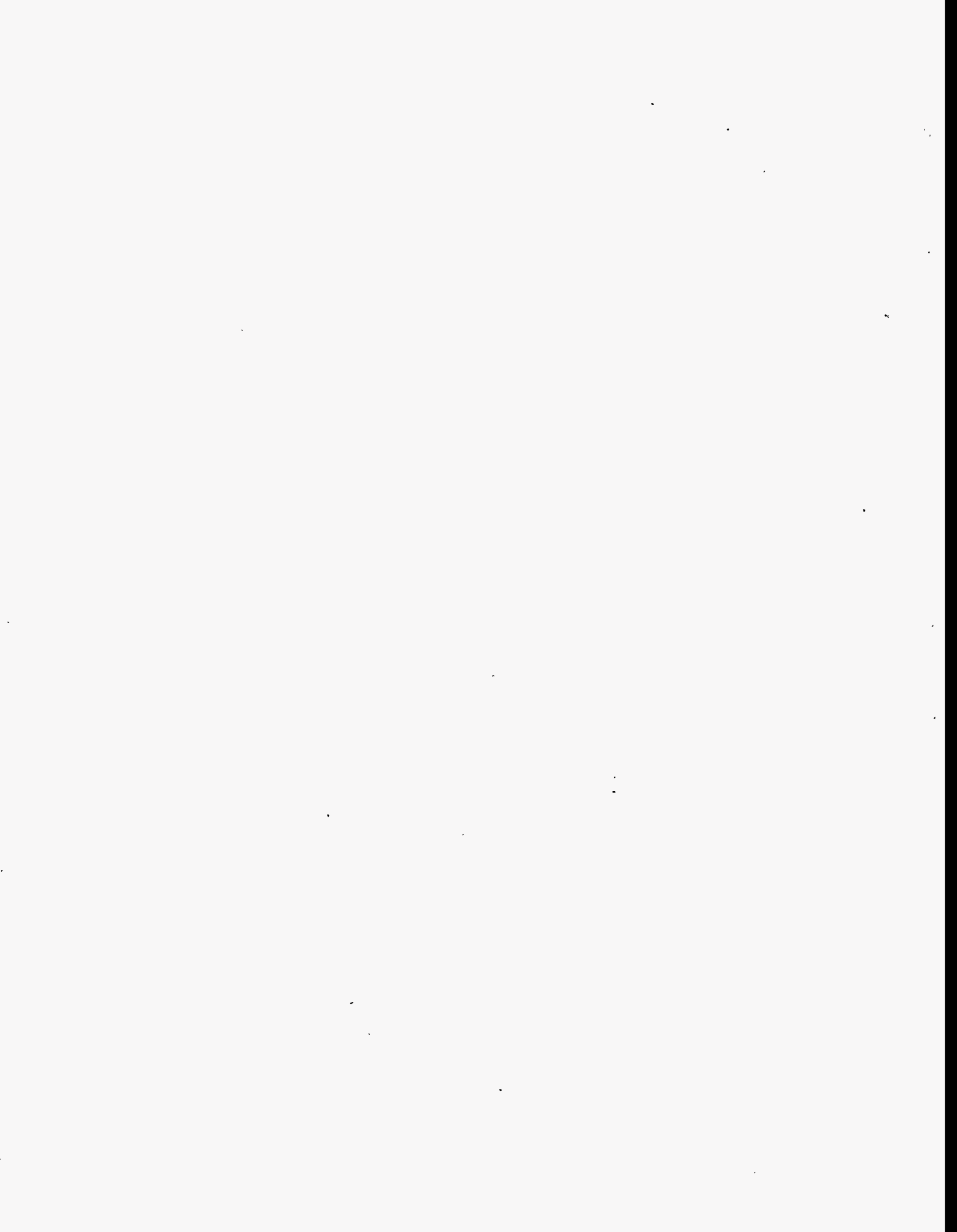
**Volatilization and Redox Testing in
a DC Arc Melter: FY-93 and FY-94**

**J. D. Grandy
J. W. Sears
N. R. Soelberg
G. A. Reimann
M. E. McIlwain**

Published July 1996

**Idaho National Engineering Laboratory
Lockheed Martin Idaho Technologies Company
Idaho Falls, ID 83415**

**Prepared for the
U.S. Department of Energy
Assistant Secretary for Environmental Management
Under DOE Idaho Operations Office
Contract DE-AC07-94ID13223**



DISCLAIMER

**Portions of this document may be illegible
in electronic image products. Images are
produced from the best available original
document.**

DISCLAIMER

This report was prepared as an account of work sponsored by an agency of the United States Government. Neither the United States Government nor any agency thereof, nor any of their employees, makes any warranty, express or implied, or assumes any legal liability or responsibility for the accuracy, completeness, or usefulness of any information, apparatus, product, or process disclosed, or represents that its use would not infringe privately owned rights. Reference herein to any specific commercial product, process, or service by trade name, trademark, manufacturer, or otherwise does not necessarily constitute or imply its endorsement, recommendation, or favoring by the United States Government or any agency thereof. The views and opinions of authors expressed herein do not necessarily state or reflect those of the United States Government or any agency thereof.

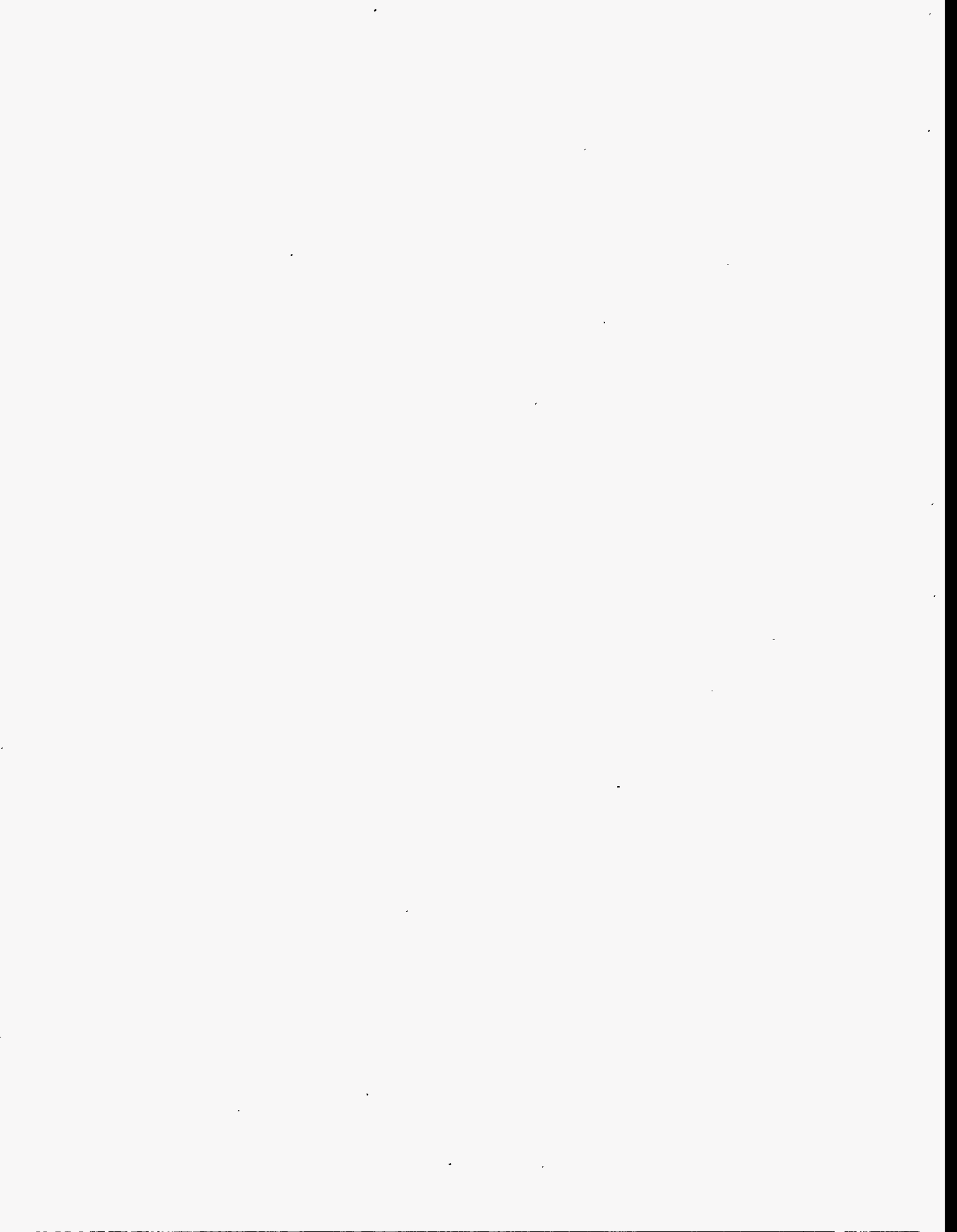
ABSTRACT

This work was a preliminary study of the effects of high-temperature arc melting on emissions of transuranic (TRU) surrogates, cesium, and high vapor pressure metals (HVPMs), both with and without a cold cap of feed materials in an iron-enriched basalt waste form with TiO_2 and ZrO_2 (IEB4). The effect of the reducing/oxidizing (redox) conditions on the retention of HVPMs and surrogate elements was also studied. Volatilization experiments were conducted in FY-93 and again in FY-94. Redox testing took place in FY-93.

Exhaust gas samples were obtained for melts ranging in temperature from 1200 to 2300°C during FY-93. The off gas samples were collected by a "Modified Method 5" system and analyzed to determine the volatilization rates of the HVPMs and surrogates. The comparison of volatilization rates between open melt vs. cold cap conditions did not reveal a definite correlation for reduced volatilization in the cold cap melts. Slag samples were also analyzed. By comparing the concentrations of HVPMs in the slags, a slight improvement in HVPM retention was seen for the cold cap melts. Except for chromium, most of the HVPMs volatilized from the melt. The surrogate elements tended to remain in the slag, but there was no definite correlation for improvement in surrogate retention in the cold cap experiments.

During the FY-93 campaign, the redox state was adjusted by adding carbon powder to produce a reducing state and by introducing air through a lance to produce an oxidizing state. Iron oxide ratios were analyzed for these samples to determine their final redox state. With the exception of chromium, the HVPMs evaporated from the melt regardless of the redox conditions. Of the surrogates, only cerium remained in the slag in significant amounts. The slags produced under oxidizing conditions formed many more crystalline phases than the glassy slags produced under reducing conditions.

Additional volatilization tests conducted in FY-94 under open melt and cold cap conditions were also used to collect mass balance data. Like the previous experiments, zinc and particularly cadmium and lead, evaporated from the melt while chromium remained. Cesium partitioned half into the slag and half into exhaust gas particulates. On average, the detailed mass balance closures for the HVPMs and surrogates were low. Mass balance closure for the HVPMs was approximately 60-70%, except for chromium which was 35%. Surrogate mass balance closures ranged from only 20-30%. This result may be the result of the surrogates partitioning to the high alumina refractory that lines the inside of the arc melter crucible.



EXECUTIVE SUMMARY

The Idaho National Engineering Laboratory (INEL) small DC arc melter was designed and constructed in FY-92. The primary purpose of this melter system was to investigate the synthesis and properties of waste forms expected to result after thermal processing of INEL radioactive mixed wastes. After an initial series of tests in FY-92, the arc melter system was greatly modified in FY-93 so that experiments using toxic heavy metals could be conducted. Several programs, including Buried Waste Integration Demonstration (BWID), Private Sector Participation Initiative (PSP), and Integrated Waste Processing Facility (IWPF) took advantage of the capabilities of the INEL small arc melter to investigate the effects of various processing conditions on the properties of thermally treated final waste forms. The arc melter was slightly modified again in FY-94 to accommodate collection of complete mass balance data. The arc melter generally operates between 10 and 40 kW with typical operating current and voltages at 110 A and 180 V, respectively. The system operates with two side-by-side carbon electrodes in a melt chamber dimensioned 14 inches high and 9 inches in diameter when lined with a cast ceramic crucible one-half inch thick. It operates in batch mode, but an auger feeder can be used to add more material once the initial batch has been melted. The water cooled crucible jacket prevents slag/metal tapping.

Experimental work to evaluate the extent of vaporization in the small arc melter was conducted over a 2-year period with simulated mixed radioactive waste and soil over a temperature range of 1300 to 1900°C. Organics and halogens were not used as part of the simulated waste streams since they were assumed to have burned off or volatilized in an incinerator prior to entering the melter. The radionuclide surrogates used in the program that were expected to mimic the chemical characteristics of transuranics (TRUs) and U compounds were Ce, Sm, Nd, Eu and Gd for the early FY-93 tests. Later in FY-93 and all of FY-94, only cerium and samarium were used as TRU surrogates. Cesium is highly volatile metal and acts as a study for the radioactive isotope Cs¹³⁷. The HVPMS used in the testing programs were Cd, Cr, Cs, Pb, and Zn. These elements cover the range of boiling points of interest and are the major toxic contaminants in the wastes that may remain in the solids after incineration. Hg is present in INEL radioactive wastes but was not used in the experiments since it was assumed that it will completely volatilize during processing and end up in the air pollution control system where it must be treated as a secondary waste stream.

FY-93 Volatilization Tests

There were three experimental campaigns conducted during FY-93 and FY-94. The first of these was the volatilization testing in FY-93 consisting of experiments that employed open melt and cold cap processing conditions. In these tests, the exhaust gases were collected while feed material containing the HVPMS and surrogates was introduced into the melt with the auger feeder. The exhaust gas particulates were collected using an "EPA modified Method 5" exhaust gas analyzer commonly used to monitor industrial stack emissions. Samples were sent to an independent laboratory for analysis. Data from the analysis were used to calculate volatilization rates in units of milligrams per hour for the elements of interest, specifically the HVPMS and radionuclide surrogates.

Examination of the data did not reveal an overwhelming correlation for reduction in volatilization in the cold cap melts vs. the open melts. This conclusion, however, may only point to the need for a thicker cold cap layer. Only in the case of chromium was there a clear indication of reduced volatilization in the cold cap experiments. Results for the other HVPMS show only a slight reduction in volatilization in most cases during cold cap conditions. The surrogates tended to remain in the slag under open melt or cold cap conditions.

Measured volatilization rates can be expected to be system dependent since the geometry, temperature profiles, exhaust gas flow rates, etc. that will affect volatilization will be unique for each melter system. Primary factors affecting volatilization are the amount and surface area of the slag, concentration of the volatile material in the slag, and slag temperature. The measured rates for the INEL small arc melter show in general the expected correlation between temperature and volatilization, i.e. higher rates for higher slag temperatures, although there are some exceptions. Lack of a strict correlation can likely be attributed to uncertainties in slag temperature and unknown HVPM and surrogate concentrations during exhaust gas sampling. In order to obtain reliable volatilization rate data for any processing system, detailed slag temperature must be taken along with slag samples to determine volatile element concentrations.

Redox Tests

A second set of tests conducted in FY-94 tested the extremes in reducing or oxidizing conditions and their effect on melt chemistry and crystallization. Reducing conditions for two melts were achieved by using different levels of carbon blended into the melt mix. In the case of these two melts, one-half the stoichiometric amount of carbon needed to reduce iron oxides to metals was added and the second melt used twice the stoichiometric amount. Two levels of oxidation were maintained by introducing air under the surface of the melt with a water cooled air lance.

The redox state of the molten slag affects the types of minerals produced upon cooling in the glass-ceramic waste forms. The type of minerals produced determine the waste form chemical and physical durability. Since minerals have different affinity for toxic metals, cesium, and TRUs, the redox state may also affect their retention in the final waste form.

An overall generalization of the difference between slag material processed under reducing and oxidizing conditions is that the reduced melts produced mostly glassy slag while the oxidized melts developed substantially more crystalline structure even though the cooling rates were very similar. Redox conditions had little influence on the disposition of the HVPMS. With the exception of chromium, the HVPMS evaporated from the melt in both reducing and oxidizing environments. Chromium showed a strong tendency to form crystals in conjunction with iron, although the crystalline structures formed in reducing conditions tended to be much smaller and finer. Surrogates did not tend to collect preferentially in the crystalline phases as was hoped. This may be due primarily to relatively fast slag cooling rates once the melter is turned off. Of the surrogates, only cerium demonstrated an ability to remain in the slag in significant amounts retaining about half of the original amount in the simulated waste mix. The cerium was found in the glassy phases of the slag. In general, the rest of the surrogates were not found in the slag although there were exceptions. For instance, cesium showed modest retention under oxidizing conditions but was completely volatilized in the reducing environment.

FY-94 Volatilization Tests

Volatilization testing was continued in FY-94, again under open melt and cold cap conditions. In these experiments the arc melter exhaust system was modified to streamline the

task of obtaining a global mass balance. Masses of the slag (including metal, if any), particulates in the melter chamber, and particulate in the exhaust system were collected and measured. In order to do elemental masses balances, the slag and particulates were analyzed using energy dispersive x-ray spectroscopy and x-ray fluorescence spectroscopy. Additionally, they were also analyzed using inductively coupled plasma-atomic emission absorption spectroscopy. All of these analytical methods produced similar results.

A general mass balance comparing the amount of starting material with the amount of material after processing revealed an average mass loss of 10.7 wt%. This is a typical amount expected to be lost from carbonated and hydrated compounds in the starting material, which will be released as carbon dioxide and water vapor during processing. A more complete mass balance would include measurement of the exhaust gas flow rate and input air flow rate rather than assuming the deficit mass was part of the off-gas. While measurement and analysis of exhaust gas flows are necessary to obtain a complete mass balance, in practical terms, it is somewhat complex and expensive. Also, since conservation of total mass must hold, measurements of only solid masses may be considered adequate for the scope and requirements of this project.

The elemental mass balance for the HVPs revealed that the majority zinc, cadmium and lead ended up in particulates in the melt chamber and exhaust system while chromium tended to remain in the slag. The elemental mass balances in general did not account for the metal amounts originally introduced, particularly for chromium having a mass balance closure of just 35%. Mass balances for the other toxic metals on average were 80% for lead, 73% for zinc and 67% for cadmium. Cesium tended to partition half into the slag and half into the off-gas particulates. The mass balance closure for cesium was just 60%. The partitioning behavior of the surrogate elements, cerium and samarium, is uncertain due to the very poor mass balance results which range from 20-30%. These elements are expected to remain in the slag and indeed while the relative mass amounts found in the slag are much higher (about 10 times) than for the off-gas particulates, the poor mass balance closure leaves open the question about the ultimate fate of the surrogate elements.

A reason for the poor mass balances may be the result of two factors. First, the mass of the slag is substantially larger than that of the particulates. Therefore, a small discrepancy in the measured concentrations of HVPs and surrogates could cause large discrepancies in the overall mass balance for an element. Second, the widely varying mass closure results suggest the possibility of elemental partitioning to different parts of the slag. Although this

possibility was taken into account by taking samples from the top and bottom parts of the melt, elements may have been concentrated in regions of the slag that were not sampled. Based on these possibilities, more samples should be analyzed to determine average concentrations of an element in the slag. Another possibility is that the surrogates, in particular, may have partitioned into the high alumina refractory liner that contains the slag inside the water cooled crucible of the arc melter.

Conclusions and Recommendations

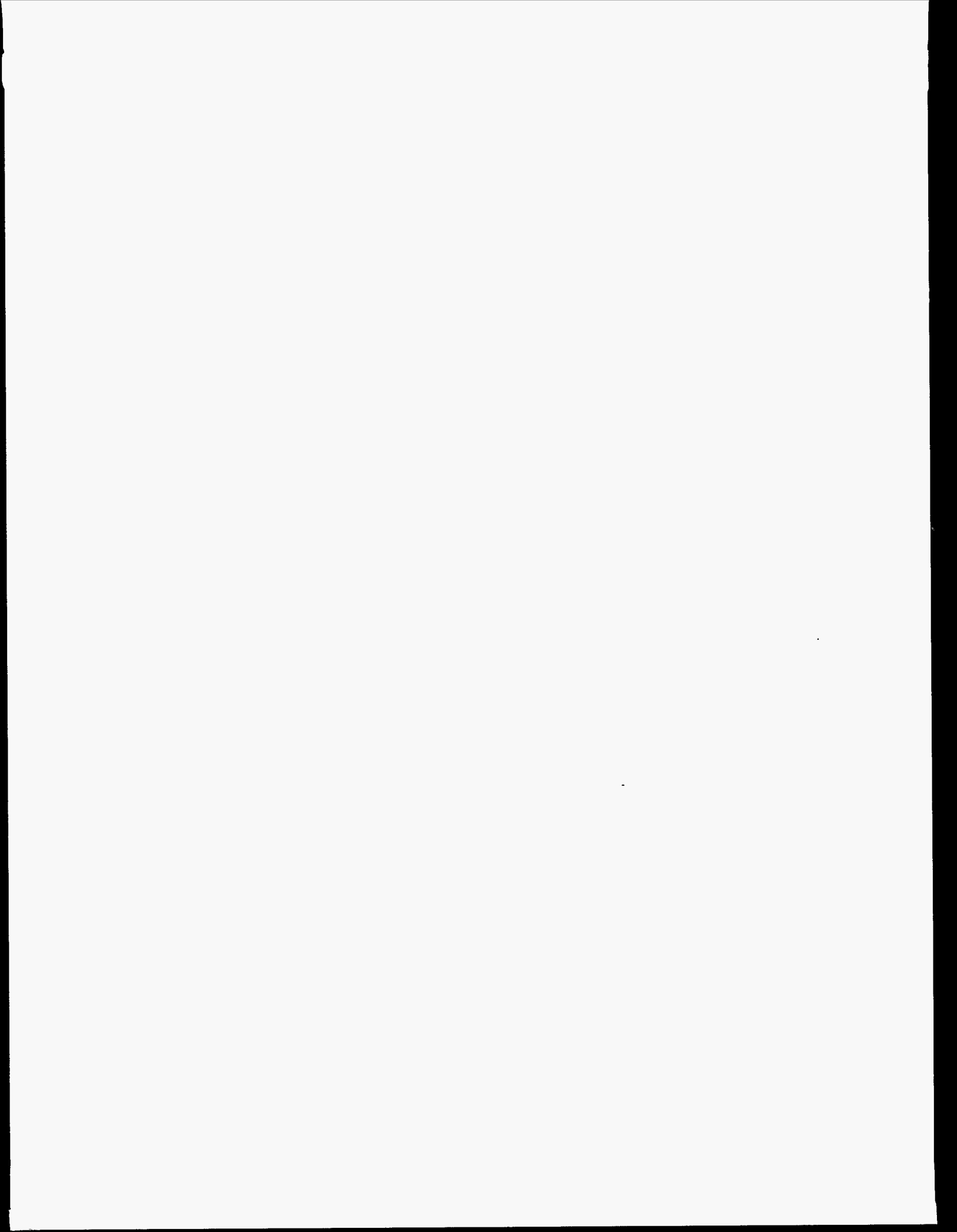
The volatilization experiments conducted in FY-93 and FY-94 provided valuable information on partitioning of toxic heavy metals and radionuclides via surrogate elements in a high-temperature arc melter processing system. During the course of the experiments many improvements to the data gathering and analysis procedures were made, and areas where further improvements could be made were identified. As a minimum, data collection must include measurement of solid mass amounts distributed during processing and elemental analysis of specific areas where solids have accumulated within the processing system. Exhaust gas mass amounts and elemental analysis can be done if budget constraints allow and if the scope of a project requires it. This may be dictated for preproduction systems where EPA and other environmental regulations will necessitate exhaust gas measurements to ensure compliance of that system and future production systems. Off-gas mass measurements will allow total mass balance measurements to be made but are not necessary to determine solid mass partitioning within the melter and air pollution control systems.

Measurement of volatilization rates for any specific processing system requires good temperature and volatile element concentration measurements of the slag. Although individual processing systems will affect volatilization due to geometry, surface area of the melt, energy input mechanism, etc., slag temperature and volatile element concentration are the primary factors affecting volatilization. Future testing must include radioactive bench-scale testing where these considerations are taken into account. Also, modeling of the partitioning mechanisms within specific processing systems may prove to be an important aspect in gaining knowledge for control of volatilization during radioactive waste processing.

Overall results of these experiments show that provisions must be made for the air pollution control system of any high-temperature radioactive processing system containing toxic metals to deal with them since the majority of these metals volatilized. Approximately half or more of any cadmium, zinc, lead, and cesium will be volatilized or entrained and end up in the exhaust treatment system. In addition, some of the radionuclide elements (based on results from the surrogate elements) will also end up in the off-gas system. Particulates containing these elements must either be rerouted back to the melter or treated as a separate secondary waste stream.

ACKNOWLEDGMENTS

This work was supported through several related projects within the Environmental Management Branch at the INEL and the Office of Waste Technology Development, Environmental Management Technology Evaluation Project (EMTEP). The assistance of O. Wiersholm (IWTP), A. L. Ayers, Jr., and L. G. Gale (IWPF) in monitoring and assisting in the implementation of the project is appreciated. The guidance of G. L. Anderson, Advanced Mixed Waste Treatment Project (AMWTP), Private Sector Participation Initiative (PSPI), in coordinating this activity with other concurrent projects is also appreciated. Technical consultation, construction, and operational support by B. C. Benefield, R. J. Bitsoi, A. D. Donaldson, J. M. Hillary, D. Duford, A. L. Jones, J. E. Lee, B. K. Marshall, J. G. Rodriguez, J. Devoran, R. Thompson, A. D. Watkins, J. D. Choules, and G. C. Wilson is greatly appreciated. Assistance in the preparation of the manuscript by T. K. Pettingill, T. A. Ward and M. M. Siefken is also appreciated.



CONTENTS

ABSTRACT	iii
EXECUTIVE SUMMARY	v
ACKNOWLEDGMENTS	xi
ACRONYMS	xxi
1. INTRODUCTION	1-1
1.1 Objective	1-1
1.2 Overview	1-1
2. BACKGROUND	2-1
3. ARC MELTER DESCRIPTION AND HISTORY	3-1
3.1 Original Arc Melter	3-1
3.2 FY-93 Arc Melter Modifications	3-1
3.3 FY-94 Arc Melter Modifications	3-5
4. ARC MELTER OPERATIONS	4-1
4.1 Introduction	4-1
4.2 Operating the Arc Melter	4-1
4.3 Energy Balance	4-1
4.4 Electrode Erosion	4-5
4.5 Temperature Monitoring	4-9
5. VOLATILIZATION AND REDOX TESTING OVERVIEW	5-1
5.1 Introduction	5-1
5.2 HVPM Tests (FY-93)	5-1
5.3 Cold Cap Tests (FY-93)	5-3
5.4 Redox Tests (FY-93)	5-4
5.5 Volatilization Tests (FY-94)	5-4

6. HVPM RETENTION AND EXHAUST GAS ANALYSIS (FY-93)	6-1
6.1 Introduction	6-1
6.2 Data Collection	6-1
6.2.1 Slag Sampling	6-1
6.2.2 Exhaust Gas Sampling	6-4
6.3 XRD Analysis of Exhaust Particulate	6-9
6.4 HVPM Tests: Analysis and Results	6-9
6.4.1 Slag Composition Evaluation	6-9
6.4.2 Slag Characterization	6-12
6.5 Cold Cap Tests: Analysis and Results	6-19
6.5.1 Slag Characterization	6-19
6.6 Exhaust Particulate Composition	6-24
6.7 Volatilization Rates	6-26
7. REDOX MEASUREMENTS (FY-93)	7-1
7.1 Introduction	7-1
7.2 Experimental Conditions	7-2
7.3 Analytical Results	7-5
7.3.1 Fe ⁺² /Fe ⁺³ Ratios	7-5
7.3.2 SEM/EDXS Analysis of Slag	7-7
7.4 Discussion	7-21
8. VOLATILIZATION TESTS (FY-94)	8-1
8.1 Introduction	8-1
8.2 Experimental Conditions	8-1
8.3 Data Collection	8-4
8.4 General Mass Balance	8-5
8.5 Off-Gas Particulate Analysis	8-8
8.5.1 EDXS and XRF Analysis of Exhaust Filter Particulate	8-8
8.5.2 ICP Analysis of Exhaust Filter Particulate	8-9
8.5.3 EDX and XRF Analysis of Melter Chamber Particulate	8-10
8.5.4 ICP Analysis of Melter Chamber Particulate	8-12
8.6 Slag Composition Analysis	8-12
8.6.1 EDXS and XRF Slag Analysis	8-13
8.6.2 ICP and FLAA Slag Analysis	8-26
8.7 Detailed Mass Balance for HVPMs and Surrogates	8-27

8.7.1 Detailed Mass Balances for HVPMS	8-27
8.7.2 Detailed Mass Balances for Radionuclide Surrogates.	8-30
8.8 Discussion	8-36
9. CONCLUSIONS AND RECOMMENDATIONS	9-1
9.1 Arc Melter System and Operations	9-1
9.2 Effects of Redox Conditions	9-3
9.3 Volatilization in a DC Arc Melter	9-4
9.4 Conclusions	9-6
10. REFERENCES	10-1
APPENDIX A - LDRD FY-94 Annual Report	A-1
APPENDIX B - Melter Off-Gas Sampling Procedures	B-1
APPENDIX C - Composition and Normalization Calculation Worksheets	C-1
APPENDIX D - Volatilization Rate Calculations	D-1
APPENDIX E - EDXS and XRF Data	E-1
APPENDIX F - ICP and FLAA Data	F-1

FIGURES

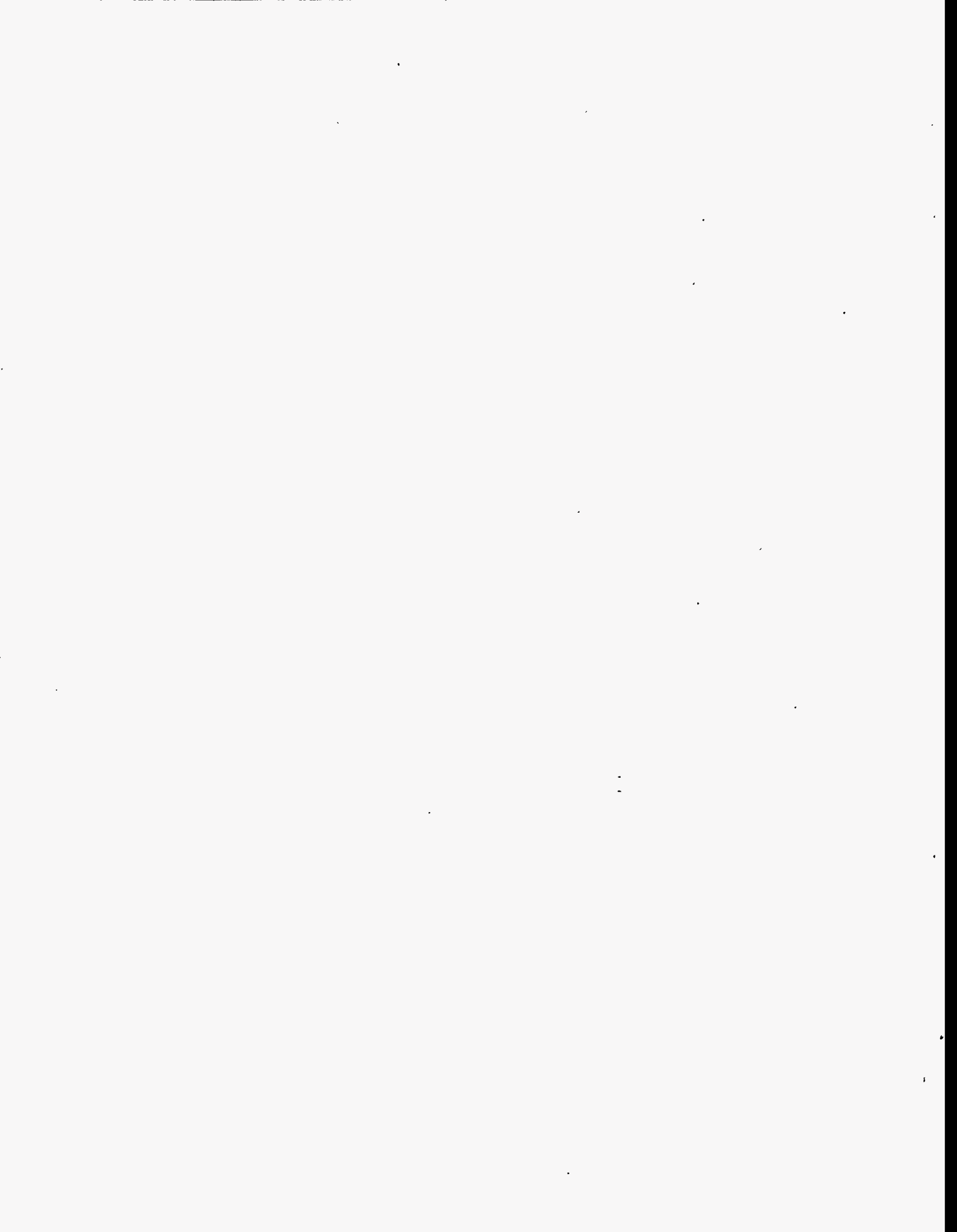
3.1	Photograph of the modified bench-scale arc melter in FY-93	3-3
3.2	Schematic of the modified bench-scale arc melter	3-4
3.3	Photograph of the arc melter system as configured for FY-94 tests	3-6
3.4	Photograph of the off-gas system used during the FY-94 tests	3-7
3.5	Schematic of the off-gas system utilized during the FY-94 tests	3-8
3.6	Micarta seal and rod-wiper assembly for the electrodes used during FY-94	3-10
3.7	Schematic of the modified electrode drive mechanism	3-11
3.8	Schematic of the arc melter crucible assembly	3-12
3.9	Schematic of the pin-hole camera assembly	3-13
4.1	Energy input data for the HVPM run ARM090894 with a cold cap.	4-3
4.2	Energy balance data for the HVPM run ARM090894 with a cold cap	4-3
4.3	Energy input data for the HVPM run ARM092094 without a cold cap	4-4
4.4	Energy balance data for the HVPM run ARM020894 without a cold cap	4-4
4.5	Anode and cathode carbon loss rates in grams per amp-hour	4-8
4.6a	Used carbon electrodes coated with ZYP silicon carbide	4-10
4.6b	Used carbon electrodes coated with plasma-sprayed silicon	4-10
4.7a	Carbon feed tube extender with SiC coating	4-11
4.7b	Carbon feed tube extender with no coating	4-11
4.8	Schematic of a water cooled TC probe	4-12
4.9	Temperature response of the slag and power input vs. time	4-14
6.1	Sketch of the slag sampling system used during the FY-93 HVPM studies	6-3
6.2	Schematic of exhaust gas sampling train	6-5
6.3	Open melt vs. cold cap cesium volatilization rates	6-30
6.4	Open melt vs. cold cap cadmium volatilization rates	6-30
6.5	Open melt vs. cold cap cerium volatilization rates	6-31
6.6	Open melt vs. cold cap samarium volatilization rates	6-31
7.1	Schematic of the air/oxygen lance	7-3
7.2	SEM micrographs for the slightly reduced slag	7-8
7.3	SEM micrographs for the highly reduced slags	7-10
7.4	SEM micrographs for the slightly oxidized slags	7-14
7.5	SEM micrographs for the highly oxidized slags	7-18

8.1 XRF and EDXS chemistry results from slag material - ARM082394	8-15
8.2 XRF and EDXS chemistry results from slag material - ARM082694	8-17
8.3 XRF and EDXS chemistry results from slag material - ARM090694	8-19
8.4 XRF and EDX chemistry results from slag material - ARM090894	8-21
8.5 EDXS chemistry results from slag material - ARM092094	8-23
8.6 EDXS chemistry results from slag material - ARM092294	8-25
8.7 Calculated composition of the starting IEB4/A-40 waste-soil mixture	8-29

TABLES

2.1	Weight percent compositions of the IEB series waste forms	2-2
4.1	Operating conditions and electrode erosion data for the FY-93 experiments	4-6
4.2	Operating conditions and electrode erosion data for the FY-94 experiments	4-7
5.1	Melting and boiling points of HVPMs and surrogates plus oxides	5-2
5.2	HVPM analyses for FY-93 HVPM and cold cap experiments	5-3
6.1	FY-93 HVPM and cold cap test series	6-2
6.2	Metals sample information for the FY-93 HVPM and cold cap test series	6-7
6.3	Metals sample conditions for FY-93 HVPM and cold cap test series	6-8
6.4	Chemical compositions for 1 kilogram of IEB4 mixes	6-10
6.5	Chemical composition of the FY-93 HVPM experiments	6-11
6.6	HVPM02 slag materials characterization	6-14
6.7	HVPM03 Slag Materials Characterization	6-15
6.8	HVPM05 slag materials characterization	6-16
6.9	HVPM06-01 Slag Materials Characterization	6-17
6.10	HVPM06-02 Slag Materials Characterization	6-18
6.11	Cold-cap CC01 slag materials characterization	6-20
6.12	Cold-cap CC02 slag materials characterization	6-21
6.13	Cold-cap CC03 slag materials characterization	6-22
6.14	Cold-cap CC05 slag materials characterization	6-23
6.15	FY-93 HVPM experiments - particulate elemental analysis.	6-25
6.16	FY-93 cold cap experiments - particulate elemental analysis	6-25
6.17	Volatilization rates for the HVPMs in open melt conditions	6-28
6.18	Volatilization rates for the surrogates in open melt conditions	6-28
6.19	Volatilization rates for the HVPM's under cold cap conditions	6-29
6.20	Volatilization rates for the surrogates under cold cap conditions	6-29
7.1	Summary of FY-93 redox tests	7-2
7.2	Redox results over a range of reducing and oxidizing conditions	7-7
7.3	EDXS analysis of designated spots in the slightly reduced slag (RED01)	7-10
7.4	EDXS analysis of designated spots in the highly reduced slag (RED02)	7-13
7.5	EDXS analysis of designated spots for the slightly oxidized slag (OX02)	7-18
7.6	EDXS analysis of designated spots in the highly oxidized slag (OX03)	7-21
7.7	EDX general area scan analysis for the redox tests	7-23
8.1	General parameters and feeding information for the FY-94 HVPM runs	8-2

8.2	Data and operating conditions for the FY-94 experiments	8-3
8.3a	Mass balance information for the FY-94 HVPM experiments	8-6
8.3b	Mass balance information for the FY-94 HVPM experiments	8-7
8.4	EDXS and XRF analysis - Average concentrations for HVPMs and surrogates in exhaust filter particulate	8-9
8.5	ICP analysis - Average concentrations for HVPMs and surrogates in exhaust filter particulate	8-10
8.6	EDX and XRF melter chamber condensate/particulate analysis	8-11
8.7	ICP analysis - Average concentrations for HVPMs and surrogates for particulate collected from the melter chamber	8-12
8.8	EDX and XRF analysis of ARM082394 slag	8-14
8.9	EDX and XRF analysis of ARM-082694 slag	8-16
8.10	EDX and XRF analysis of ARM-090694 slag	8-18
8.11	EDX and XRF analysis of ARM-090894 slag	8-20
8.12	EDX analysis of ARM-092094 slag	8-22
8.13	EDX Analysis of ARM-092294 Slag	8-24
8.14	ICP analysis - Average concentrations for HVPMs and surrogates in the slag ..	8-26
8.15	IEB4/A-40, HVPMs, and surrogates composition for the FY-94 tests	8-28
8.16	Mass balance information for solid materials in the arc melter system	8-30
8.17a	HVPM mass balance using EDXS and XRF spectroscopic analysis	8-31
8.17b	HVPM mass balance using EDXS and XRF spectroscopic analysis	8-32
8.18a	HVPM mass balance using ICP spectroscopic analysis.	8-33
8.18b	HVPM mass balance using ICP spectroscopic analysis.	8-34
8.19	Surrogate mass balance for ARM082394.	8-35



ACRONYMS

AES	atomic emission spectroscopy
ASG	aluminosilicate glass
BN	boron nitride
BWID	Buried Waste Integration Demonstration
DC	direct current
DOE	Department of Energy
EDXS	energy dispersive X-ray spectroscopy
EPA	Environmental Protection Agency
FLAA	flame atomic absorption (spectroscopy)
FWF	final waste form
HEPA	high efficiency particulate air (filter)
HVPM	high vapor pressure metal
ICP	inductively coupled plasma
IEB	iron-enriched basalt
IEB4	iron-enriched basalt with ZrO ₂ and TiO ₂ additions
INEL	Idaho National Engineering Laboratory
IRC	INEL Research Center
MFP	mixed fission product
PSPI	Private Sector Participation Initiative
RFP	Rocky Flats Plant
RTD	resistance temperature device
RWMC	Radioactive Waste Management Complex
SDA	Subsurface Disposal Area
SEM	scanning electron microscopy
slpm	standard liters per minute
TC	thermocouple
TCLP	toxicity characteristic leach procedure
TRU	transuranic
TSA	Transuranic Storage Area
WSL	Waste Stream Limits
XRD	X-ray diffraction
XRF	X-ray fluorescence

1. INTRODUCTION

The purpose of these experiments was to study the dissolution, retention, volatilization, and trapping of transuranic radionuclide elements (TRUs), mixed fission and activation products, and high vapor pressure metals (HVPMs) during processing in a high temperature arc furnace. In all cases, surrogate elements (lanthanides) were used in place of radioactive ones. The experiments were conducted utilizing a small DC arc melter developed at the Idaho National Engineering Laboratory (INEL) Research Center (IRC). The small arc melter was originally developed in 1992 and has been used previously for waste form studies of iron enriched basalt (IEB) and IEB with zirconium and titanium additions (IEB4). Section 3 contains a description of the small arc melter and its operational capabilities are discussed in Chapter 4. The remainder of the document describes each testing program and then discusses results and findings.

In any high temperature melter system, the exhaust gases will contain particulate that must be processed by the air pollution control system (APCS) or rerouted back to the melter. In general, this material or "carryover" can arise from two sources, either from small particles of the waste material that become entrained in the flow or from material that is vaporized from the melt and that subsequently condenses into particulates which are carried away in the off-gas stream. Once carryover has been collected, it is intimately mixed, and it is difficult to differentiate which part was entrained and which part was volatilized from the melt. Elements or compounds with very low boiling points, can be expected to contribute heavily to carryover in the exhaust gas stream. This behavior can be verified if high concentrations of these materials end up in the carryover mass. This turns out to be true, particularly in the case of the HVPM's. Therefore, while most of the data and discussions in this report refer to volatilized material, it is recognized that some portion of the material collected for analysis was due to entrainment.

1.1 Objective

The overall objective of the testing efforts described in this report is to discover the conditions under which HVPMs will volatilize from the melt and to determine methods to trap and dispose of these elements. These tests indicated the extent of dissolution and maximum retention of these elements in the slag. Along with the major objective, valuable experience in operating an arc melter was gained. Improvements to the arc melter system were made regarding electrode erosion, refractory performance, slag temperature monitoring, and process control. Vaporization of some of the HVPMs is unavoidable but it may be minimized through the use of proper engineering and operational controls. Vaporization of TRUs and mixed fission products (MFPs), on the other hand, could cause excessive

contamination in the off-gas components and possibly lead to criticality or unacceptable exposure limits. It is preferred that TRUs and MFPs remain in the melt and go into the primary final waste form.

1.2 Overview

The experiments consisted of melting simulated waste materials mixed with typical INEL soil obtained from the Radioactive Waste Management Complex (RWMC). Both solid and gaseous products were collected and analyzed to determine the partitioning behavior of each of the elements of interest. Test variables were molten slag temperature, open melt vs. cold cap, the method for feeding material into the melter, and oxidizing vs. reducing conditions in the melter. Melter operations that control these variables were material feed rate, material composition, power input, arc length, refractory insulation, and insertion of air into the melt. Results identify the extent of volatilization of HVPM under these controlled conditions. Specific results from these experiments are intended to help in determining optimum parameters for subsequent processing, maximum retention of radionuclides, and minimum vaporization of HVPM elements.

2. BACKGROUND

The RWMC contains over 50,000 metric tons of low-level and TRU-contaminated wastes in addition to contaminated soil in the Subsurface Disposal Area (SDA) and the Transuranic Storage Area. The RWMC radioactive wastes also contain a variety of toxic materials and HVPs requiring them to be designated as "mixed wastes." Treatment of these wastes for disposal is expected to be necessary in to meet Environmental Protection Agency (EPA) land disposal restrictions and Department of Energy (DOE) disposal requirements.

A high-temperature thermal treatment process (involving arc or plasma torch melters) for dealing with the INEL mixed wastes has been evolving from preliminary buried waste system design studies^{1,2} and stored waste system design studies.³ This approach for treating TRU contaminated waste results in an IEB final waste form. Previous research performed with IEB has shown that this waste form is long lived.^{4,5,6} Present waste form research at the INEL is focused on the improvements attainable with zirconium and titanium additives.^{7,8} These studies have shown that titanium and zirconium may increase the longevity of the waste form by producing a durable ceramic phase (Zirconolite) within a glass matrix. The TRU elements form a solid solution in the crystalline phase that is locked into the glass matrix structure.^{9,10,11}

Surrogate waste mixtures were used for the tests. The surrogate mixtures were prepared to simulate mixed wastes stored at the INEL RWMC. This simulation was consistent with a proposed treatment system in which the mixed wastes would be incinerated. Following incineration, the ash would be melted in an arc melter and then cooled to produce a solid monolith waste form.

The "average" TRU-contaminated waste stream at the RWMC, after oxidization and removal of organics, is designated A-0. If 40 wt% soil has been added to this waste, it is designated A-40. The compositions of A-0 (100 wt% waste) and A-100 (100 wt% soil) are shown in Table 2.1.⁴ Calculated compositions for A-40 and A-80 are also included since they were the main waste form types used during the studies. The resulting slag waste form for A-40 is a basalt-like composition with increased iron, hence called iron-enriched basalt or IEB. The addition of oxides of elements Zr and Ti from Group IV of the Periodic Table produces additional minerals in IEB. These Ti/Zr minerals have an affinity for actinide elements. IEB modified in this manner is called IEB4.¹² The amount of Zr and Ti oxides used in the experiments was generally 10 wt% TiO₂ and 5 wt% ZrO₂, although this occasionally varied. Designations, such as IEB/A-40, IEB4/A-40, etc., are used to identify waste form compositions. Obviously, a composition such as IEB/A-100 (soil) is not really iron-enriched (see Table 2.1), but these designations will still be used as a matter of convenience.

Table 2.1 Weight percent compositions of the IEB series waste forms.

	SiO ₂	Al ₂ O ₃	FeO-Fe ₂ O ₃	CaO	MgO	Na ₂ O	K ₂ O	TiO ₂
A-0	38.0	7.4	34.5	8.3	4.6	4.8	2.4	-
A-40	51.0	10.2	19.5	9.7	3.5	3.2	2.6	0.3
A-80	60.4	12.0	9.4	9.9	2.8	2.2	2.8	0.5
A-100	65.4	13.0	4.5	10.2	2.4	1.7	2.9	0.6

Oxides of metals commonly found in INEL soil, such as Si, Al, Fe, Ca, and Mg, will be dissolved in the melt and retained in oxide form. Previous studies have indicated that retention of the TRU/U surrogates Ce, Gd, Nd, and Sm is high.⁷ The influence of these reactions on the behavior of the HVPMS, such as Pb, Cd, Cr, and Zn, however, is less certain. Oxidation, dissolution, and retention of the metals in the melt are desirable. The focus of this work was to determine the extent of partitioning of the metals between the gaseous and solid products. This study collected and analyzed both solid and gaseous residues to determine the partitioning behavior of each of the above elements. This information will be correlated as a function of surrogate and HVPM waste feed content and process temperature.

3. ARC MELTER DESCRIPTION AND HISTORY

The primary justification for building the small arc melter was to investigate the synthesis and properties of IEB4 formed in an arc processing environment. Additionally, it was important to study arc heated melter characteristics and processing capabilities and to determine development requirements for a waste processing demonstration facility.

3.1 Original Arc Melter

The first generation arc melter, built and tested during in 1992, consisted of a water-cooled stainless steel crucible with dual carbon electrodes attached to water cooled holders. The arc melter operates in DC mode with two graphite electrodes maintaining an arc just above the melt. The electrode feed-throughs into the melt chamber are insulated. The crucible consisted of an outer stainless steel housing into which an inner crucible fit. A rubber o-ring sealed the crucible so cooling water could flow between the outer housing and the inner stainless steel crucible. The easily removable stainless steel insert allows fast turnover during batch operations. The entire crucible was surrounded by a large water-cooled chamber to which the electrode support and drive motors were attached. Tests were conducted to investigate various system operational parameters and capabilities. The arc melter operates in direct current mode utilizing two 60 kW DC power supplies controlled manually. The overall capacity of the melter is approximately 20 kg with a maximum power input of about 40 kW. In normal operation, the electrodes are close to the melt, with short arcs occurring between the electrodes and the melt. The operator monitors the position of the electrodes through portholes in the top of the melt chamber. The melter operates in a predominantly Joule-heating mode with current passing through the relatively high resistance melt. The arc gaps above the melt are constantly adjusted via stepper motors to maintain stable operation. A complete description of this first generation arc melter and the tests that were conducted can be found in an earlier report.¹³

3.2 FY-93 Arc Melter Modifications

The arc melter underwent substantial modifications in FY-93. The large outside chamber was discarded and replaced by a lid fitting directly on top of the water-cooled crucible creating a small melt chamber within the water-cooled crucible. This change was made primarily to ensure a tight seal in the melter and exhaust system so fumes would not escape during tests with HVPs in the melt. The lid included two sealed viewing ports plus other penetrations for thermocouples, pressure transducers, etc. A separate support stand was built to hold the electrodes, connectors, and drive motors in addition to the crucible lid. The crucible itself was supported by a hydraulic lift table which could be raised up to the crucible

lid to seal the system or lowered to provide access to the removable inner stainless steel crucible. The data logger system was retained as the primary data recording device. Information on cooling water flows and temperatures, input power, exhaust temperature, etc. were automatically transmitted from the datalogger to a personal computer and saved during arc melter operation.

Also added to enhance operability were other major system elements such as a control and monitoring console, video monitoring and recording equipment, two-color infrared pyrometer, auger feeder, gas flow control and monitor system, and baghouse filter system. Operability improvements were attained by modifying the electrode drive system to include separate stepper motor control of the anode to compensate for its higher erosion rate. A stick-mounted thermocouple that could be inserted into the slag for a temperature measurement and then withdrawn before being damaged or melted also improved the system's capability. A photograph of the system, as modified for FY-93, is presented in Figure 3.1. Additional detail about this arc melter facility can be found in previous reports.¹⁴

Specialized equipment used for specific testing series included a Method 5 exhaust gas sample train and a slag sampling system used during the volatilization studies. A water-cooled air/oxygen lance was used during the redox tests. Figure 3.2 shows a schematic of the arc melter system as configured for the FY-93 volatilization tests.

Surface temperature measurements of the melt were made using the optical pyrometer which can be seen in Figure 3.1 mounted to the right of the electrode assembly. Resistance temperature detectors (RTDs) are installed to measure heat losses to the chamber, crucible cooling water, electrodes, and off-gas. Type 'C' immersion thermocouples (TCs) are used to monitor slag temperature. The TCs, RTDs readings, arc voltage, current, and water flows are recorded with time on a data logger system. Gas flow rates are monitored by an MKS M062-LS06E mass flow valve and an MKS 440 series mass flow controller. An ice cold trap was used to condense water vapor and cool exhaust gases before entering the baghouse. The high-efficiency baghouse filter collects condensed and solid particulate before the exhaust gas passes through a HEPA filter and into the building exhaust system.

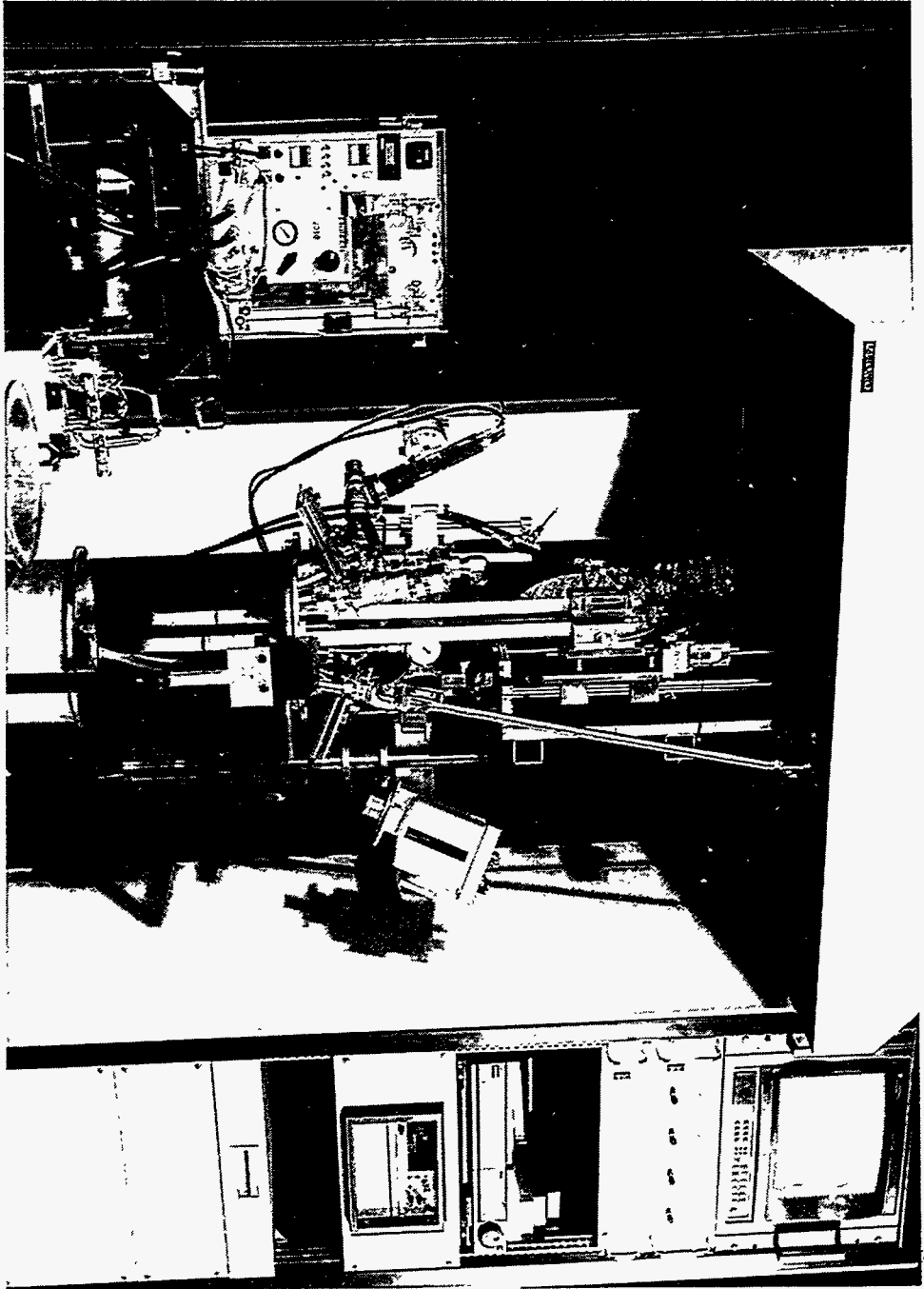


Figure 3.1 Photograph of the modified bench-scale arc melter in FY-93.

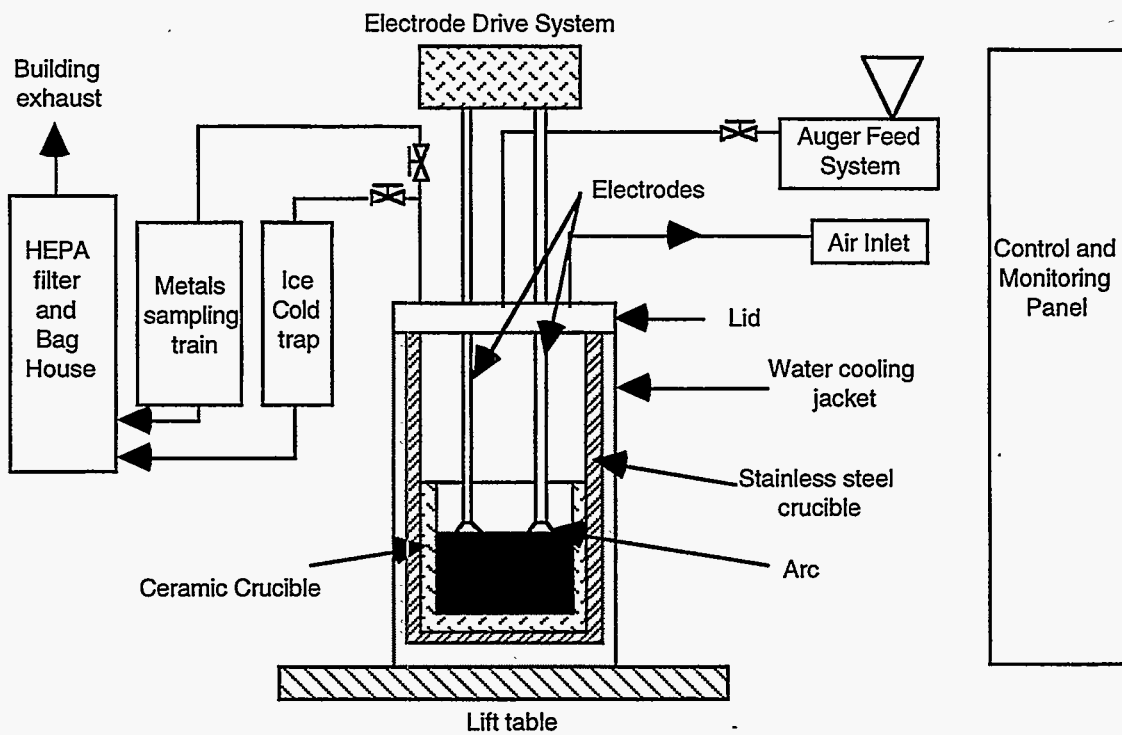


Figure 3.2 Schematic of the modified bench scale arc-melter .

3.3 FY-94 Arc Melter Modifications

The purpose of the FY-94 HVPM tests was to determine methods to retain surrogates (HVPM, Cs, and TRUs) in the final waste form (IEB4/A-40). Many modifications to the arc melter were made to ensure that useful data could be obtained. Most important, the exhaust system was entirely rebuilt so that particulate could be easily collected and an accurate mass balance attained. Further changes included improvement of the electrode penetration seals in the lid of the melter, development of a pinhole viewing device to observe the melt and arcs in dusty conditions, installation of a graphite feed chute to better control introduction of material into the furnace, and construction of a water-cooled lance to inject air or oxygen into a melt. Figure 3.3 shows the arc melter system as configured for the FY-94 tests.

In order to analyze HVPM retention, quantitative mass balances were needed during melter operations. A procedure was developed to measure all input and output materials and thus ensure an accurate mass balance. Of particular importance, the arc melter exhaust system was modified to provide for easy material collection. The new exhaust system, presented in Figures 3.4 and 3.5, was redesigned and built to allow easy assembly, access for cleaning, and particulate collection, which facilitated mass balance accountability within the melter system.

Additionally, the new exhaust system was modified to prevent blockages that were experienced during the FY-93 tests. The size of the exit port was increased and the 90-degree exit line was replaced with one having a gradual radius. Downstream, the exhaust line also included an air dilution nozzle and eductor to provide extra motive force for maintaining negative pressure in the melt chamber and gas cooling. A type 'K' thermocouple inserted upstream of this nozzle monitored the exhaust gas temperature. A cyclone separator was installed downstream of the nozzle for particle collection. A removable Watman quartz microfiber filter (8 x 10 inches) was placed in the exit gas stream prior to the baghouse to collect the remainder of entrained particulates and provide for mass balance closure. These filters are rated to retain 99.997% of particles 0.3 μm in size at flows up to 1000 slpm. Isolation and bypass valves were installed around the filter so the filter could be replaced during operation. The loading condition of the filter was determined by a Magnehelic® (0-10 inches of water) differential pressure gage installed across the filter. The filter is determined to be loaded with particulate when the pressure gage reads 5 inches of water.

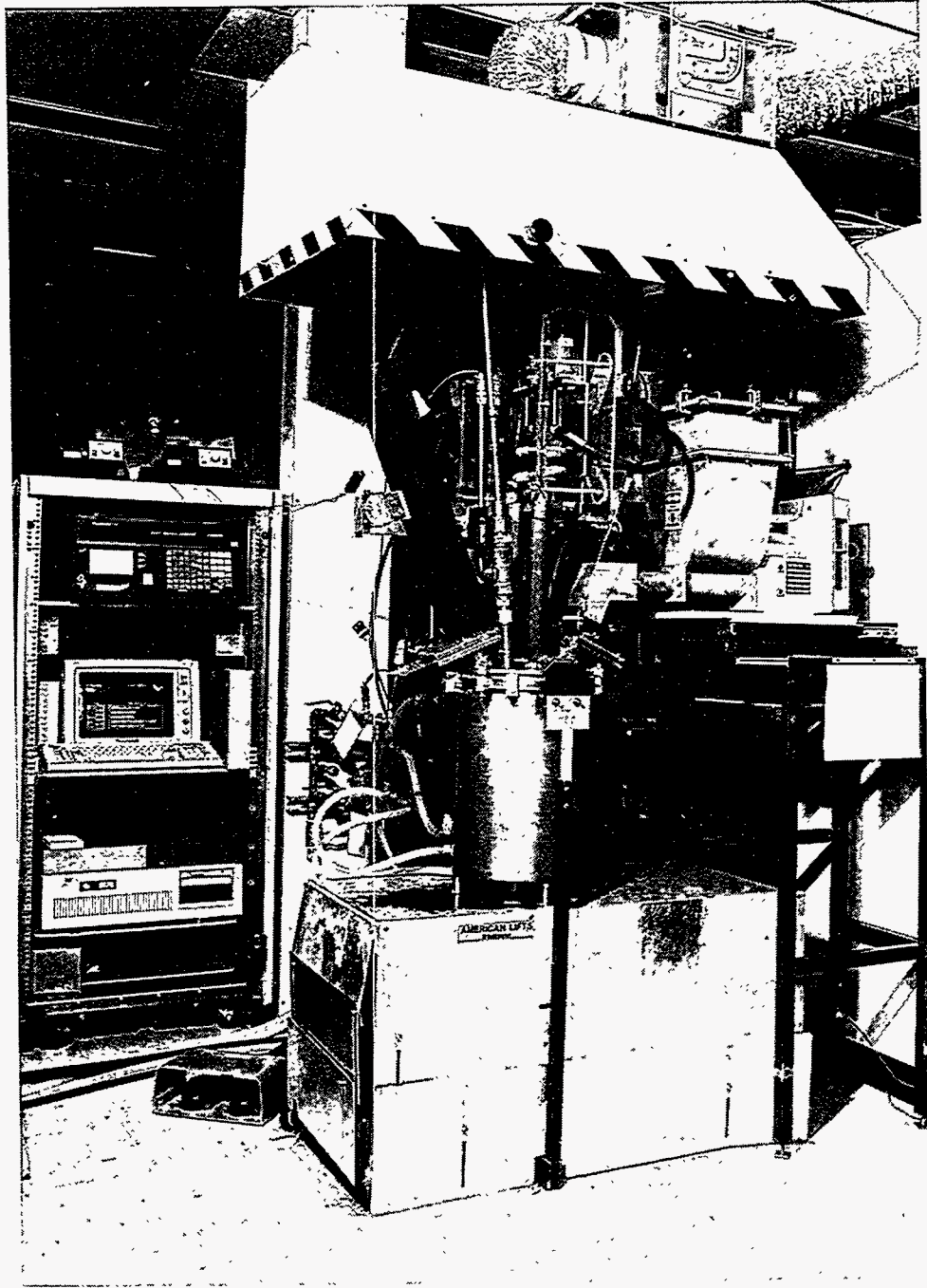
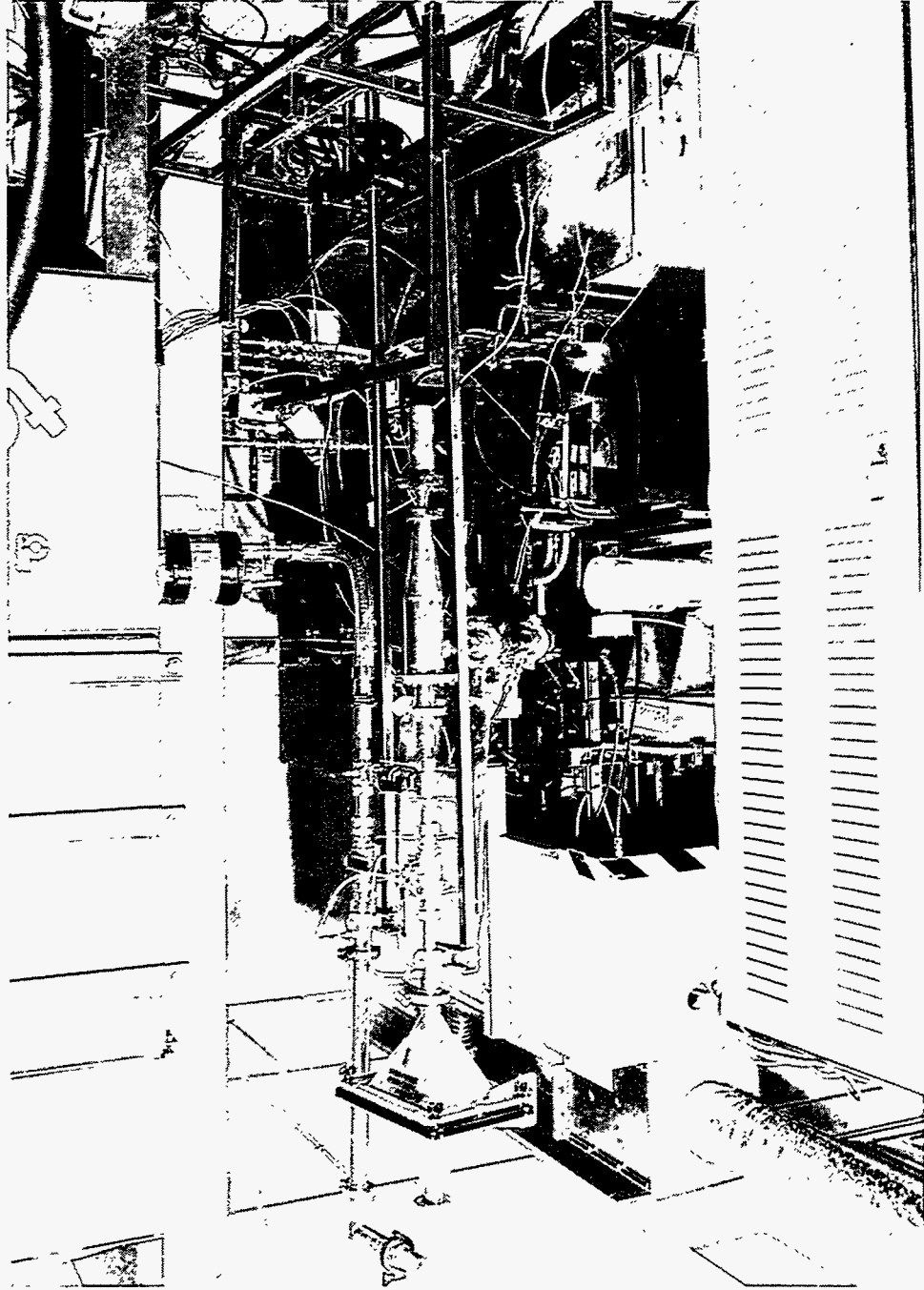


Figure 3.3 Photograph of the arc melter system as configured for the FY-94 tests.

Figure 3.4 Photograph of the off-gas system used during the FY-94 tests.



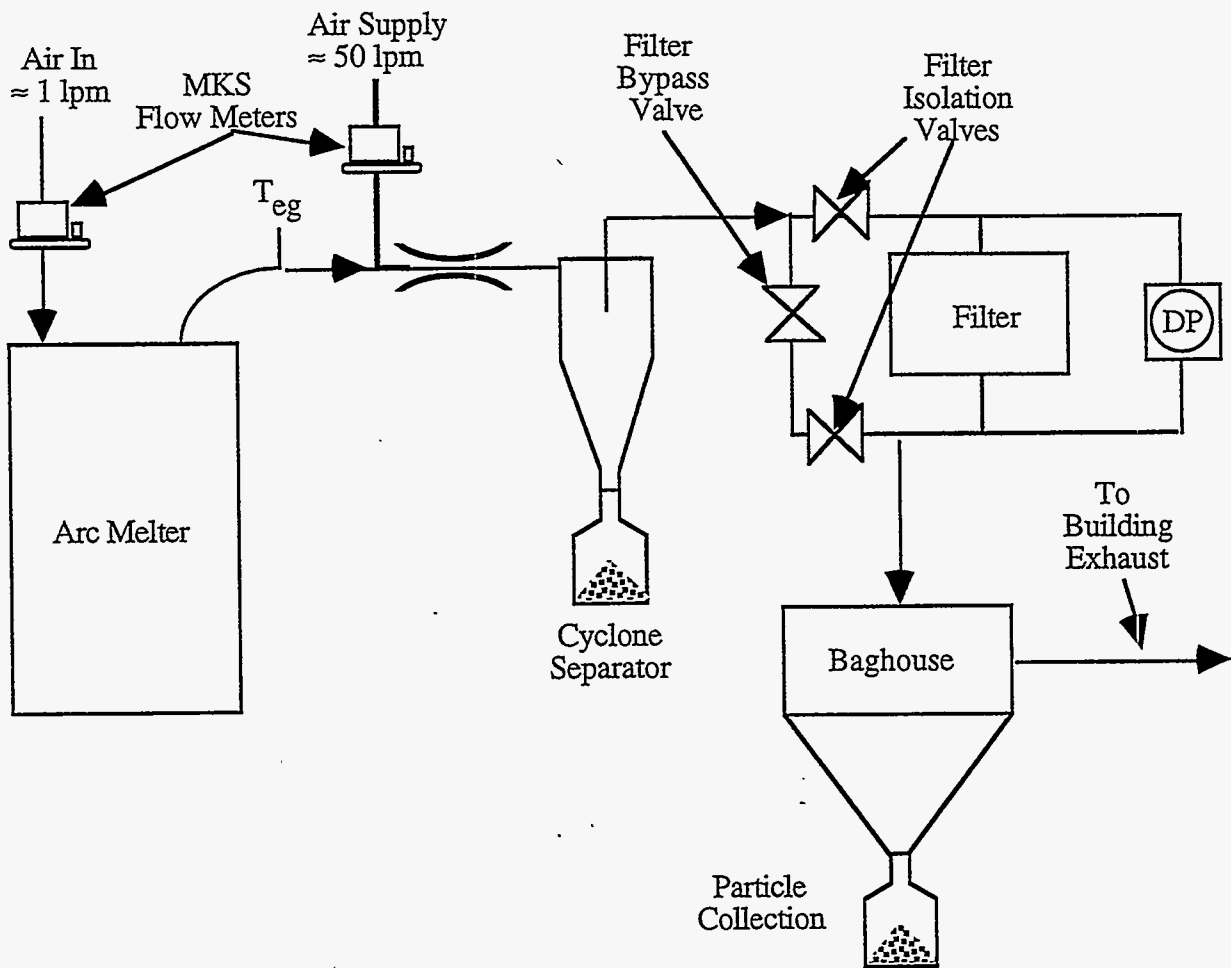


Figure 3.5 Schematic diagram of the modified offgas system utilized during the FY-94 tests.

The sealing system on the arc melter was upgraded to ensure negative pressure in the melt chamber for extended operations. The boron nitride (BN) electrode seals, used previous to FY-94, exhibited poor wear characteristics. The replacement seals, constructed of micarta (a resin-bonded fiber board), are shown in the schematic in Figure 3.6. The micarta seal and rod wiper assembly improved operation of the electrode motion while providing excellent sealing. A small piece of BN attached to the bottom of the micarta seal was required for thermal protection. The electrodes themselves were provided with individual drive mechanisms along with a master drive as shown schematically in Figure 3.7.

The feed system was modified to allow for installation of a graphite downcomer or feed chute that would direct material onto the top of the melt. Figure 3.8 shows the relative position of the feed tube, graphite extension, carbon steel starter ring, and soil mixture. Also shown in Figure 3.8 is the new cooling system used for the FY-94 tests.

The control of the melter through visual observation of the electrode arcs was critical in determining the existence of a cold cap and position of the electrodes relative to the melt surface. A pinhole camera assembly (see Figure 3.9) was incorporated into the viewing system to permit an unobstructed view of the melt surface for monitoring the arcs and cold cap. The pin-hole camera eliminated the need to constantly clean the porthole windows as required when viewing the melt directly through the portholes.

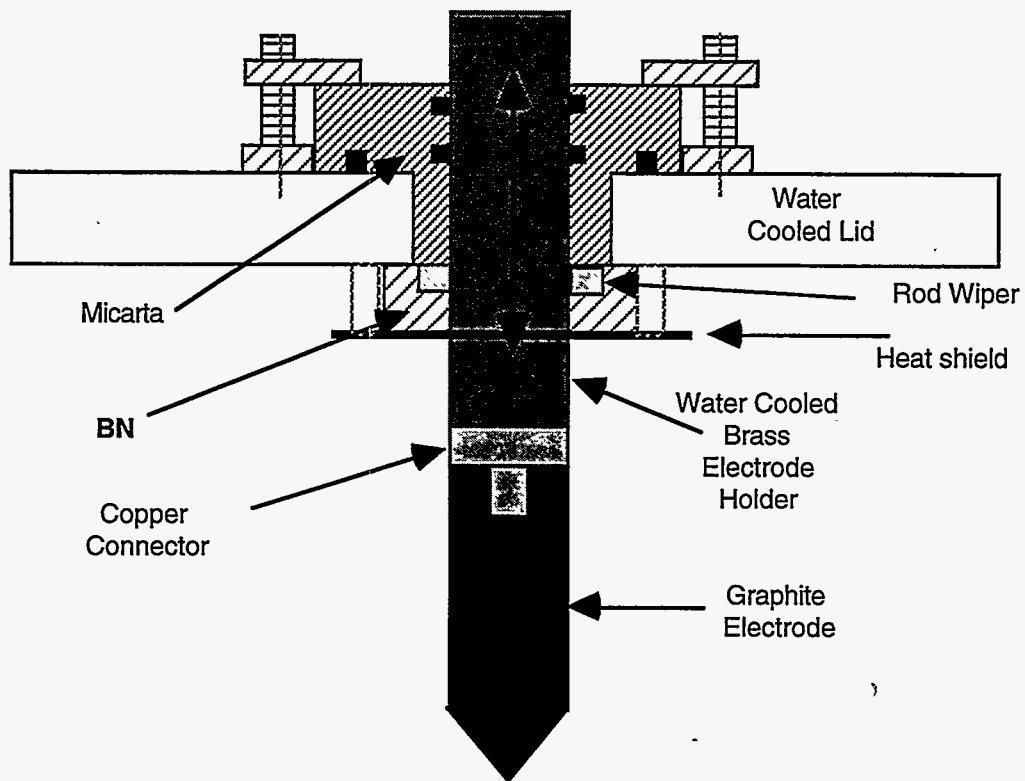


Figure 3.6 Micarta seal and rod-wiper assembly used for the electrodes during FY-94.

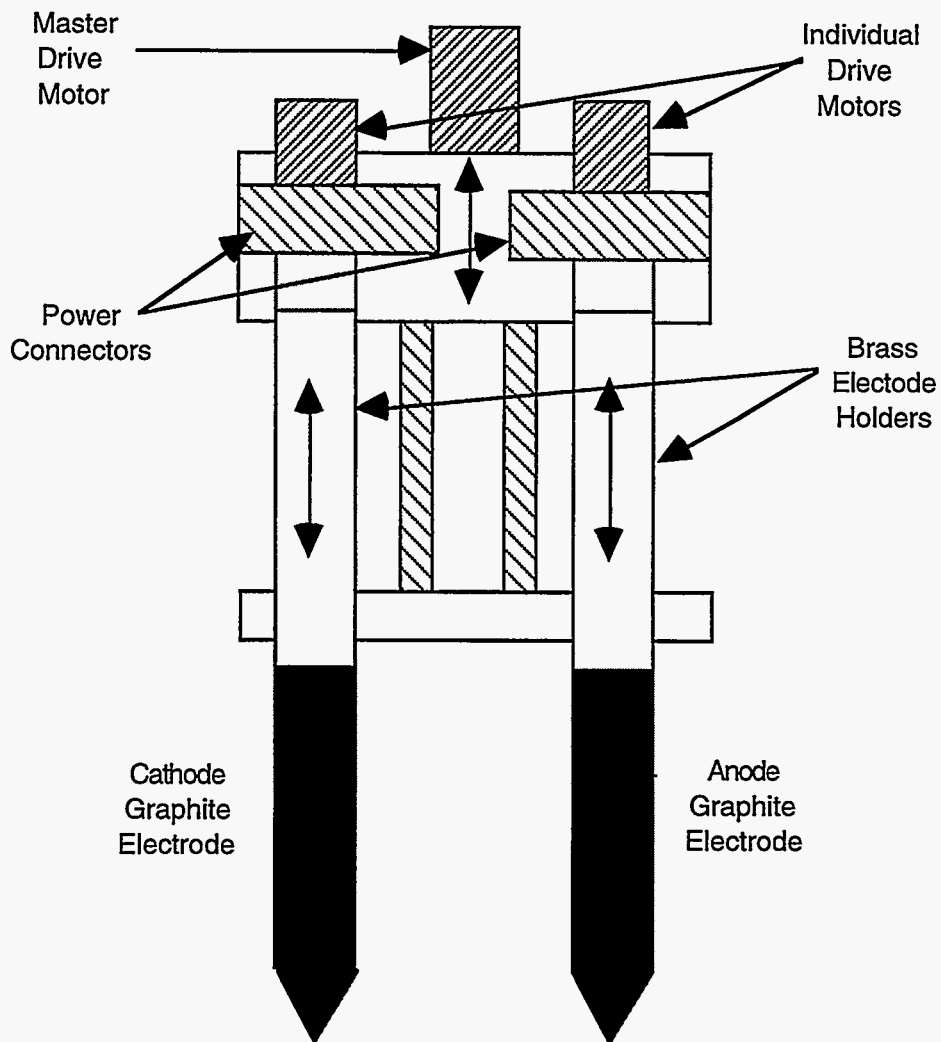


Figure 3.7 Schematic of the modified electrode drive mechanism showing the individual drive motors and master drive motor.

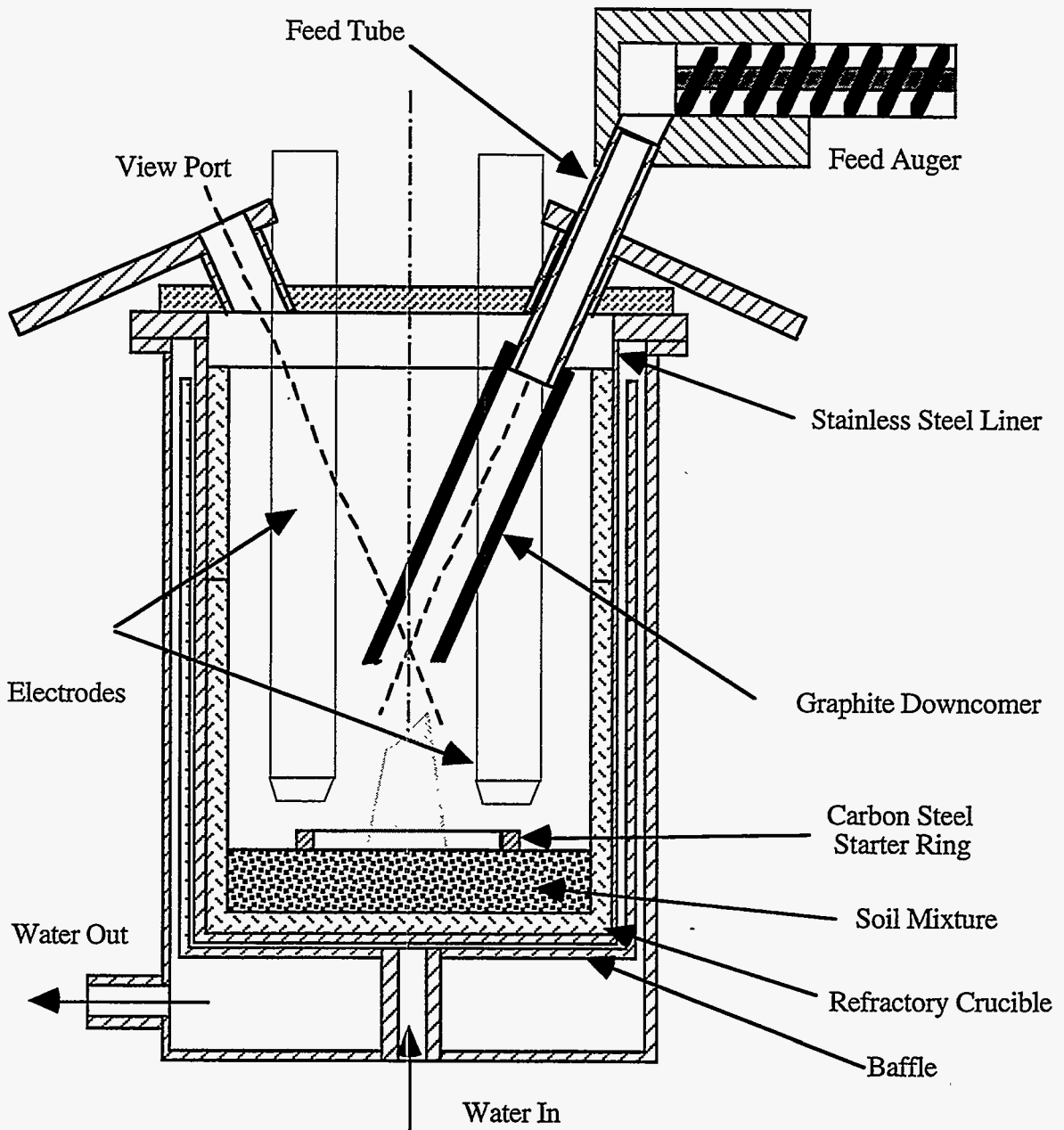


Figure 3.8 Schematic of the modified arc melter crucible assemble showing the material feed system used during FY-94.

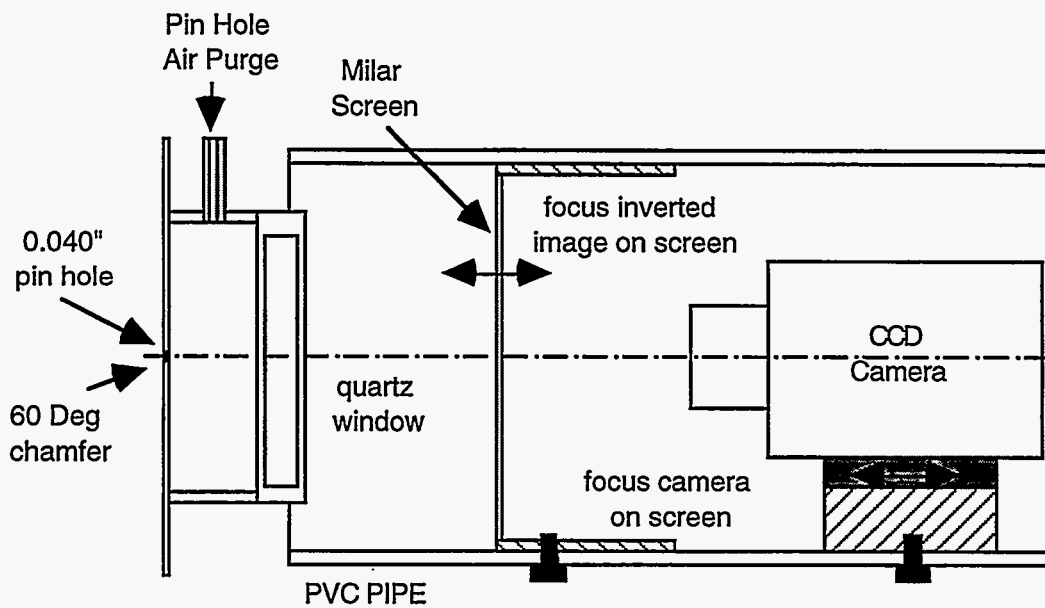


Figure 3.9 Schematic of the pin-hole camera assembly used during the FY-94 tests.

4. ARC MELTER OPERATIONS

4.1 Introduction

During the various experimental campaigns, several aspects of melter operation were found to be important, including the energy balance during arc melter operation, carbon electrode erosion, and melt temperature monitoring. Electrode erosion is problematic because it limits the duration that the arc melter can be operated. Temperature measurements on the slag were challenging due to sometimes high ($>2000^{\circ}\text{C}$) temperatures.

The general routine in all melter operations consisted of weighing the electrodes and mounting them onto the electrode drive mechanism. All thermocouples, water flow meters, and voltage probes were set in place, including those inside the crucible, and operationally checked and calibrated. An initial charge of soil/waste mixture was loaded into the crucible and the system secured. When the crucible cover is closed and sealed, a cooling water leak check is performed prior to starting the arc melter.

4.2 Arc Melter Operation

Two 80 kW power supplies were used to run the arc melter. A thin carbon strip or a metal ring was placed in the initial charge material to provide a current path to start the melting process. When melt pools beneath the electrodes coalesced providing a current path through molten slag, joule heating in the slag would increase energy input into the melt. After the startup phase and the electrodes have been adjusted to a stable operating position above the slag (approximately one-half inch), power input to the melt is controlled primarily by decreasing or increasing the current. The typical operating voltage is 180 V, although this may vary somewhat depending upon the material being melted. Melting soil, rather than an A-40 mixture for example, will typically result in an operating voltage of over 200 V. The arc melter is normally operated between 10 and 40 kW with the current at 50 to 200 A.

4.3 Energy Balance

An understanding of the energy or heat balance of the system is critical to operating the arc melter. During the FY-93 tests, the arc melter was difficult to control when the viewport windows became covered with dust obstructing the operator's view of the electrodes above the melt. Also excessive foaming of the melt caused by gaseous evolution sometimes made control difficult. Control was improved during FY-94 with the addition of a pin-hole camera. During FY-94 less material was preloaded into the crucible for startup, which substantially reduced problems related to foaming during the initial melt stage. It should be

noted that nearly all the materials are already in oxide form and inert, and therefore in all of these tests, the amount of chemical energy supplied by the melt materials is negligible.

During volatilization experiments, changing conditions in the melter were evident from energy balance measurements. Crucible heat transfer calculations are given elsewhere.¹³ Voltage and current traces with time can also be informative. The energy balance description for the FY-93 tests was described by T. L. Eddy et al.¹³

Examples of energy balance data are presented in Figures 4.1-4.4. Figure 4.1 shows the input energy data for the FY-94 cold cap run ARM090894. Compare this data with the curves in Figure 4.3, ARM092094 a run without a cold cap. During the cold cap run the power input was generally under 20 kW and lasted only 66 minutes where the run without a cold cap operated over 20 kW for 89 minutes to process the same amount of material. The difference in melt time and power levels can be attributed mainly to the insulating effect of the cold cap. In both cases, the molten slag was maintained at about 1600°C. For all the FY-94 runs it took about 20 minutes to achieve a fully molten surface with slag temperature at 1600-1700°C. The "power out" traces shown in Figures 4.2 and 4.4 reveal the difference in operating with and without a cold cap. Although they are similar in that they both level off at 21-22 minutes into the run, the 'power out' trace in Figure 4.3 is almost equal to the 'power in' trace. This indicates energy is being removed from the melt via the water-cooled crucible almost as fast as it is being supplied, thus the increased amount of time required to completely melt the material. Since the melt is open, heat energy can quickly radiate away from the surface of the melt. The larger difference between "power in" vs. "power out" in Figure 4.2 shows that significantly more energy is being supplied to the melt in this case, thus the reduced amount of time necessary to melt it. The cold cap prevents heat energy from radiating away. Only near the end of the run after 60 minutes does the amount of energy being lost increase, indicating that the cold cap has completely melted.

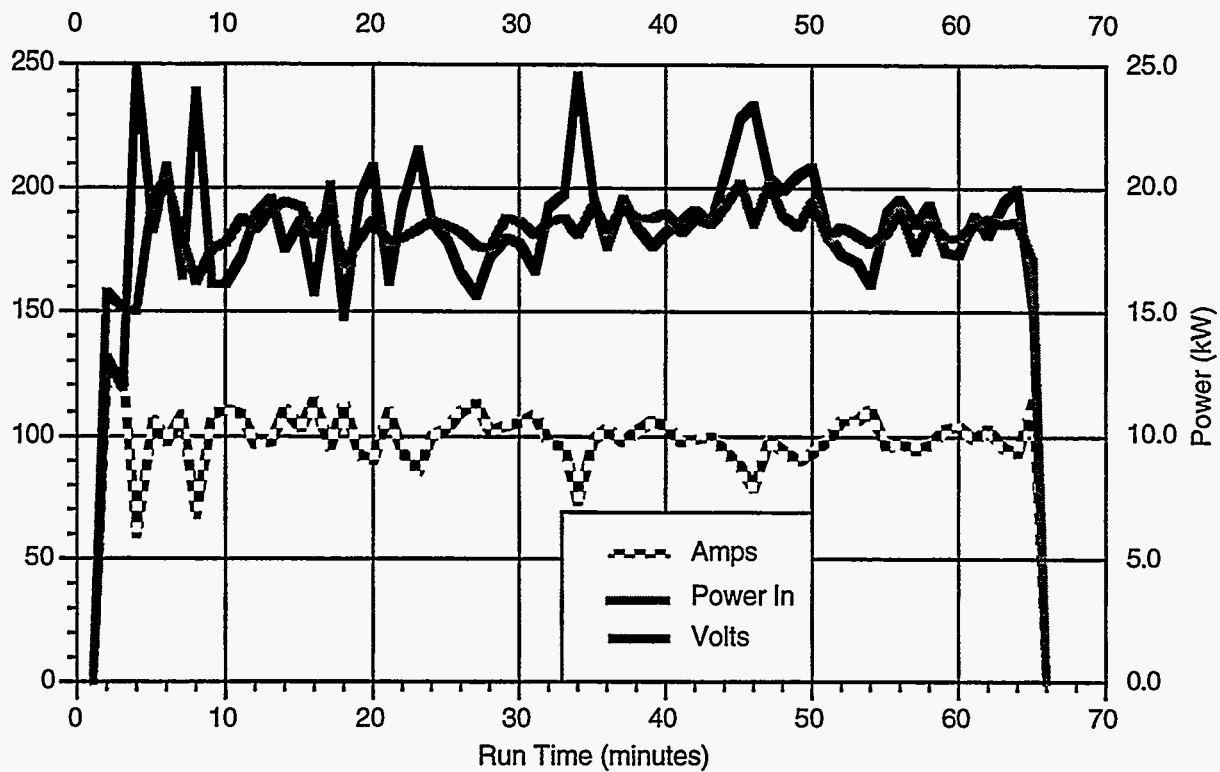


Figure 4.1 Energy input data for the HVPM run ARM090894 with a cold cap.

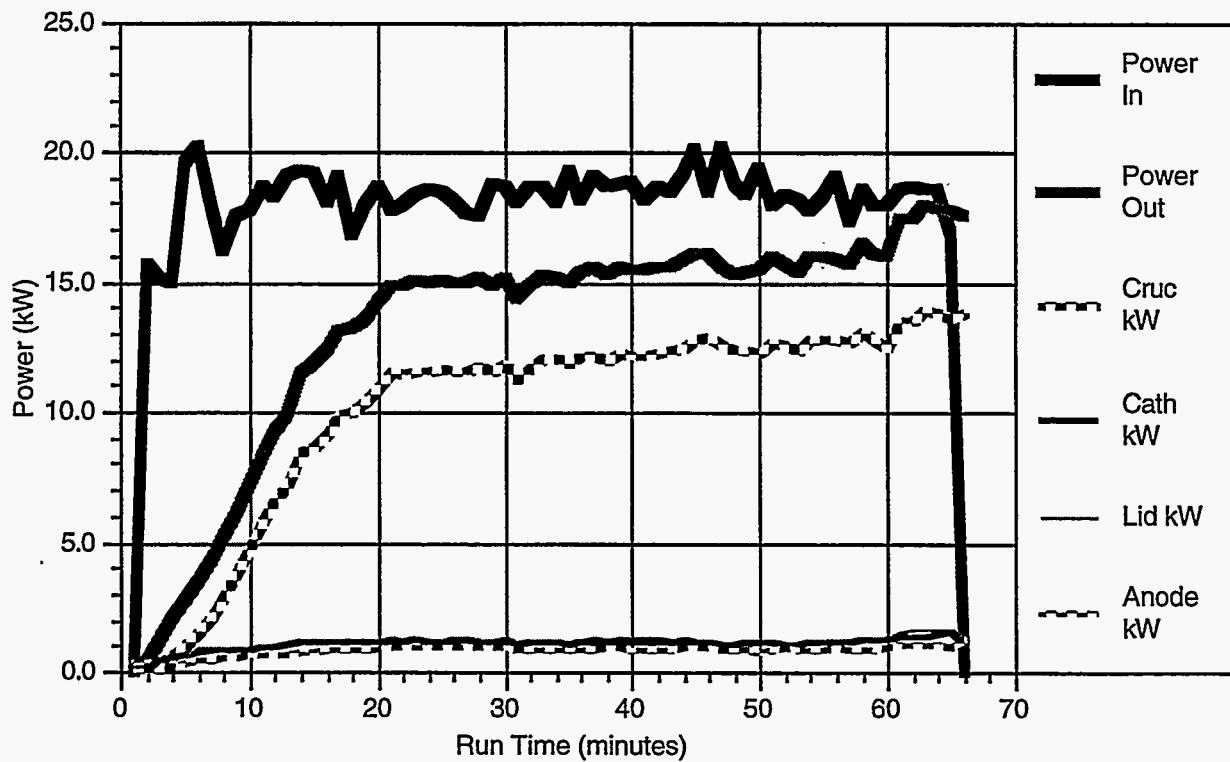


Figure 4.2 Energy balance information from HVPM run ARM090894 with a cold cap.

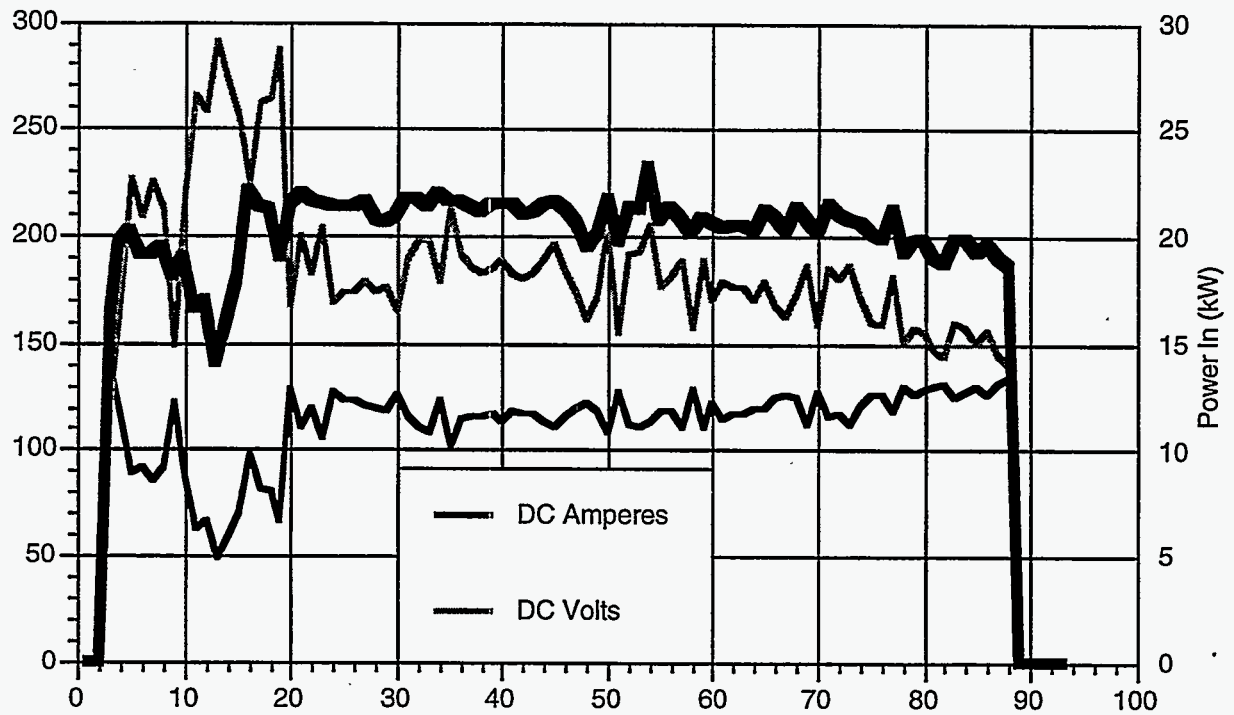


Figure 4.3 Energy input data for the HVPM run ARM092094 without a cold cap.

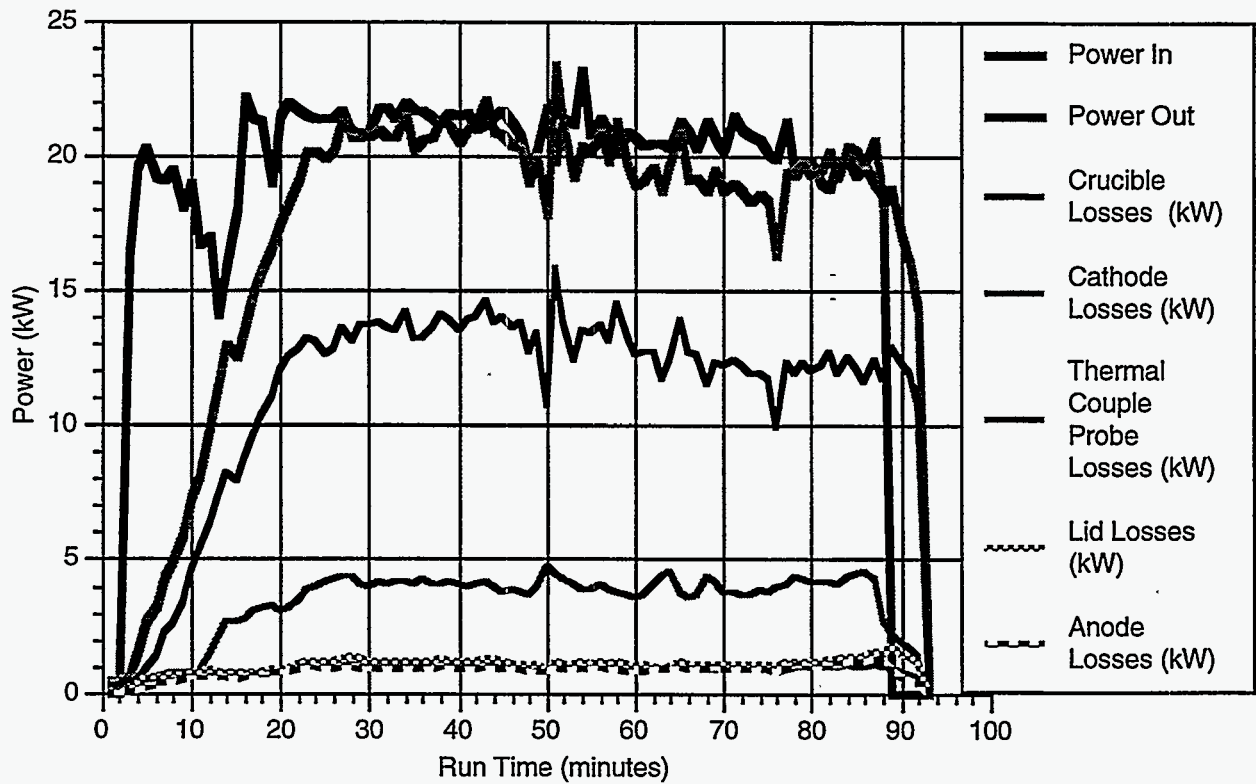


Figure 4.4 Energy balance information from HVPM run ARM092094 without a cold cap.

4.4 Electrode Erosion

Graphite electrode erosion is one of the factors that limit the operating time of the arc melter. In Tables 4.1 and 4.2, data from the FY-93 volatilization and redox experiments and FY-94 volatilization experiments show that the anode consumption rate is 25 to 50% higher than that of the cathode most of the time. During FY-93 tests, all the electrodes were coated with 0.060 inches of zirconia to inhibit erosion. Previous work had shown that zirconia coating reduced electrode erosion.¹³ During FY-94 two types of silicon based coating were used: a paint on silicon carbide (ZYP Coatings, Inc., 48% SiC) coating and plasma sprayed silicon coating applied through the Vartech company. Although, the anode is consumed faster than the cathode (about 2 to 1), without information about arc length or submerged arc, it is difficult to formulate a relationship between power input, temperature, chamber atmosphere (redox conditions), and electrode erosion rates.

Figure 4.5 shows that electrode erosion rate (in grams per amp-hr) when using the cold cap is, in general, higher than that without the cold cap. Electrodes submerged in a cold cap erode faster than electrodes held above a liquid melt in the case without a cold cap because they are in contact with the reactive slag. Except for the oxidizing run #OX03A, where excessive foaming stopped the run, the erosion or loss rates for all electrodes were very similar.

It was observed that the noncoated and ZYP SiC coated electrodes were consumed differently from the ZrO or Si coated electrodes. Noncoated electrodes and the ZYP SiC coated electrodes became pencil-shaped during the run indicating reaction with the graphite above the melt surface. Figure 4.6a, shows ZYP SiC coated electrodes from FY-94 cold cap run ARM082394, giving an example of the pencil-shaped wear. In Figure 4.6b, the plasma-sprayed Si coated electrodes from FY-94 cold cap run ARM090894 show little evidence of reaction above the arc-affected zone, and the wear is more uniform from anode to cathode. The zirconia-coated electrodes used during FY-93 tests produced results similar to the plasma-sprayed Si coating.

• During the FY-93 volatilization runs without the cold cap, it was difficult to see the position of the electrodes above the melt because of the dust. The cold cap material also made it difficult to observe the position of the electrodes and, therefore, to keep them just above the melt. Some initial oscilloscope measurements were made in an attempt to identify a signature related to electrode position, but they were inconclusive. During FY-94, a pin-hole camera was used to observe the electrode arc gaps. This proved to be a useful tool, and

Table 4.1 Operating conditions and electrode erosion data for the FY-93 experiments.

Test	Time (min)	Ave power (kW)	Total (A-h)	Anode loss (g)	Cathode loss (g)	Anode loss rate (g/A-h)	Cathode loss rate (g/A-h)	Max. slag temp (°C)
------	------------	----------------	-------------	----------------	------------------	-------------------------	---------------------------	---------------------

Volatility tests without cold cap (IEB4/A-80 and IEB4/A-40)

HVPM01	169	15.7	230	73.2	43.3	0.32	0.19	1460
HVPM02	125	18.8	223.7	73.2	43.3	0.33	0.19	1650
HVPM03	98	-	-	-	-	-	-	1900
HVPM04	60	16.1	113.4	22.6	9.7	0.20	0.09	-
HVPM05	136	16.3	251	61.1	37.9	0.24	0.15	1600
HVPM06	144	12.7	213	48.9	31.6	0.23	0.15	1460

Volatility test with cold cap (IEB4/A-80 and IEB4/A-40)

CC01	62	14.3	96.2	37.3	31.2	0.39	0.32	2300
CC02	112	9.5	82.2	31	10.7	0.38	0.13	1400
CC03	86	14.4	144.2	69.1	24.3	0.48	0.17	2000
CC04	62	14.6	66.5	35.8	25.1	0.54	0.38	-
CC05	80	13.6	83	48.7	21.3	0.59	0.26	2100

Reduction tests (IEB4/A-40)

RED01	110	10.9	103.5	51.5	35.6	0.50	0.34	2000
RED02	95	11.5	106.1	22.8	11.3	0.21	0.11	1800

Oxidizing tests (IEB4/A-40)

OX01	115	6.6	84.4	36	3.3	0.42	0.04	1665
OX02	125	12.8	161.3	77.2	51	0.48	0.32	1850
OX03A	95	13.0	36.5	57.3	43.2	1.57	1.18	1700
OX03B	120	13	-	133.1	37.7	-	-	1900

Table 4.2 Operating conditions and electrode erosion data for the FY-94 experiments.

Test	Time (min)	Ave power (kW)	Total (A-h)	Anode loss (g)	Cathode loss (g)	Anode loss rate (g/A-h)	Cathode loss rate (g/A-h)	Max. slag temp (°C)
ARM082394	109	19.06	246.0	72.8	43.8	0.300	0.178	2005
ARM082694	64	21.0	119.0	39.9	19.1	0.335	0.161	2113
ARM090694	75	17.4	106.8	35.3	11.9	0.331	0.111	1962
ARM090894	64	18.0	106.0	32.7	24.1	0.308	0.227	1677
ARM092094	89	19.9	161	40.8	17.6	0.253	0.109	1625
ARM092294	56	20.3	99.5	40.9	37.8	0.411	0.380	1763

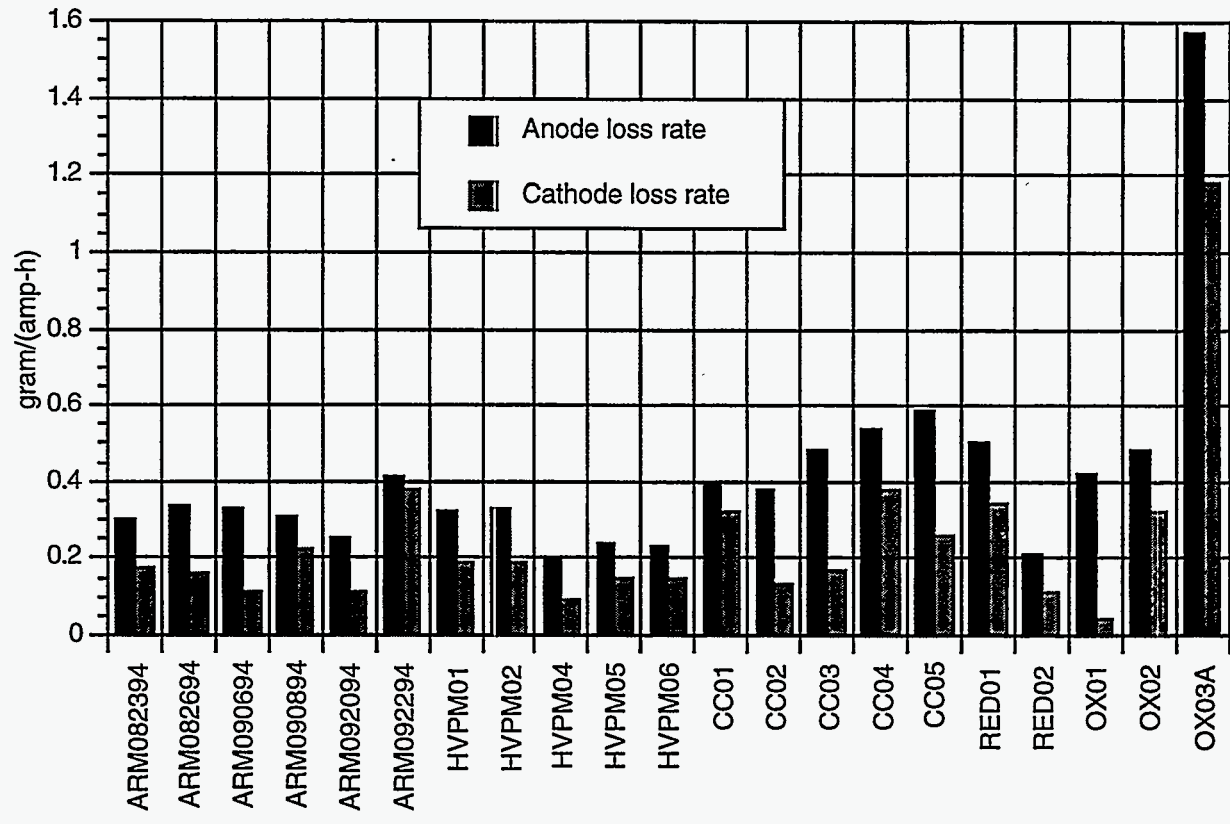


Figure 4.5 Anode and cathode electrode loss rates in grams per amp-h for FY-93 and FY-94 operations.

reduced the variability in electrode loss rates. Also during FY-94, a Laboratory-Directed Research and Development (LDRD) project examined the electrical signature of the electrodes. The year end LDRD report is located in Appendix A.

Plasma-sprayed Si coatings were also used during the FY-94 tests on the graphite feed tube extension and thermocouple sheaths. A photograph of an uncoated and coated feed tube extension is shown in Figure 4.7. In both cases, the extenders were in the melter for three HVPM runs. Although the uncoated extender was originally shorter than the SiC coated extender, it is obvious that the coating had a favorable effect. The SiC coated extender had little weight loss and is very close to original dimensions, where the uncoated extender had 25% weight loss and is tapered at the end.

4.5 Temperature Monitoring

During FY-93 and early FY-94, it was almost impossible to maintain a constant temperature reading on the molten slag. Thermocouple sheath material usually failed within 10 to 20 minutes of exposure to molten slag. Various sheath materials, such as alumina, zirconia, BN and silicon carbide, were used to protect the TCs, but none survived an entire run. A combination graphite, water-cooled probe was developed that allowed the TCs to survive a run. A schematic of the graphite, water-cooled probe is shown in Figure 4.8.

Improved methods of slag temperature monitoring evolved during the course of the FY-94 tests. Type 'C' thermocouples were utilized to monitor the slag and soil temperatures for all the runs. Initially, an alumina single sleeve and wire insulator were utilized for the runs, but the alumina was slowly consumed in each case finally resulting in TC failure. The TCs were double sleeved with alumina increasing their life. However, even using the highest grade of alumina did not solve the reaction problem with the molten slag. The double-sleeved TCs were used for ARM082694 run and were left in the melt the whole run. For the ARM090694, run BN sleeves were utilized, which lasted for approximately 70% of the run with continuous monitoring before the BN material eroded away. BN was also used as sleeve material for the ARM090894 TCs. During this run the TCs were periodically dipped into melt to ensure operability through the entire run. For the ARM92094 and ARM92294 runs, water cooled thermocouples were utilized. These TCs used a graphite sleeve covering the alumina TC wire insulator and survived the entire run for both cases. The graphite sleeves used for ARM92094 did not extend far enough away from the water-cooled wand and resulted in causing lowered indicated melt temperatures. The slag TCs used during the ARM92294 run were longer and coated with the ZYP SiC coating for added protection. Substantial erosion occurred on these sleeves, but both lasted the entire run.

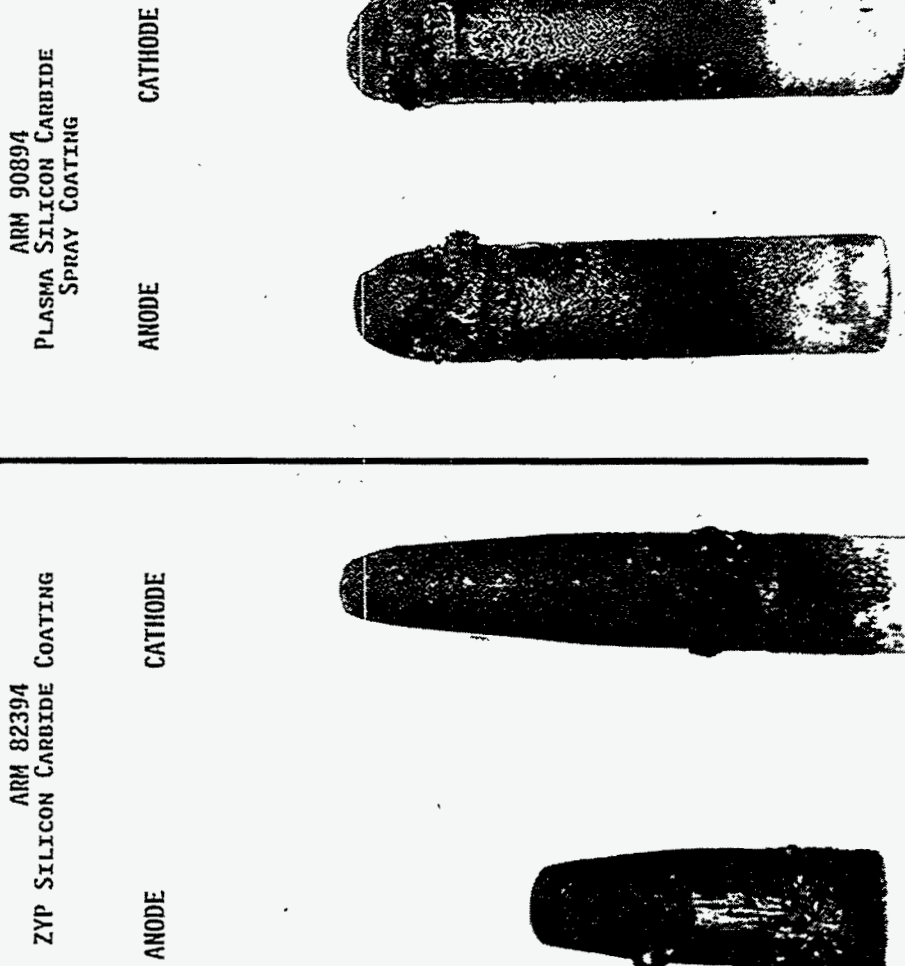
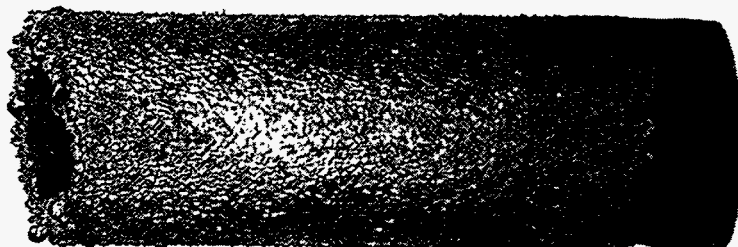


Figure 4.6 Used carbon electrodes coated with (a) ZYP silicon carbide and (b) plasma-sprayed silicon.

ARM 92294
GRAPHITE FEED TUBE EXTENSION
WITH SILICON CARBIDE COATING



ARM 81194
GRAPHITE FEED TUBE EXTENSION
WITHOUT COATING

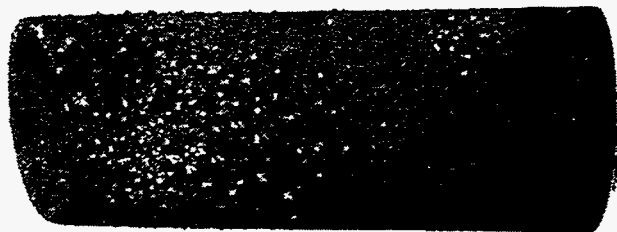


Figure 4.7 Carbon feed tube extenders (a) with and SiC coating and (b) without coating.

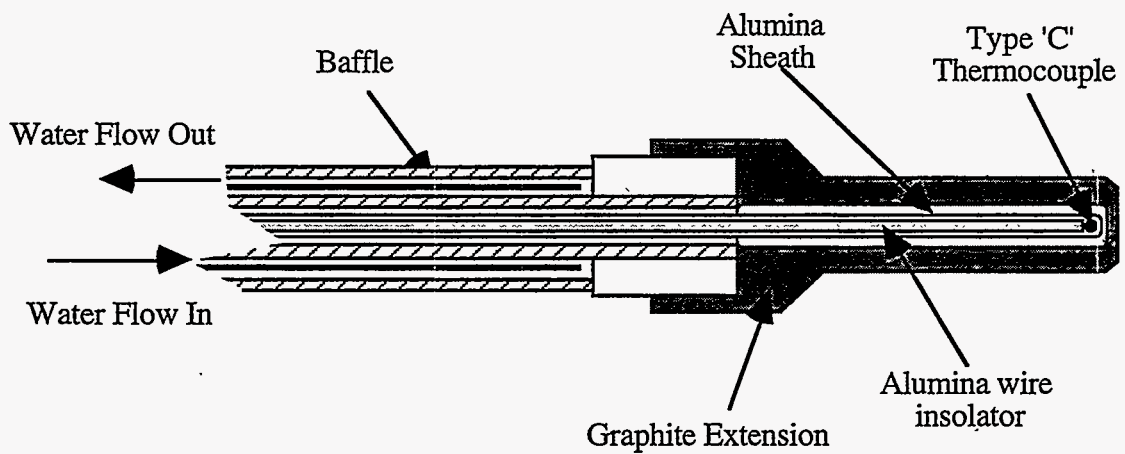


Figure 4.8 Schematic of the water-cooled TC probes used during the FY-94 HVPM tests.

Two TCs were used for each of the FY-94 tests. One was located near the center of the melt zone, and the other was placed near the edge. In Figure 4.9 the black line is the temperature response near the edge, and grey line is the response in the center. The temperature response of the slag at the two locations shows that the operating slag temperature of 1600-1700°C was reached after 44 minutes in both locations. At this point in time, the power in and out curves begin to parallel each other (the power out curve is not displayed).

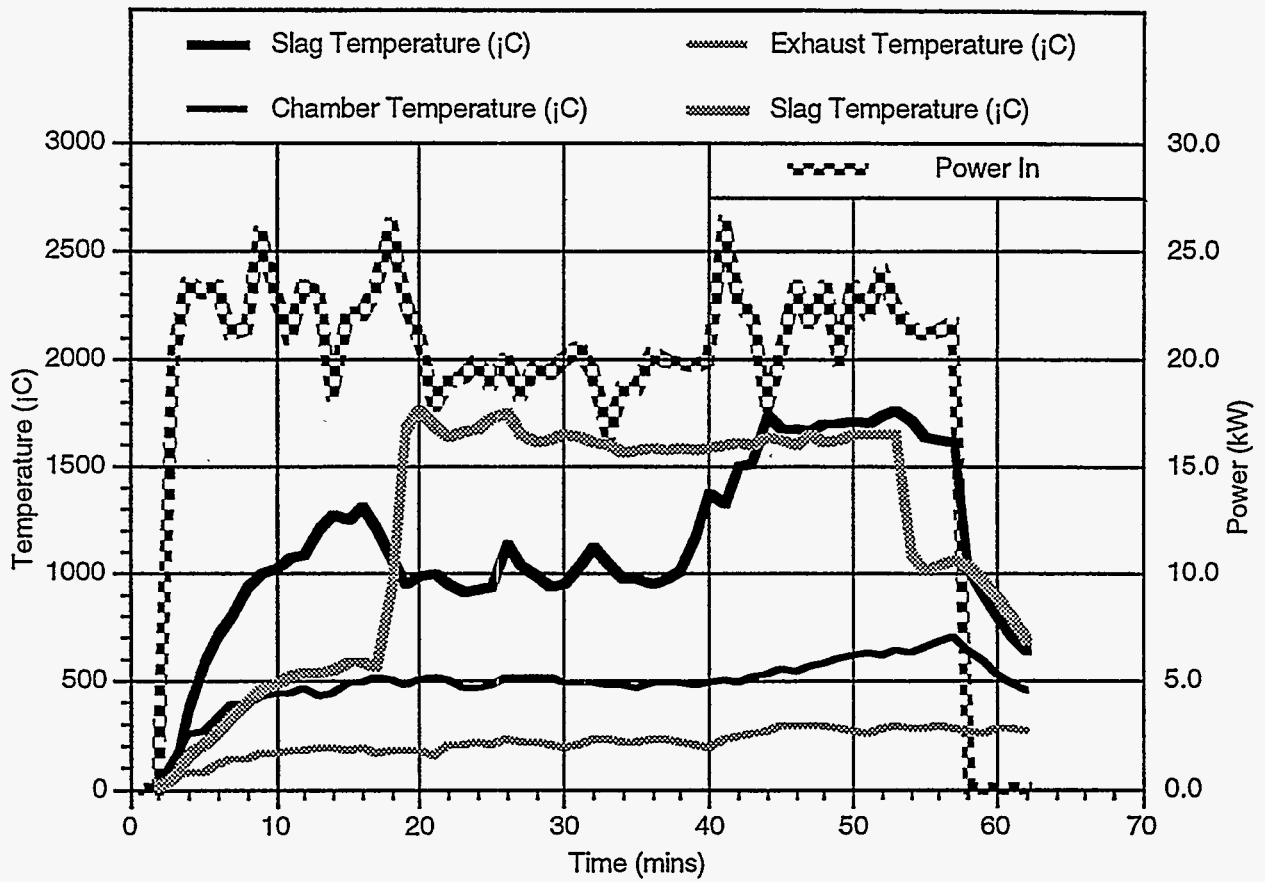


Figure 4.9 Temperature response of the slag and power input versus time for the HVPM run ARM092294.

5. VOLATILIZATION AND REDOX TESTING OVERVIEW

5.1 Introduction

This work was performed over a 2-year period in a bench-scale arc melter^{13,14} that was constructed to process simulated TRU waste and soil over a temperature range of 1300 to 1900°C and to evaluate the extent of vaporization. Surrogates used in the program that were expected to mimic volatilization characteristics of the TRUs and U compounds were CeO₂, SmO₂, NdO₂, Eu₂O₃, and Gd₂O₃ for the early FY-93 tests. Later in FY-93 and in all of FY-94, only CeO₂ and SmO₂ were used as TRU surrogates. In early FY-93, the HVPMS used in the testing were Cd, Cr, Cs, Pb, and Zn and were all added as metals except for cesium. For later tests, the HVPMS were added as oxides. Due to extremely reactive nature of pure cesium, it was always added as a carbonate (Cs₂CO₃). These elements cover the range of boiling points of interest and are the major toxic contaminants in TRU wastes that may remain in the solids after incineration. Cs is not toxic, but is a mixed fission product and has high volatility. Cr is not highly volatile, but is toxic. Hg was not considered for this series of tests, since it was already assumed that it will completely volatilize and end up in the off-gas collection system. The simulated waste mixtures contained 10% TiO₂ and 5% ZrO₂ by total weight and 1% each of the HVPMS and TRU surrogates.

As a convenient reference, the melting and boiling points of the elements above plus their relevant oxide forms are listed in Table 5.1 as contained in the CRC Handbook of Chemistry and Physics.¹⁵ Both metals and oxides are listed since conditions within the melter (oxidizing vs. reducing) may transform the metals into oxide forms or reduce metal oxides to metals.

5.2 HVPM Tests (FY-93)

This series of tests was designed to measure the extent of volatilization of several HVPMS and radionuclide surrogates to be processed in an arc melter environment. In these experiments, particulates in the exhaust gases were collected using an exhaust gas analyzer. The off-gas samples were intended to be obtained at melt temperatures 1900, 1600, 1450, and 1300°C. Control of the arc melter was not that precise, but the melt temperatures for the various experiments spanned the desired range. The exhaust gas particulates and slag were analyzed for composition. Table 5.2 below summarizes analytical testing for both the HVPM and cold cap experiments.

Table 5.1 Melting and boiling points of HVPMS and surrogates plus oxides.

Metal	Melting point (°C)	Boiling point (°C)		Oxides	Melting point (°C)	Boiling point (°C)
Cd	320.9	765		CdO amph	>1500	d 900-1000
				CdO cub	>1500	subl 1559
Cr	1857±20	2672		CrO		
				CrO ₂	300	
				Cr ₂ O ₃	2266±25	4000
Pb	327.5	1740		PbO	886	
				PbO ₂	290	
				Pb ₂ O	d	
				Pb ₂ O ₃	370	
				Pb ₃ O ₄	500	
Zn	419.6	907		ZnO	1975	
Cs	28.4±0.01	669.3		Cs ₂ O	d 400;	
				Cs ₂ O ₂	400	650
				Cs ₂ O ₃	400	
				Cs ₂ CO ₃	d 610	
Ce	798	3443		CeO ₂	ca 2600	
				Ce ₂ O ₃	1692, ign 200	
Sm	1074	1793		Sm ₂ O ₃		
Nd	1021	3074		Nd ₂ O ₃	~1900	
Eu	822	1527		Eu ₂ O ₃		
Gd	1313	3273		Gd ₂ O ₃	2330±20	

amph - amorphous, ca - calculated, cub - cubic, d - decomposes, ign - ignites, subl - sublimates

Table 5.2 HVPM analyses for FY-93 HVPM and cold cap experiments.

Sample type	Method	Elements
slag (TCLP only)	SW-846 1311, 3010, USEPA 200.8, and any furnace AA methods necessary to meet TCLP requirements provided in ERD-SOW-107	Cd, Cr, Pb
slag	USEPA 200.8	Al, Ca, Cd, Cr, Ce, Cs, Fe, Gd, K, Mg, Na, Nd, Pb, Si, Sm, Ti, Zn, Zr
soil	USEPA 200.8	Al, Ca, Cd, Cr, Fe, K, Mg, Na, Pb, Si, Ti, Zn, Zr
glass fiber filters	USEPA 200.8	Cd, Ce, Cs, Cr, Gd Nd, Pb, Sm, Zn
impinger liquid	USEPA 200.8	Cd, Ce, Cs, Cr, Gd Nd, Pb, Sm, Zn

5.3 Cold Cap Tests (FY-93)

A cold cap of IEB4/A40 with HVPM and TRU surrogates was used during these tests to study its effect on volatilization of the HVPM and TRU surrogates. The tests focused on global (total mass as opposed to elemental mass) volatilization from the melt having a cold cap of feed material over the surface of the melt. One technique sometimes employed to minimize volatilization from a molten surface is to over load that surface with feed material, effectively placing a cold cap on the melt surface. Materials will condense on the cold cap and be returned to the melt as the cold cap is consumed from beneath. Raw material is added from above to maintain a desired thickness of cap material. In a batch-type operation, the cold cap will be consumed prior to securing the operation.

5.4 Redox Tests (FY-93)

Oxidizing and reducing conditions were varied during melting in a preliminary effort to determine the effect, if any, of redox on retention and distribution of the HVPMs, Cs, and TRU surrogates in the melt. Four experiments were run that may individually be described as highly reducing, slightly reducing, slightly oxidizing, and highly oxidizing. All redox melts were made without a cold cap, and the exhaust gas analyzer was not used. Compositional analysis and examination of crystalline and amorphous phases of the slags were done using SEM/EDXS. Compositions were also determined using inductively coupled plasma/ atomic emission spectroscopy (ICP/AES) and flame atomic absorption (FLAA) Spectroscopy. An independent lab, determined the Fe^{+2}/Fe^{+3} ratios.

5.5 Volatilization Tests (FY-94)

The purpose of the FY-94 HVPM tests was to determine methods to retain surrogates and HVPMs in the final waste form (IEB4/A-40). In order to analyze these methods, quantitative mass balances were needed during melter operations. An accurate mass balance was obtained by a procedure developed to measure all input and output materials. Prior to FY-94 testing, the arc melter system was modified to improve its operabililty and performance with the goal of total material recovery, which would allow accurate mass balances to be made.

XRF and EDXS analyses were done to determine elemental compositions of both the filter particulates and slags. An independent ICP analysis was also conducted by a commercial analytical lab to determine metals basis compositions for particulates and slags.

6. HVPM RETENTION AND EXHAUST GAS ANALYSIS (FY-93)

6.1 Introduction

These experiments began with a 6.0 kg charge of IEB4/A-80 mix in the melter. This amount of material would take 45 minutes to 1 hour to melt depending upon the input power and whether a cast ceramic insert or crucible was installed in the melter. A crucible insert provides some insulation from the water-cooled stainless steel wall and thus reduces the overall amount of energy needed to melt a charge of material. Once this initial charge had melted, the A-40 mix with HVPMs and TRUs was added via the auger feeder system. Slag and off-gas samples were collected during the feeding operations. Problems with the electrodes and exhaust plug ups limited the length of most of these runs. Table 6.1 outlines some of the basic parameters of the HVPM and cold cap experiments.

Additions of alkali (IEB4/A-40 + KOH and NaOH) and adjusting power input were to be used to control melt viscosity and temperature. Melt viscosity varies mainly as a function of temperature: the higher the temperature the lower the viscosity. Only in experiment HVPM05 was alkali added to decrease viscosity. For this series of tests, the melt temperature was monitored using a type C thermocouple probe sheathed with a high-temperature alumina tube. The probe would be lowered into the melt and held there until the temperature reading stabilized, whereupon it would be withdrawn to prevent damage.

6.2 Data Collection

The primary goal of determining the extent and nature of volatilization within the arc melter system requires that volatile materials be tracked through the system as it is operating. To achieve this, both the melt and particulates entrained in the exhaust gases were sampled and analyzed to determine the concentrations of HVPMs and TRU surrogates they contained.

6.2.1 Slag Sampling

Slag samples were extracted directly from the melt just before and just after each exhaust gas sample collection. Slag samples were collected during FY-93 by using a quartz tube with an aspiration device, shown schematically in Figure 6.1. The aspiration device consists of three components: a venturi vacuum pump, a vacuum control valve, and a vacuum cut-off valve. The quartz tube is used to collect the sample. As 90 psi air is forced

Table 6.1 FY-93 HVPM and cold cap test series.

Test name	Date	Starting material	Additions	Cruc. insert	Run time	Shutdown condition
HVPM01	6/18	6.0 kg IEB4/A-80 + HVPM's + Surrogates	1.0 kg IEB4/A-40 + HVPM's + Surrogates	no	2 hr 49 m	Normal (some damage to anode)
HVPM02	6/23	6.0 kg IEB4/A-80	1.0 kg IEB4/A-40 + H + S	no	2 hr 5 m	Exhaust plug up
HVPM03	6/24	6.0 kg IEB4/A-80	1.0 kg IEB4/A-40 + H + S	no	1 hr 38 m	Exhaust plug up
HVPM04	6/25	HVPM03 remelt + 0.7 kg alkali	(none)	yes	1 hr	Exhaust plug up
HVPM05	7/01	HVPM04 remelt + 0.5 kg IEB4/A-40	2.0 kg IEB4/A-40 + H + S +.87 kg alkali	yes	2 hr 16 m	Exhaust plug up
HVPM06	7/02	HVPM05 remelt + 0.5 kg IEB4/A-40	4.0 kg IEB4/A-40 + H + S	yes	2 hr 24 m	Normal
CC01	7/09	6 kg IEB4/A-80 + 0.5 kg IEB4/A40	6.0 kg IEB4/A-40 + H + S	yes	1 hr 02 m	Normal
CC02	7/13	6 kg-IEB4/A-80	6.0 kg IEB4/A-40 + H + S	yes	1 hr 52 m	Normal
CC03	7/14	6 kg-IEB4/A-80	6.0 kg IEB4/A-40 + H + S	yes	1 hr 26 m	Auger feed tube plug
CC04	7/15	6 kg-IEB4/A-80	(none)	yes	1 hr 02 m	Water leak
CC05	7/16	6 kg-IEB4/A-80	6.0 kg IEB4/A-40 + H + S	yes	1 hr 20 m	Normal (damage to anode occurred)

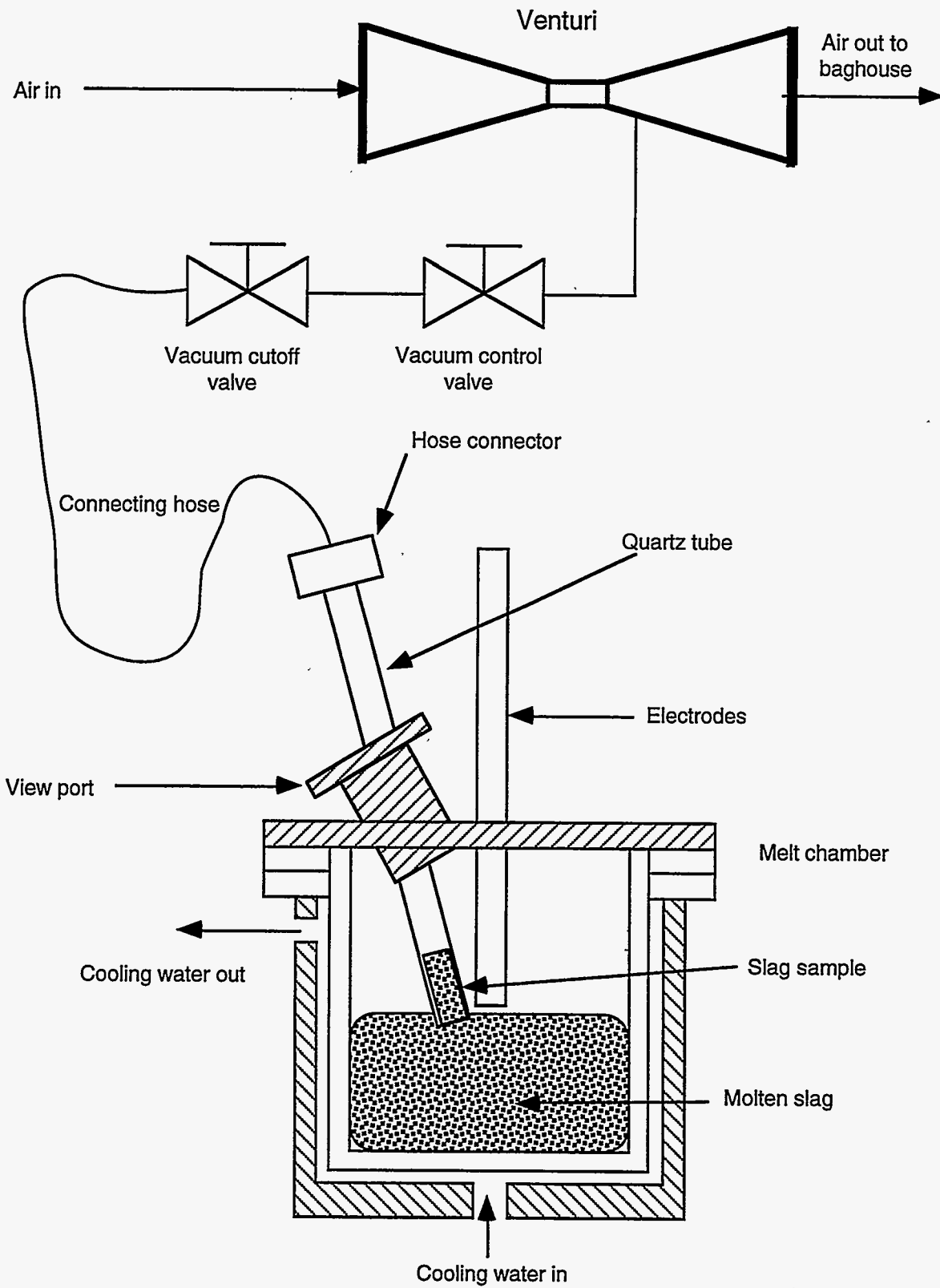


Figure 6.1 Sketch of the slag sampling system used during the FY-93 HVPM studies.

through it, the venturi vacuum pump creates a negative pressure in the quartz tube causing slag to be sucked up inside it. The transparent quartz tube allows the operator to see the amount of slag collected. The vacuum in the quartz tube is controlled by adjusting the control valve, and the vacuum cut-off valve provides a means to put a vacuum lock on the sample, holding the molten material inside the quartz tube. To prevent slag samples in large tubes from draining out of the quartz tube back into the melt, the arc melter was shut off to allow the sample to become more viscous prior to extraction.

6.2.2 Exhaust Gas Sampling

The off-gas sampling train used during the FY-93 experiments was an EPA "Modified Method 5" system and is illustrated in Figure 6.2. It consists of a series of bubblers containing nitric acid solutions for the digestion of the metals content of the off-gas stream. The entire off-gas volume flows through the solutions, depositing soluble species, and proceeds to the scrubber. The bubblers collect residues for a period of time, determined by the expected species concentration present in the off-gas, volume flow rate, and detection limits of the analytical techniques employed. At the end of the sampling period, the train is isolated from the melter outlet, and the solutions are recovered for off-line analysis. Operating procedures for the off-gas sampling train are located in the Appendix B.

As the procedure describes, two leak checks before and one after train operation were performed. The first leak check took place off-line and confirmed that all impinger and filter connections met EPA specifications for seal integrity. Leaks were detected at this stage during some tests. In those cases, the leak location was determined by observation of bubbling in the impinger fluids. Leaks were reduced to an acceptable level by repositioning components, careful application of appropriate sealant to contacting surfaces, or replacement of components. When this check was successfully concluded, the second pretest check took place with the train connected to the melter assembly through the swagelok fitting, with the valve to the train closed. That check confirmed the integrity of the fitting. When a leak was detected at this stage, it was resolved by adjusting the fitting, or by applying sealant to the outer fitting surface. A similar procedure was carried out at the conclusion of the sampling procedure. One post-test leak check fell short of the EPA requirements by a small amount during one sample collection run. In that case, the leak flow rate at the lowest level of vacuum attained during sample collection was recorded. That flow rate was used in a correction procedure applied to the data in the analysis phase.

Off-gas sample collection began when the melter sampling valve was opened and the baghouse valve closed. The gas flow rate through the sample train was controlled via the METHOD-5 BOX bypass valve, with the coarse valve fully open. Significant flow rate

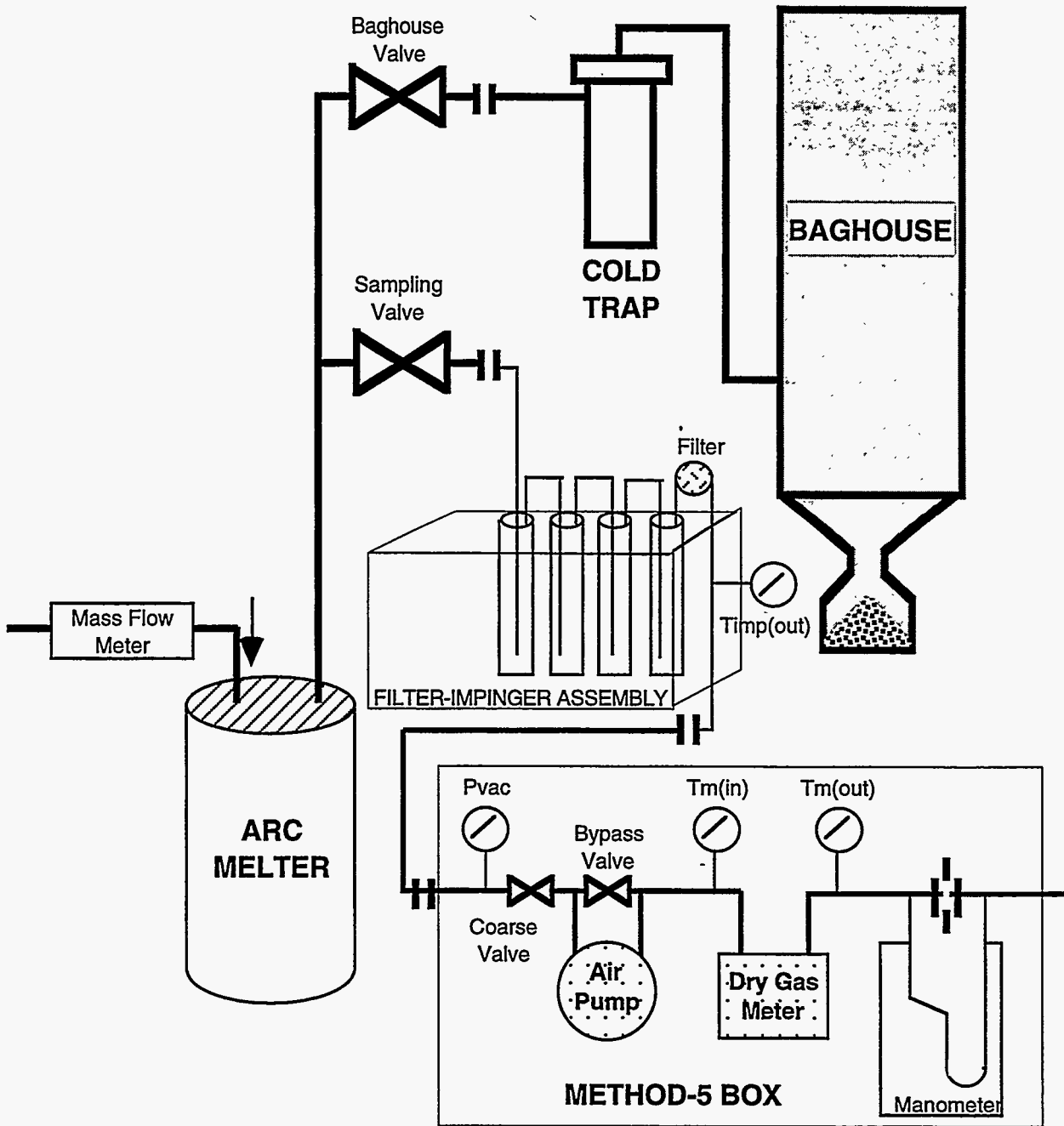


Figure 6.2 Schematic of the exhaust gas sampling train circa FY-93.

fluctuation occurred during soil addition to the melter. The bypass valve was used during these times to attempt to maintain the flow rate as closely as possible to the undisturbed flow rate.

Exhaust sample collection times varied from 9 to 30 minutes. These sampling time durations are expected to be more than adequate for collection of samples exceeding analytical detection limits, particularly since the loading in exhaust gases was very high. Some general information about the tests is contained in Table 6.2 and summarized in Table 6.3. After just a few minutes of operation, off-gas condensates were readily visible on the sampling train assembly filter and glass fittings prior to the impingers. In fact, during some tests in which the particulate loading was heavy, the sampling train filter capacity was nearly exceeded. This resulted in a notable increase in pressure drop across the filter assembly as condensible matter built up on the filter. In some cases, the filter ruptured. Consequences of this were increasing difficulty in maintaining the desired flow rate through the sample train with the available pump capacity, and also loading of the impinger fluids and fittings with excessive particulates and condensible matter. To remedy this and to ensure adequate sampling train capacity to extract all particulates and condensible matter from the off-gas stream, the following modifications were made to the sample train assembly, beginning with run HVPM06:

1. An additional nitric acid impinger was added to the train, bringing the total number of active impingers for solids digestion to three.
2. The volume of nitric acid in each of the first two impingers was doubled from 100 to 200 ml. The volume of the third impinger remained at 100 ml, increasing the total nitric acid volume in the train to 500 ml compared to the original 300 ml.
3. To help deal with the high particulate loadings, two filters were used in the filter assembly rather than just one. This increased the pressure drop across the filter assembly, but added strength to the filter, preventing the rupturing that had occurred previously during intervals with heavy particulate loadings.

Table 6.2 Metals sample information for the FY-93 HVPM and cold cap test series.

Test name	Experimental conditions and comments
HVPM01	Start with 6.0 kg of HVPM and surrogates in A-80 mix. Melt temperature of 1220°C prior to sampling 16.2 kW. Feed 1.0 kg A-40 + H + S mix during first 15 minutes of sample.
"	Melt temperature of 1350°C prior to sampling, 1460°C just after, 24 kW. No materials fed.
HVPM02	Start with 6.0 kg of IEB4/A-80 mix. Melt temperature 1650°C prior to sampling, 21 kW. Fed 1.0 kg A-40 with HVPM and surrogates for first 15 minutes.
HVPM03	Start with 6.0 kg of IEB4/A-80 mix. Melt temperature 1900°C prior to sampling, 1800-1900°C after. Fed 1.0 kg of IEB4/A-40. Train filter clogged during sampling.
HVPM04	Restart of HVPM03 with 0.7 kg of IEB4/A-40 + alkali, extremely thick green smoke, exhaust system plugged 1 hour after starting.
HVPM05	Remelt of HVPM04 with 0.5 kg of IEB4/A-40. Melt temperature before and after sample was 1600°C, 18 kW. Fed in 1.0 kg of IEB4/A-40 + H + S for first 15 minutes. Fed in 0.87 kg of alkali mix.
"	Melt temperature at 1500°C before sampling. Fed in 1.0 kg of IEB4/A-40 + H + S during sampling time, sampling was cut short due to a clog in the exhaust pipe.
HVPM06	Restart previous melt with 0.5 kg of IEB4/A-40. Added 1.0 kg of IEB4/A-40 + H + S. The filter in the metals sample train clogged up after only 6 minutes.
"	Melt temperature 1420°C before sampling and 1460°C after, 4.9 kW (one power supply). Fed IEB4A-40 + H + S during sampling interval. Fed 2.0 kg IEB4/A-40 after sampling.
CC01	Start with 6.0 kg of IEB4/A-80. Restart with 0.5 kg IEB4/A-40. Measurements (>2300°C) before and during sampling, 18.8 kW, cold-cap established 40 seconds after starting sample, momentarily lost cold-cap after 10 minutes. Fed total of 7.068 kg of IEB4/A-40 + H + S.
CC02	Start with 6.0 kg of IEB4/A-80. Melt temperature during sampling, 1400, 1350 & 1250°C, 3.2 kW, cold-cap established 40 s after starting sample. Fed 3.196 kg of IEB4/A-40 + H + S
CC03	Start with 6.0 kg of IEB4/A-80. Melt temperature at 1870-2000°C at 12.8 kW cold cap established just before sampling, the feeder plugged up forcing termination of sampling when the cold cap was lost, the melt temperature after sampling was 1750°C. Fed 6.684 kg of IEB4/A-40 + H + S.
CC04	Start with 6.0 kg of IEB4/A-80. Pinhole water leak prevented taking a sample.
CC05	Start with 6.0 kg of IEB4/A-80. Initial melt temperature of 2000-2100°C at 13.8 kW, cold-cap took over a minute to establish at highest feed rate setting, after 15 minutes melt temperature was 2000°C at 16.0 kW. Fed 4.031 kg of IEB4/A-40 + H + S.

Table 6.3 Metals sample conditions for FY-93 HVPM and cold cap test series.

Test name	Date	Sample time	Temperature (°C)	Power (kW)	Alkali
HVPM01	6/18/93	27 min	1220	16.2	no
		15 min	1350, 1460	24.0	no
HVPM02	6/23/93	30 min	1650	21.0	no
HVPM03	6/24/93	17 min	1900	unk	no
HVPM04	6/25/93	0 min			0.7 kg
HVPM05	7/01/93	30 min	1600	18.0	0.7 kg
		8 min	1500	14.5	1.6 kg
HVPM06	7/2/93	6 min	1740, 1720	18.2	no
		11 min	1420, 1460	4.9	no
CC01	7/09/93	16 min	2300+	18.8	no
CC02	7/13/93	22 min	1400, 1350, 1250	3.2	no
CC03	7/14/93	12 min	1870-2000, 1750	12.8	no
CC04	7/15/93	0 min			no
CC05	7/16/93	21 min	2000-2100, 2000	14.9	no

At the end of each sample collection period, after the final leak check was performed, the sample train assembly inlet and outlet were sealed, and the assembly was carried to a designated chemistry laboratory for sample recovery. Recovered samples were stored in glass jars and refrigerated until shipment to the analytical laboratory for analysis.

6.3 XRD Analysis of Exhaust Particulate

Particulates collected in the cold trap and crucible wall were used to make some semi-qualitative phase identifications using x-ray diffraction techniques. In the case of a no-cold-cap experiment x-ray diffraction profiles of material from the crucible wall and from the cold trap were found to be very similar. This fact suggests that most of the chemistry, such as oxidation, etc., has taken place within the melt and shortly after leaving the melt surface. The nature of particulates remains basically the same as they traverse the top of the melter and out the exhaust system. The same conclusion can be made in regard to the cold cap runs for which the XRD analyses of particulates collected from the crucible wall and the cold trap are again very similar.

In addition to the usual SiO_2 , TiO_2 , ZrO_2 , and iron oxides, CrO , CdO , ZnO , and Sm_2O_3 were identified. The original HVPM metal phases were not detected. The metals may have been oxidized while still in the melt or as they volatilized from the surface. Metal vapors just above the melt would be well above 500°C and easily oxidized by the incoming air. The Cr reaction would be different than that of other HVPMs in the melt. Cr metal is a strong reducing agent that can reduce the iron oxides in the melt to metal and itself will be oxidized to oxides. Cr_2O_3 can be dissociated at high temperature, particularly under the influence of an arc, to volatile suboxides such as CrO , CrO_2 or CrO_3 . The oxides of Pb and Cs were most likely present. However, they were not specifically identified by the XRD analysis in either cold cap or non cold cap cases.

6.4 HVPM Tests: Analysis and Results

6.4.1 Slag Composition Evaluation

In order to evaluate the extent of volatilization, it is necessary to compare the compositions of the starting materials with those of the final product or slag. Using the listed compositions of the IEB series in Table 2.2, the IEB4 compositions can be determined since known quantities of TiO_2 and ZrO_2 were added. Table 6.4 lists the IEB4 compositions and alkali mixture used in the experiments. TiO_2 and ZrO_2 additions were based on 10 wt% and 5 wt% loadings in the soil. The IEB4/A-80 therefore had total additions of 8 wt% TiO_2 and 4 wt% ZrO_2 , and the IEB4/A-40 had total additions of 4 wt% TiO_2 and 2 wt% ZrO_2 . The alkali mix was composed of 50 wt% IEB4/A-40 plus 33.3 wt% NaOH and 16.7 wt% KOH. Materials added to the melts are mentioned in Table 6.2.

Table 6.4 Chemical compositions for 1 kilogram of IEB4 mixes and alkali mix.

Chemical constituent	IEB4/A-80 (grams)	IEB4/A-40 (grams)	IEB4/A-40+H+S (grams)	Alkali mix (grams)
SiO ₂	531.5	479.4	436.3	239.7
Al ₂ O ₃	105.6	95.9	87.3	47.9
Fe _x O _y	82.7	183.3	166.8	91.7
CaO	87.1	91.2	83.0	45.6
MgO	24.6	32.9	29.9	16.5
Na ₂ O	19.4	30.1	27.4	348.3*
K ₂ O	24.6	24.4	22.2	178.9**
TiO ₂	84.4	42.8	39.0	21.4
ZrO ₂	40.0	20.0	18.2	10.0
Pb			10	
Cd			10	
Zn			10	
Cr			10	
CeO ₂			10	
Sm ₂ O ₃			10	
Gd ₂ O ₃			10	
Nd ₂ O ₃			10	
Cs ₂ CO ₃			10	

* - Na₂O and NaOH combined

** - K₂O and KOH combined

Table 6.5 Chemical composition of the FY-93 HVPM experiments.

Chemical constituent	HVPM02 (grams)	HVPM03 (grams)	HVPM05* (grams)	HVPM06 (grams)
SiO ₂	3625.37	3625.37	5113.91	7184.92
Al ₂ O ₃	720.85	720.85	1018.56	1432.76
Fe _x O _y	663.12	663.12	1232.27	2024.13
CaO	605.69	605.69	888.81	1282.71
MgO	177.78	177.78	279.93	422.06
Na ₂ O	143.53	143.53	760.26	890.21
K ₂ O	170.08	170.08	507.64	613.22
TiO ₂	545.37	545.37	678.32	863.30
ZrO ₂	258.20	258.20	320.30	406.70
Pb	10.00	10.00	30.00	50.00
Cd	10.00	10.00	30.00	50.00
Zn	10.00	10.00	30.00	50.00
Cr	10.00	10.00	30.00	50.00
CeO ₂	10.00	10.00	30.00	50.00
Sm ₂ O ₃	10.00	10.00	30.00	50.00
Gd ₂ O ₃	10.00	10.00	30.00	50.00
Nd ₂ O ₃	10.00	10.00	30.00	50.00
Cs ₂ CO ₃	10.00	10.00	30.00	50.00
Total	7000	7000	11070	15570

* Sodium hydroxide and potassium hydroxide were added to the melt to decrease viscosity.

6.4.2 Slag Characterization

The chemical analyses for selected slag samples from HVPM 02, 03, 05, and 06 were examined to determine residual composition of primary and added constituents. In the case of HVPM06, two slag samples were analysed. Tables 6.6 through 6.11 list the input composition of material for each of the HVPM experiments and (in the next column) the metals basis in parts per million (ppm) for each compound. Analytical results for the slag composition in terms of metals concentrations in ppm are also listed. Due to varying mass losses for each compound during processing, however, direct comparison of input metals concentrations to those of the slag in order to directly determine mass losses will not work. One method that will adjust the input metals concentrations so they can be directly compared to the analytical results is to normalize the input metals concentrations with a metal that has undergone no mass loss during processing. These "corrected" values will only be as good as the assumption of no mass loss for the element used to normalize the data. One can verify this using a simple example with 4 or 5 elements (see last page of Appendix C). The percentage of loss for each element can be determined exactly if the data is normalized to an element that has undergone no mass loss. The results from using this normalization method are, of course, only as good as the assumption that all of one component remains in the final product. In general, the percentage of error in the final results are about the magnitude as any original error in the assumption of no mass loss. For instance, if 15% of the mass of the element used for normalization has actually been lost, the normalized values for the other elements will be off by approximately the same amount. These errors will be compounded by errors in the analytical data when the comparisons are made.

Zirconia and titania have the highest boiling points of all the compounds in the melt (ZrO_2 - 5000 C, TiO_2 - >2500 C) and should, therefore, be more resistant to volatilization. Using Ti or Zr to normalize the data results in only a 1 or 2 percent difference in the "Amount retained" column in the tables. Titanium was chosen for the normalization in the HVPM experimental data since when Zr is used, it results in a greater than 100% amount retained for Ti. A ratio of the calculated metals basis concentration of titanium to the chemical analysis value was used to normalize the calculated metal concentrations. Appendix C contains the spread sheet work for the calculated compositions and normalization.

By comparing the corrected values with the slag metals analysis, the amount of each constituent compound retained can be determined. In Table 6.6 for HVPM02, the overall amount of material retained is approximately 50%. This result, however, is known to be incorrect. Even accounting for mass losses from hydrates and carbonates into H_2O and CO_2 and volatilization from all the compounds, still upward of 85% of the original mass should be retained. This suggests that the analytical metals concentrations for Ti and Zr may be over-

valued. This being the case, the (Ti or Zr) correction process would result in lowering the amount retained percentage of the other compounds below what they actually are.

Direct comparison of the calculated metals basis values with the slag metals analysis values, while inaccurate, is still useful for making some generalizations. This approach suggests that metals like Si, Al, Ca, and Mg have increased slightly in percentage as expected. The HVPMs like Pb, Cd, and Zn have decreased as expected. The metals Ti and Zr and in some cases Fe, have increased dramatically to twice or more their original concentrations. An increase in concentration is expected due to the loss of other constituents, but as stated in the previous paragraph, they appear to be abnormally high. The data contained in Table 6.6 for HVPM02 is consistent with the other HVPM experiments.

Some general conclusions concerning volatilization can still be drawn by direct examination of the analytical data. In all the HVPM experiments, the majority of Pb and Cd tended to volatilize. Zinc was also heavily volatilized but less so than for Pb and Cd. Sodium also was heavily volatilized in most cases. Chromium apparently stayed in the melt as did the surrogates, Ce and Sm.

Table 6.6 HVPM02 slag materials characterization.

HVPM02					
	Final composition (grams)	Metals basis (ppm)	Correct with titanium (ppm)	Slag metals analysis (ppm)	Amount retained (%)
SiO ₂	3625.37	241864	554544	276000	50
Al ₂ O ₃	720.85	54476	124901	54300	43
Fe _x O _y	663.12	66217	151823	161000	106
CaO	605.69	61867	141848	96400	68
MgO	177.78	15314	35113	20100	57
Na ₂ O	143.53	15214	34883	5150	15
K ₂ O	170.08	20167	46238	24900	54
TiO ₂	545.37	46668	107000	107000	100
ZrO ₂	258.20	27295	62583	53900	86
Pb	10.00	1429	3275	262	8
Cd	10.00	1429	3275	463	14
Zn	10.00	1429	3275	1320	40
Cr	10.00	1429	3275	1550	47
CeO ₂	10.00	1163	2666	1220	46
Sm ₂ O ₃	10.00	1231	2823	1210	43
Gd ₂ O ₃	10.00	1224	2843	1190	42
Nd ₂ O ₃	10.00	1166	2807	1250	45
Cs ₂ CO ₃	10.00	1171	2673	1210	45

Table 6.7 HVPM03 Slag Materials Characterization.

HVPM03					
	Final composition (grams)	Metals basis (ppm)	Correct with titanium (ppm)	Slag metals analysis (ppm)	Amount retained (%)
SiO ₂	3625.37	241864	689294	261000	38
Al ₂ O ₃	720.85	54476	155251	56900	37
Fe _x O _y	663.12	66217	188714	116000	61
CaO	605.69	61867	176316	90600	51
MgO	177.78	15314	43645	21500	49
Na ₂ O	143.53	15214	43359	2500	6
K ₂ O	170.08	20167	57473	21400	37
TiO ₂	545.37	46668	133000	133000	100
ZrO ₂	258.20	27295	77790	69700	90
Pb	10.00	1429	4071	549	13
Cd	10.00	1429	4071	463	11
Zn	10.00	1429	4071	940	23
Cr	10.00	1429	4071	1800	44
CeO ₂	10.00	1163	3314	1600	48
Sm ₂ O ₃	10.00	1231	3509	1460	42
Gd ₂ O ₃	10.00	1224	3534	1550	44
Nd ₂ O ₃	10.00	1166	3489	1450	42
Cs ₂ CO ₃	10.00	1171	3322	1210	36

Table 6.8 HVPM05 slag materials characterization.

HVPM05					
	Final composition (grams)	Metals basis (ppm)	Correct with titanium (ppm)	Slag metals analysis (ppm)	Amount retained (%)
SiO ₂	5113.91	215736	670060	262000	39
Al ₂ O ₃	1018.6	48674	151177	52900	35
Fe _x O _y	1232.27	77810	241672	97600	40
CaO	888.81	57407	178303	70800	40
MgO	279.93	15248	47360	19200	41
Na ₂ O	760.26	50959	158274	22700	14
K ₂ O	507.64	38062	118216	26400	22
TiO ₂	678.32	36704	114000	114000	100
ZrO ₂	320.30	21411	66502	60000	90
Pb	30.00	2710	8417	524	6
Cd	30.00	2710	8417	210	2
Zn	30.00	2710	8417	1420	17
Cr	30.00	2710	8417	3130	37
CeO ₂	30.00	2206	6852	2960	43
Sm ₂ O ₃	30.00	2336	7256	2700	37
Gd ₂ O ₃	30.00	2352	7306	2880	39
Nd ₂ O ₃	30.00	2322	7213	2880	40
Cs ₂ CO ₃	30.00	2211	6868	2310	34

Table 6.9 HVPM06-01 Slag Materials Characterization.

HVPM06-01					
	Final composition (grams)	Metals basis (ppm)	Correct with titanium (ppm)	Slag metals analysis (ppm)	Amount retained (%)
SiO ₂	7184.92	215501	700775	280000	40
Al ₂ O ₃	1432.76	48679	158296	50100	32
Fe _x O _y	2024.13	90871	295499	127000	43
CaO	1282.71	58904	191547	70500	37
MgO	422.06	16346	53153	18000	34
Na ₂ O	890.21	45401	137955	45000	33
K ₂ O	613.22	32689	106300	41600	39
TiO ₂	863.30	33212	108000	108000	100
ZrO ₂	406.70	19329	62856	58500	93
Pb	50.00	3211	10443	587	6
Cd	50.00	3211	10443	125	1
Zn	50.00	3211	10443	1620	16
Cr	50.00	3211	10443	4030	39
CeO ₂	50.00	2614	8500	2840	33
Sm ₂ O ₃	50.00	2768	9002	3390	38
Gd ₂ O ₃	50.00	2787	9064	3610	40
Nd ₂ O ₃	50.00	2752	8949	3540	40
Cs ₂ CO ₃	50.00	2620	8521	2840	33

Table 6.10 HVPM06-02 Slag Materials Characterization.

HVPM06-02					
	Final composition (grams)	Metals basis (ppm)	Correct with titanium (ppm)	Slag metals analysis (ppm)	Amount retained (%)
SiO ₂	7184.92	215501	687798	192000	32
Al ₂ O ₃	1432.76	48679	155364	49800	36
Fe _x O _y	2024.13	90871	290026	199000	78
CaO	1282.71	58904	187999	72500	44
MgO	422.06	16346	52169	20000	44
Na ₂ O	890.21	45401	135400	21000	18
K ₂ O	613.22	32689	104332	30300	33
TiO ₂	863.30	33212	106001	106000	100
ZrO ₂	406.70	19329	61692	54200	88
Pb	50.00	3211	10249	589	6
Cd	50.00	3211	10249	147	1
Zn	50.00	3211	10249	1320	13
Cr	50.00	3211	10249	3310	32
CeO ₂	50.00	2614	8343	2860	34
Sm ₂ O ₃	50.00	2768	3534	2660	75
Gd ₂ O ₃	50.00	2787	8896	2800	31
Nd ₂ O ₃	50.00	2752	8784	2820	32
Cs ₂ CO ₃	50.00	2620	8363	2230	27

6.5 Cold Cap Tests: Analysis and Results

6.5.1 Slag Characterization

Tables 6.11 through 6.14 show the slag analysis results for the cold cap tests. The same normalization technique described above was again used except in this case Zr was used for the normalization rather than Ti. If Ti were to be used, it would result in a greater than 100% amount retained for Zr, with the exception of CC03.

In general the results are very similar to the HVPM experiments. Once again the amount retained percentages for most elements are far lower than expected using the Ti-corrected values, and therefore direct comparison of analytic values to the calculated (metals basis) values will be used to make some general conclusions. In all the cold cap experiments, the majority of Pb and Cd tended to volatilize. Zinc was also heavily volatilized but less so than for Pb and Cd. Again, Na was heavily volatilized for each of the cold cap experiments. Chromium tended to remain in the melt as did the surrogates, Ce and Sm.

Direct comparison of the open melt (HVPM) data and the cold cap (CC) data show a slight decrease in the amount of Pb and Cd volatilization. This can be seen most easily by comparing the analytical results directly. The concentrations of Pb and Cd in the slag are just slightly higher overall in the cold cap experiments. This is true also for Zn and Cr. For these tests, there is no discernable effect of the cold cap on surrogate element retention in the slag.

Table 6.11 Cold-cap CC01 slag materials characterization.

CC01					
	Final composition (grams)	Metals basis (ppm)	Correct with zirconium (ppm)	Slag metals analysis (ppm)	Amount retained (%)
SiO ₂	6512.26	224147	676207	231000	34
Al ₂ O ₃	1298.23	50616	152700	54400	36
Fe _x O _y	1766.93	91029	274617	186000	68
CaO	1154.77	60854	183583	71400	39
MgO	375.90	16706	50399	17900	36
Na ₂ O	324.67	17755	53565	2500	5
K ₂ O	317.26	19408	58550	21500	37
TiO ₂	803.22	35461	106978	103000	96
ZrO ₂	378.64	20651	62300	62300	100
Pb	70.68	5209	15715	1940	12
Cd	70.68	5209	15715	805	5
Zn	70.68	5209	15715	3240	21
Cr	70.68	5209	15715	5790	37
CeO ₂	70.68	4240	12792	3960	31
Sm ₂ O ₃	70.68	4490	13547	3700	27
Gd ₂ O ₃	70.68	4522	13641	3840	28
Nd ₂ O ₃	70.68	4464	13468	4020	30
Cs ₂ CO ₃	70.68	4251	12824	4030	31

Table 6.12 Cold-cap CC02 slag materials characterization.

CC02					
	Final Composition (grams)	Metals basis (ppm)	Correct with zirconium (ppm)	Slag metals analysis (ppm)	Amount retained (%)
SiO ₂	4583.39	232758	613083	225000	37
Al ₂ O ₃	912.45	52489	138255	58100	42
Fe _x O _y	1029.42	78248	206103	169000	82
CaO	787.90	61260	161359	71300	44
MgO	243.53	15969	42062	20600	49
Na ₂ O	203.64	16431	43280	2500	6
K ₂ O	218.92	19759	52045	20700	40
TiO ₂	630.94	41098	108251	103000	95
ZrO ₂	298.17	23994	63199	62300	100
Pb	31.96	3475	9154	1100	12
Cd	31.96	3475	9154	482	5
Zn	31.96	3475	9154	2440	27
Cr	31.96	3475	9154	2090	23
CeO ₂	31.96	2829	7452	1840	25
Sm ₂ O ₃	31.96	2996	7891	1640	21
Gd ₂ O ₃	31.96	3017	7946	1740	22
Nd ₂ O ₃	31.96	2978	7845	1720	22
Cs ₂ CO ₃	31.96	2836	7470	1760	24

Table 6.13 Cold-cap CC03 slag materials characterization.

CC03					
	Final composition (grams)	Metals basis (ppm)	Correct with zirconium (ppm)	Slag metals analysis (ppm)	Amount retained (%)
SiO ₂	5563.27	222359	505554	230000	45
Al ₂ O ₃	1108.43	50185	114100	58300	51
Fe _x O _y	1404.08	84000	190981	152000	80
CaO	974.27	59620	135552	81700	60
MgO	310.77	16039	36465	23500	64
Na ₂ O	265.13	16837	38281	2780	7
K ₂ O	268.88	19101	43427	20600	47
TiO ₂	778.99	39936	90799	108000	119
ZrO ₂	498.62	31580	71800	71800	100
Pb	56.84	4865	11061	1130	10
Cd	56.84	4865	11061	125	1
Zn	56.84	4865	11061	1440	13
Cr	56.84	4865	11061	4800	43
CeO ₂	56.84	3960	9003	4100	46
Sm ₂ O ₃	56.84	4193	9534	3780	40
Gd ₂ O ₃	56.84	4223	9601	3990	42
Nd ₂ O ₃	56.84	4169	9479	3930	41
Cs ₂ CO ₃	56.84	3970	9025	3830	42

Table 6.14 Cold-cap CC05 slag materials characterization.

CC05					
	Final composition (grams)	Metals basis (ppm)	Correct with zirconium (ppm)	Slag metals analysis (ppm)	Amount retained (%)
SiO ₂	4872.83	222359	574481	255000	44
Al ₂ O ₃	970.34	50185	129586	58800	45
Fe _x O _y	1140.09	84000	201184	220000	109
CaO	842.95	59620	152155	78200	51
MgO	263.39	16039	40095	21100	53
Na ₂ O	221.80	16837	41547	2500	6
K ₂ O	233.68	19101	48964	16300	33
TiO ₂	699.71	39936	105809	91000	83
ZrO ₂	423.41	31580	79099	79100	100
Pb	40.31	4865	10176	2170	21
Cd	40.31	4865	10176	464	5
Zn	40.31	4865	10176	5400	53
Cr	40.31	4865	10176	6340	62
CeO ₂	40.31	3960	8284	5240	63
Sm ₂ O ₃	40.31	4193	8772	5080	58
Gd ₂ O ₃	40.31	4223	8833	5440	62
Nd ₂ O ₃	40.31	4169	8721	5400	62
Cs ₂ CO ₃	40.31	3970	8304	5510	66

6.6 Exhaust Particulate Composition

Table 6.15 presents the chemical analysis results obtained for a combination of material collected on the filter and trapped in the liquid in the bubblers for HVPM runs. The volatile heavy metals, cadmium, lead, and zinc were found in the highest concentration. The amount of each metal for a particular run varied, but all were significantly higher in concentration than the next highest metal which was cesium. As indicated by the analyses, rare earth elements were also found in the particulate samples, but their concentration was significantly less than cadmium, cesium, lead, and zinc.

Particulate analyses for the cold cap runs are given in Table 6.16. With the exception of the CC01 run, the particulate obtained from the cold cap runs has slightly less cesium, lead, and zinc relative to that found for the HVPM runs.

The high levels of lead, cadmium and zinc in the exhaust particulates indicate that significant volatilization of these elements has taken place. The competing process for carryover of material, which is entrainment of feed material, would contribute much less of these elements, consistent with the amounts in the feed (less than 1 wt%). The significant levels of these HVPM's, 27 wt% in the case of Cd for CC01, can only be the result of volatilization.

Table 6.15 FY-93 HVPM experiments - particulate elemental analysis.

Metal	HVPM02 (ppm)	HVPM03 (ppm)	HVPM05 (ppm)	HVPM06-1 (ppm)	HVPM06-2 (ppm)
Cd	94700	44900	66600	20600	19100
Cr	326	226	862	1230	888
Pb	136000	47300	71300	16200	2550
Zn	99100	58100	57400	33800	3200
Cs	16400	7390	12400	9900	1200
Ce	623	569	424	141	50
Gd	1010	1070	549	185	50
Nd	924	1220	558	179	50
Sm	698	756	512	177	5

Table 6.16 FY-93 cold cap experiments - particulate elemental analysis.

Metal	CC01 (ppm)	CC02 (ppm)	CC03 (ppm)	CC05 (ppm)
Cd	270000	81600	111000	158000
Cr	114	50	50	50
Pb	223000	11700	56400	14100
Zn	133000	10700	21000	17600
Cs	11300	489	1650	6550
Ce	288	318	103	592
Gd	4550	1040	1010	9440
Nd	4360	728	1110	11400
Sm	4210	919	863	9130

6.7 Volatilization Rates

Data gathered during the exhaust gas sampling included the total off-gas, sample volume and temperature, ambient temperature, barometric pressure, differential pressure drop across the sample train, sampling time, etc. With this data the amount of volatilization for the HVPMS and surrogates, averaged over the sample time, can be calculated once the sampling train solutions have been analyzed. Calculations were done on a spread sheet, and Appendix D contains a printout. The results are in units of lb/hr and kg/hr, and they have been converted to units of mg/hr in Tables 6.17 through 6.20 below.

Volatilization rates listed in the tables are specific only to the INEL arc melter, since the geometry and temperature profiles within the melter will influence volatilization. Primary factors affecting the volatilization rate are the amount of slag in the melter, slag surface area, concentration of the volatile material in the slag, and slag temperature. Actual volatilization rates may actually be much higher since volatilized material condenses on the walls of the melt chamber and exhaust lines and this material will not be captured downstream by the sampling train. Condensed particulates and entrained particulates on which volatilized metals have condensed also collect on surfaces inside the melter. This further reduces the total load of volatilized material reaching the sampler, which would in turn cause an underestimation of the actual volatilization rate.

Examination of the data in the tables reveals in general the expected correlation between temperature and volatilization, i.e., the higher the temperature the higher the rate of volatilization, although there are exceptions. Lack of a strict correlation between temperature and volatilization rates may be related to the uncertainty in temperature and to unknown HVPM and surrogate concentrations in the slag at the specific time the sampling was done. The averaged temperatures consist of only two or three individual measurements. In the experiments where only one temperature measurement was made, the associated uncertainty in that temperature must be assumed to be quite large.

There appears to be no definite correlation for reduction of volatilization in the cold cap melts vs. the open melts. In fact the volatilization rate for specific elements is higher in many cases for the cold cap melts. This may be related to how the feed material is distributed in the melt. In the open melt case, the waste feed material (IEB4/A-40 plus HVPMS and surrogates) was slowly introduced into the melter allowing the feed to quickly melt into the slag and become well distributed. In the cold cap case, the waste feed is quickly fed in to cover the surface of the melt. The cold cap melts from underneath, and this may cause higher concentrations of HVPMS and surrogates near the melt surface resulting in higher volatilization rates, even in the presence of the cold cap. If true, this would argue for

a thicker cold cap in order for it be effective.

A further complication in the interpretation of the results is caused by entrainment of particulate as material is fed into the melt. Thus the total carryover load is a combination of volatilized and entrained material. Some of the data follow the expected trend for volatilization such as cesium and chromium. The data for cesium for the open and cold cap melts are shown below in Figure 6.3. The trend of the data clearly shows the expected volatilization rate vs. temperature relationship and also a reduction in the volatilization rate for the cold cap data. The data for chromium are very similar showing a marked reduction in volatility for the cold cap case. Only data with averaged temperatures have been plotted since the uncertainty in the single temperature measurements is too great for the data to be of any value. The data for cadmium in Figure 6.4 show the opposite trends than that for cesium. Correlation with higher volatilization rates to higher temperatures is weak, and the volatilization rates for the cold cap melt are higher. Figures 6.5 and 6.6 show data for cerium and samarium. The cerium data show no difference between open melt and cold cap conditions. Below 1800°C, the plot shows no temperature dependence for the volatilization rates. Volatilization rates for samarium shown in Figure 6.6 are higher for the cold cap case than for the open melt case. Results for gadolinium and neodymium are similar.

The results for the surrogates seem to indicate that entrainment is the primary mode of transport for them. As material is dropped into the melter chamber, fine particulate becomes airborne and can be carried away in the off-gas stream. The argument that the transport rates for the surrogates are mostly due to entrainment rather than volatilization is easy to make. First of all, the transport rates are very small. Since these elements are less than 1 wt% of the feed makeup, a substantial amount of entrainment would have to occur for them to be higher. The entrainment mechanism is completely independent of melt temperature, and this fact is indicated by the data for the surrogates. Entrainment may be affected by feed, however, with higher feed rates producing more entrainment. The data for the surrogates would seem to support this idea since most of the time the rates are slightly higher in the cold-cap cases where the feed rates were higher.

Table 6.17 Volatilization rates for the HVPMs in open melt conditions.

Experiment name/date	Average slag temp (C)	Cd [mg/hr]	Cs [mg/hr]	Cr [mg/hr]	Pb [mg/hr]	Zn [mg/hr]
HVPM02 06/23/93	(1650)*	474	82	1.63	680	496
HVPM03 06/24/93	(1900)*	396	65	1.99	417	513
HVPM05 07/01/93	1570	333	62	4.31	357	287
HVPM06 07/02/93	1730	281	135	16.8	221	461
HVPM06 07/02/93	1440	318	20	14.8	43	53

Table 6.18 Volatilization rates for the surrogates in open melt conditions.

Experiment name/date	Average slag temp [C]	Ce [mg/hr]	Gd [mg/hr]	Nd [mg/hr]	Sm [mg/hr]
HVPM02 06/23/93	(1650)*	3.12	5.05	4.62	3.49
HVPM03 06/24/93	(1900)*	5.02	9.44	10.8	6.67
HVPM05 07/01/93	1570	2.02	2.75	2.79	2.56
HVPM06 07/02/93	1730	1.92	2.52	2.44	2.41
HVPM06 07/02/93	1440	0.833	0.833	0.833	0.833

* - single measurement

Table 6.19 Volatilization rates for the HVPM's under cold cap conditions.

Experiment name/date	Average slag temp [C]	Cd [mg/hr]	Cs [mg/hr]	Cr [mg/hr]	Pb [mg/hr]	Zn [mg/hr]
CC01 07/09/93	(2300)*	2700	113	1.14	2230	1330
CC02 07/13/93	1340	556	3.33	0.34	7.98	73
CC03 07/14/93	1870	1390	20.6	0.63	705	263
CC05 07/16/93	2000	1130	46.8	0.357	101	126

Table 6.20 Volatilization rates for the surrogates under cold cap conditions.

Experiment Name/ Date	Average Slag Temp [C]	Ce [mg/hr]	Gd [mg/hr]	Nd [mg/hr]	Sm [mg/hr]
CC01 07/09/93	(2300)*	2.88	45.5	43.6	42.1
CC02 07/13/93	1340	2.17	7.09	4.96	6.27
CC03 07/14/93	1870	1.29	12.6	13.9	10.8
CC05 07/16/93	2000	4.23	67.4	81.4	65.2

* - single measurement

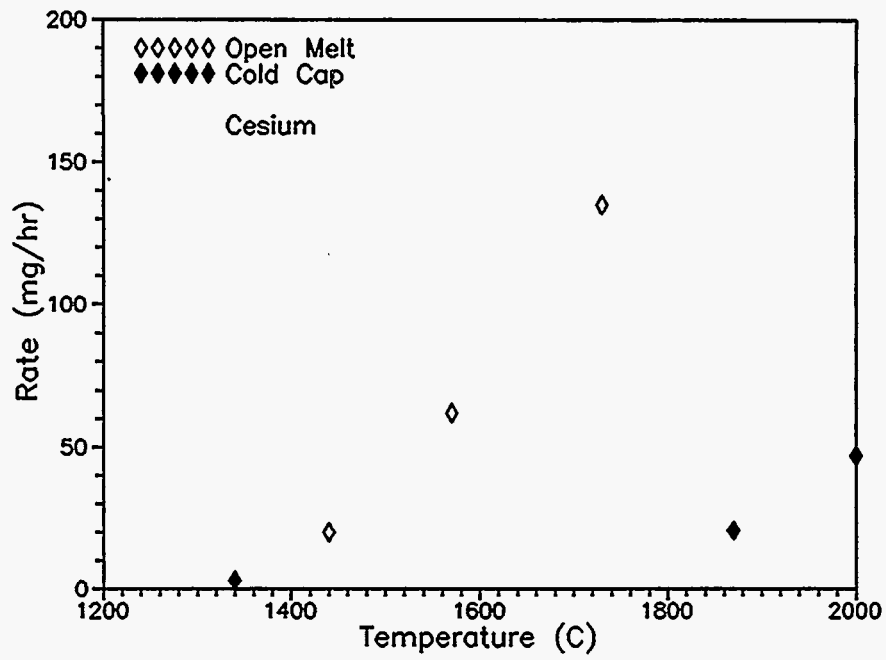


Figure 6.3 Open melt vs. cold cap cesium volatilization rates.

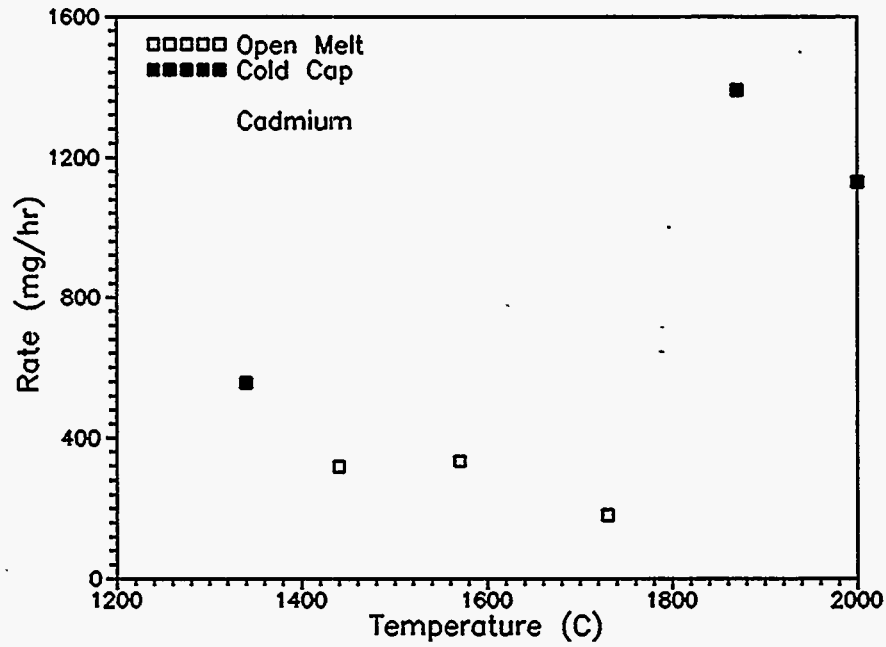


Figure 6.4 Open melt vs. cold cap cadmium volatilization rates.

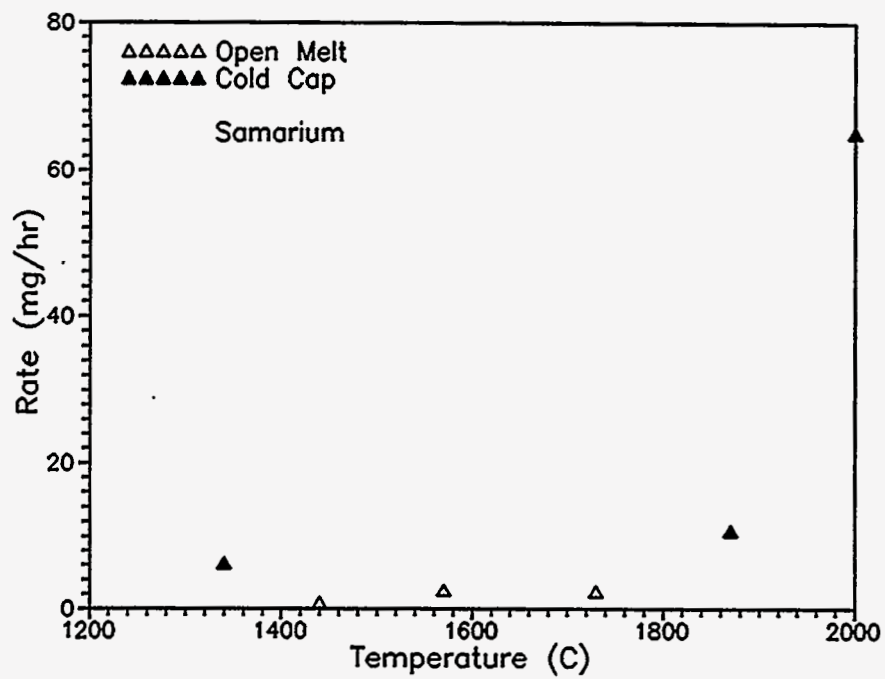


Figure 6.5 Open melt vs. cold cap cerium volatilization rates.

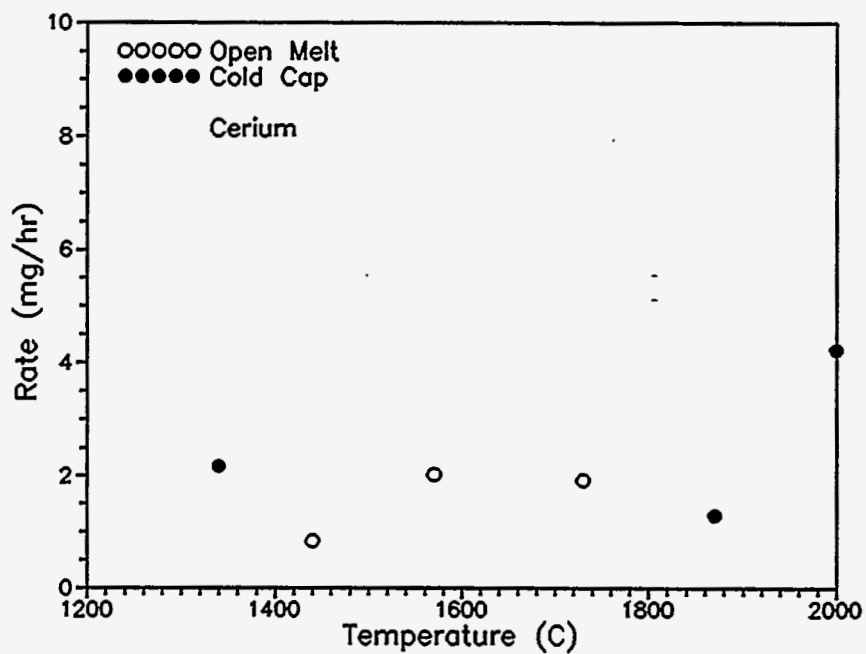


Figure 6.6 Open melt vs. cold cap samarium volatilization rates.

7. REDOX MEASUREMENTS (FY-93)

7.1 Introduction

The redox experiments tested the extremes in reducing or oxidizing conditions and their effect on melt chemistry and crystallization. Two melts had different levels of carbon blended into the melt mix to achieve two reducing conditions. Alternately, two additional melts were subjected to two levels of oxidation by injecting air under the melt surface with a lance. In the reducing cases, the first melt mix contained sufficient carbon to reduce half of the iron oxides to Fe, while the second melt contained twice as much carbon to convert all of the iron oxides to Fe. In the oxidizing experiments, which employed an air lance, sufficient air was injected into one melt to oxidize half of the iron (assuming FeO) to Fe_2O_3 , while twice as much air was introduced into the next melt to convert all of the FeO to Fe_2O_3 . The general operating conditions of each of the redox tests are summarized in Table 7.1.

In order to determine the effects of varying redox conditions on the distribution of high vapor pressure metals (Cd, Cr, Pb, and Zn), 1.0 wt% (metals basis) of each of these elements was added to the mix as oxides. So that zirconolite crystals would form, 4.0 wt% TiO_2 and 2 wt% ZrO_2 were added to the mix. The CaO already present (10 wt% for A-40) was considered sufficient to enable zirconolite formation. Also, 1.0 wt% each of CeO_2 and Sm_2O_3 was added as surrogates for actinide elements so that the zirconolite, if formed, could demonstrate its ability to remove these surrogates from the glass phase and incorporate them into its structure. In addition, 1.0 wt% of Cs_2CO_3 was added to each of the melts, and in the case of the oxidizing melts only, 1.0 wt% each of Nd_2O_3 and Gd_2O_3 was added as actinide surrogates also.

An air lance was designed and fabricated to provide submerged air/oxygen injection into the slag. The air lance was constructed from three concentric stainless steel tubes. As shown in Figure 7.1, the inner and outer tubes were welded to a copper end piece, while the intermediate tube provides a flow path for the cooling water. Air is supplied to the inner tube that delivers gas to the copper nozzle. The copper nozzle contains five 0.025-inch diameter holes, four being directed at 30 degrees from center and one on center as shown in the diagram. Air flow into the lance is monitored by a MKS M062-LS06E mass flow valve and a MKS 440 series mass flow controller. During operation the lance is earth grounded through the power supply for safety.

Table 7.1 Summary of FY-93 redox tests.

Test name	Date	Starting material	Run time (min)	Ave slag temp (C)	Ave power (kW)	Shutdown condition
RED01	7/22	6.0 kg IEB4/A-40 + HVPMs + surrogates	110	1470	10.9	Normal
RED02	7/27	6.0 kg IEB4/A-40 + HVPMs + surrogates	95	1570	11.5	Normal
OX01	6/23	6.0 kg IEB4/A-40 + HVPMs + surrogates	115	1615	6.6	Normal
OX02	6/24	OX01 remelt + 3.0 kg IEB4/A-40	125	1710	12.8	Normal
OX03A	6/25	6.0 kg IEB4/A-40 + HVPMs + surrogates + 3.0 kg IEB4/A-40	95	1700	13.0	Positive pressure buildup
OX03B	7/01	OX03A remelt	120	1700	13.0	Normal (anode consumed)

7.2 Experimental Conditions

The redox experiments were conducted in the modified bench-scale arc melter. The RED01 test used an addition of 75 grams of carbon to produce a half stoichiometric reduction of the iron assuming FeO ($\text{FeO} + \text{C} \rightleftharpoons \text{Fe} + \text{CO}$). The test was carried out for almost 2 hours, trying to maintain about 1500°C in the slag. The test was characterized by a long period of dust evolution. Visual observations indicated that direct combustion of the carbon powder may have been taking place. The slag from this experiment was slightly orange in color. Metal beads were found at the bottom of the slag.

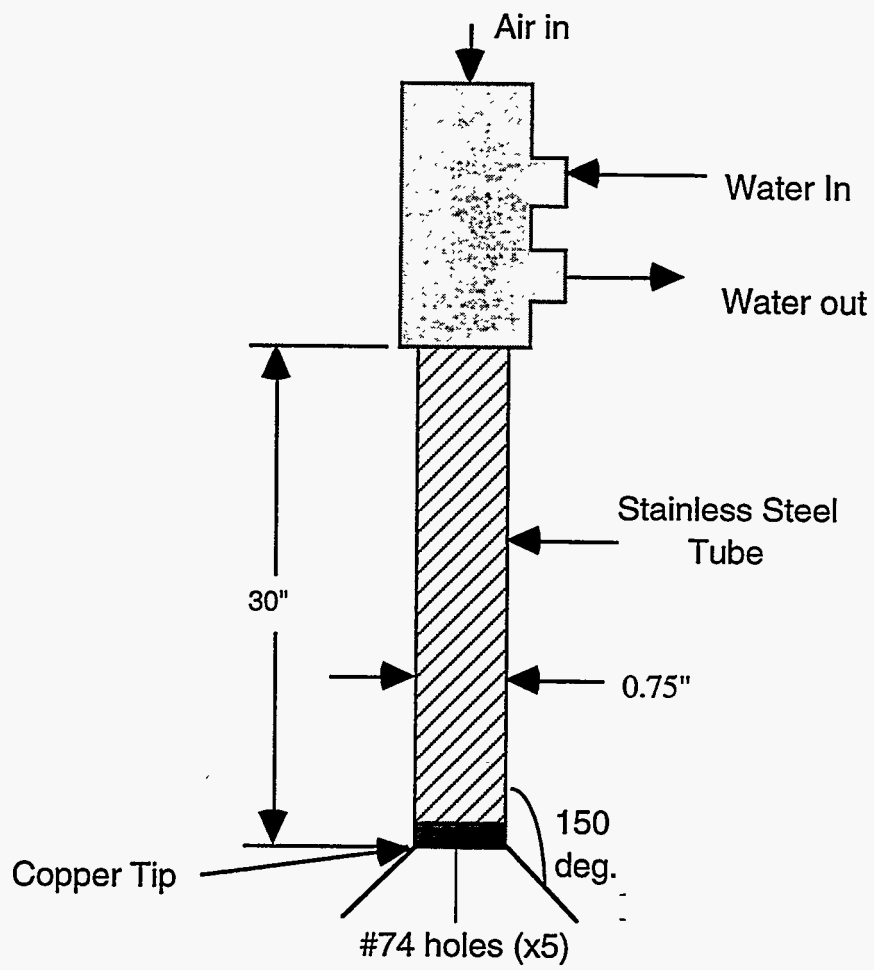


Figure 7.1 Schematic of the air/oxygen lance.

The RED02 test used an addition of 318 grams of carbon, twice the stoichiometric amount to reduce all the iron from the melt. The test was carried out for about one and one-half hours trying to maintain about 1500°C in the slag. Again, direct combustion of some of the carbon with the normal air flow through the melter appeared to be taking place. The slag from this experiment was black in color and, again, metal beads were formed in the slag at bottom of the crucible.

Forty minutes after starting the OX01 test when the mixture was completely melted, the air lance with air flow of 2.5 slpm was inserted in the molten slag. The lance was inserted for 70 minutes to provide enough oxygen to convert half the iron oxides (assuming all of it is FeO) into Fe₂O₃ ($2\text{FeO} + 1/2 \text{O}_2 \rightleftharpoons \text{Fe}_2\text{O}_3$). It was found after the run that the level of slag was too low for proper mixing of air with the slag (part of the slag froze off), and the portion of the mix directly under the lance did not melt. It was decided to run this experiment again with more material in the crucible so the lance would meet the slag directly between the electrodes.

The OX02 test started with 3.0 kg more of the IEB-4/A-40 mix added to the OX01 crucible liner. This was intended to raise the slag level so the air-lance would intercept the slag surface directly between the electrodes for maximum mixing. After 50 minutes the mix was melted and the air lance was inserted in the molten slag with air flowing through it at 5.0 slpm. The lance was inserted for 55 minutes ($2\text{FeO} + 1/2 \text{O}_2 \rightleftharpoons \text{Fe}_2\text{O}_3$ - half stoichiometry). As soon as the lance was inserted, melt began to bubble around the area of the lance insertion point. The experiment continued without incident and was shutdown by removing the air lance and turning off the power supplies. After cooling and removal from the crucible, the slag was observed to be a light brown color throughout.

The OX03A test started with 6.0 kg IEB-4/A-40 (including HVPMs and TRU/U surrogates). After 40 minutes when it was melted, an additional 3.0 kg of IEB-4/A-40 mix with HVPM and TRU/U surrogates were added using the auger feeder, raising the slag level so the air lance would intercept the slag surface directly between the electrodes for maximum mixing. After feeding and melting for another 35 minutes, the air lance was inserted in the molten slag with air flowing through it at 10.0 slpm. The lance was intended to be inserted for 55 minutes to allow for full stoichiometric oxidation of iron oxides ($2\text{FeO} + 1/2 \text{O}_2 \rightleftharpoons \text{Fe}_2\text{O}_3$). As soon as the lance was inserted, melt began to bubble around the area of the lance insertion point. After operating for another 15 minutes, the system pressure measured positive. Attempts were made to lower the pressure but failed, and the system was shut down.

The OX03B test remelted the OX03A material in the same refractory crucible liner. Because of the porous nature of the previously melted slag, a large hole quickly developed under the cathode shortly after startup, and the arc extinguished due to over voltage. The system was opened and material moved around and leveled in order to restart the run. Another graphite strip was placed under the electrode, the system sealed up and restarted without consequence. The melter was operated for another 40 minutes before the air lance was inserted in the molten slag with air flowing through it at 10 slpm. An additional 40 minutes was needed to achieve the total oxidation of 9 kgs of material based on full stoichiometry. As the lance was inserted, the melt began to boil around the insertion point. After operating for another 40 minutes, the system was shut down.

7.3 Analytical Results

7.3.1 Fe⁺²/Fe⁺³ Ratios

The Fe⁺²/Fe⁺³ ratio (or FeO/Fe₂O₃ ratio) is a convenient measure of the redox state of the melt. Influencing the Fe⁺²/Fe⁺³ ratio will affect development of several of the crystalline species during melt cooldown. For example, the transition from a Fe⁺² to Fe⁺³ dominant material may inhibit formation of augite [Ca(MgFe⁺²Al)(SiAl)₂O₆] and favor formation of pseudobrookite (Fe₂TiO₅) instead of ilmenite (FeTiO₃). One question needing resolution is whether the redox state of the melt will affect development of zirconolite (CaZrTi₂O₇), spinels (usually Fe₃O₄), or other desired phases. Zirconolite development is largely a function of the concentrations of TiO₂, ZrO₂, and CaO in the residual glass. The formation of zirconolite may be influenced indirectly by the redox state of the melt. If an oxidized melt is rich in iron, it will produce pseudobrookite early in the cooling cycle. This phase will consume TiO₂ and may deplete this oxide from the residual glass to the extent that zirconolite cannot precipitate.⁸

Slag samples from each of the redox tests were analyzed by an independent laboratory for total iron oxide content and FeO content. Total iron oxide content was determined by ICP analysis and FeO content by titration. Table 7.2 shows these results along with the calculated Fe⁺²/Fe⁺³ and Fe⁺³/Fe_{tot} ratios. For comparison, two separate IEB4/A-40 samples made for another project and produced under "normal" arc melter operating conditions are also shown. The operating state of the arc melter is slightly reducing, due to the presence of the carbon electrodes.

The Fe⁺²/Fe⁺³ ratios follow the redox conditions imposed on the melts except for the highly reducing and highly oxidizing cases. For instance, when half the carbon needed to

Table 7.2 Redox results over a range of reducing and oxidizing conditions.

Test	Operating condition	Total iron oxide (wt%)	FeO (wt%)	Fe ⁺² /Fe ⁺³ ratio	Fe ⁺² /Fe ^{tot} ratio
RED02	highly reducing	14.2	11.9	13.60	0.93
RED01	slightly reducing	12.0	10.9	infinite	1.00
PSPI03C	normal	16.9	14.5	20.49	0.95
PSPI03	normal	16.1	12.3	5.87	0.85
OX02	slightly oxidizing	17.5	8.07	1.05	0.51
OX03B	highly oxidizing	16.4	12.8	6.55	0.87

effect reduction was blended with the mix, the Fe⁺³ was eliminated from the specimen examined. Therefore, with only Fe⁺² present the Fe⁺²/Fe⁺³ ratio was infinite. The range of the Fe⁺²/Fe⁺³ ratio is infinity for complete reduction and zero for complete oxidation. In the other reducing case, when twice the needed carbon was present in the melt, not all of the Fe⁺³ was reduced in the specimen and the Fe⁺²/Fe⁺³ ratio was 13.6:1. When the air lance was inserted into the melts, the most Fe⁺³ was produced when the lesser amount of air was injected (ratio = 1.05). When enough air was injected to convert all of the Fe to Fe⁺³ the Fe⁺²/Fe⁺³ ratio increased to 6.55 rather decreasing toward zero. In both cases, the injected oxygen had to compete with reducing conditions normally present in the arc furnace.

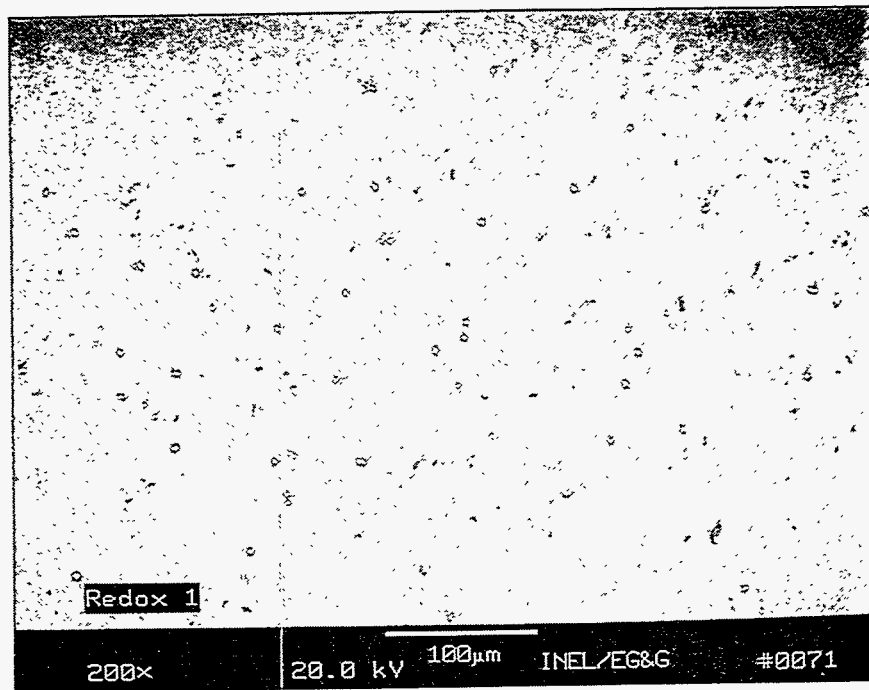
Speculation from these results is that there may have been localized effects on the redox state for these melts and that the highly reduced and oxidized samples that were analyzed were not representative of the overall redox state of the melt. Alternatively, in the case of the highly oxidizing melt, it may be argued that the increased air flow rate may have caused localized cooling to occur in the injection region and that higher flow velocities might reduce the residence time of the air in the slag. If so, the outcome would be to decrease the effective oxidation rate. After removal from the furnace, the fracture surfaces of both slags subjected to air lancing exhibited a brownish color characteristic of an elevated Fe₂O₃ content. Results for the highly reducing melt remain somewhat of a mystery, except for the possibility stated above, that the redox state was not homogenous throughout the melt and caused a sampling error.

7.3.2 SEM/EDXS Analysis of Slag

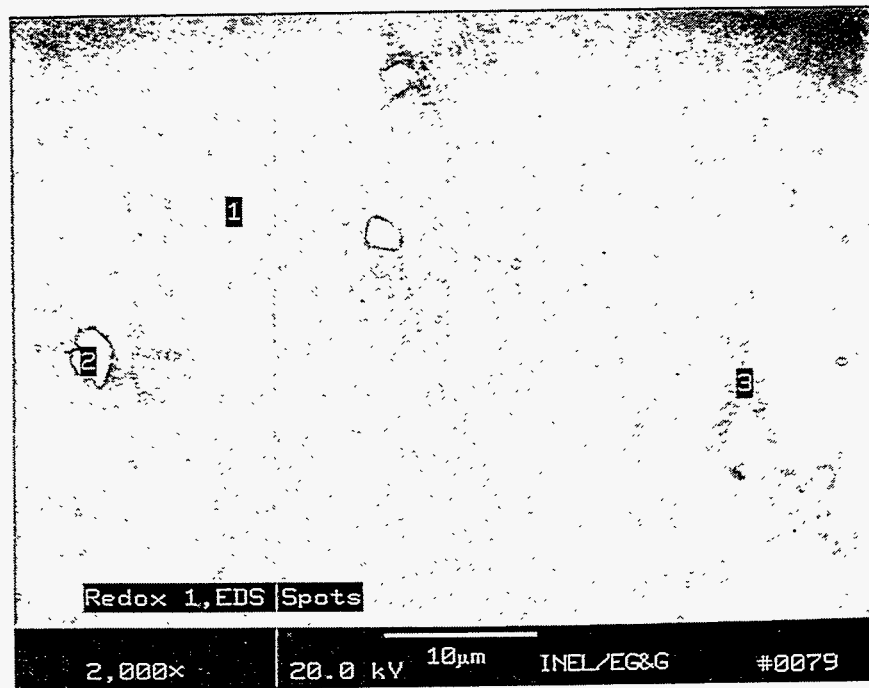
Examination of slag specimens by SEM, EDXS, and XRD indicated that the cooldown of the melts was too rapid to enable significant crystal growth to occur. Samples melted under reducing conditions were almost entirely glass, with a few feathery crystals of chromite spinel and numerous small beads of metallic iron present. These features may be observed in Figures 7.2 and 7.3. The corresponding chemistry data for the EDXS spots are contained in Tables 7.3 and 7.4. The elemental analysis by the EDXS has been converted to oxide forms based on the amount of oxygen detected, except where noted, as in column 2. In cases where the oxygen content cannot account for oxide forms (in these cases, only 1 or 2 wt%), the major components are assumed to be metallic. The conversions are done by software on the SEM/EDXS computer.

The beads of metallic iron are considerably larger in the highly reducing case. Even larger beads (up to 6 mm) settled toward the bottom of the melt and became trapped in the cooler, viscous material near the cold container liner. Spinel crystals were too small for the EDXS technique to produce a meaningful analysis. Of the additives, CdO, PbO, and ZnO were below the EDXS detection limit and were assumed to have evaporated almost entirely during melting, the Cr_2O_3 was combined with the spinels, while the Cs_2O , TiO_2 , ZrO_2 , and the surrogates remained in the glass. The CdO, PbO, and ZnO were found deposited on the furnace interior and in the cold trap, along with some of the other oxides lost as dust, or by evaporation or ejection from the melt.

The XRD patterns showed the spinels and the presence of pyroxene crystals, although pyroxenes could not be discerned in the photomicrographs. Some Fe_3C was indicated by XRD, confirming the reducing nature of the melts.



(a)



(b)

Figure 7.2 SEM micrographs for the slightly reduced slags: (a) general area and (b) associated EDXS spots.

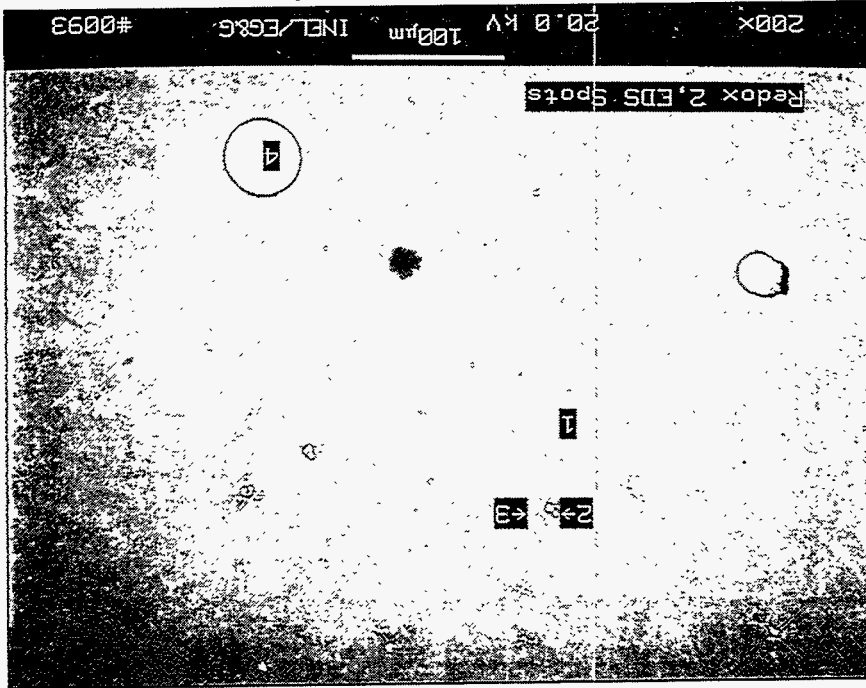
Table 7.3 EDXS analysis of designated spots in the slightly reduced slag (RED01).

	Average	1	2*	3
Na ₂ O	1.65	1.74		1.98
MgO	2.96	3.18		2.66
Al ₂ O ₃	11.33	11.49	0.81	11.11
SiO ₂	57.31	57.42	3.40	49.22
K ₂ O	1.92	1.79		2.11
CaO	6.82	7.28	0.31	2.70
TiO ₂	4.64	4.42	0.23	4.37
FeO	8.93	8.85	93.14	10.82
ZrO ₂	2.18	2.38		1.45
CeO ₂ or Ce ₂ O ₃	0.54	0.59		
Nd ₂ O ₃				
Sm ₂ O ₃	0.41	0.44		
Gd ₂ O ₃				
Cs ₂ O				
Cr ₂ O ₃	1.30	0.41	0.56	12.88
ZnO				0.74
PbO				
CdO				
Photo #	0071	0079	0079	0079

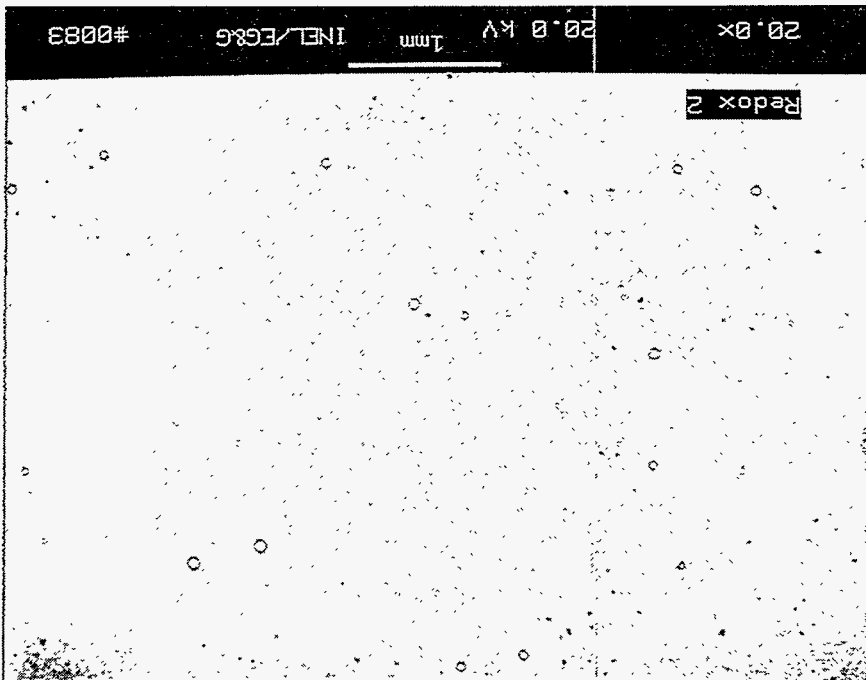
* - metallic

SEM micrographs for the highly reduced slags: (a) general area and (b) associated EDXS spots.

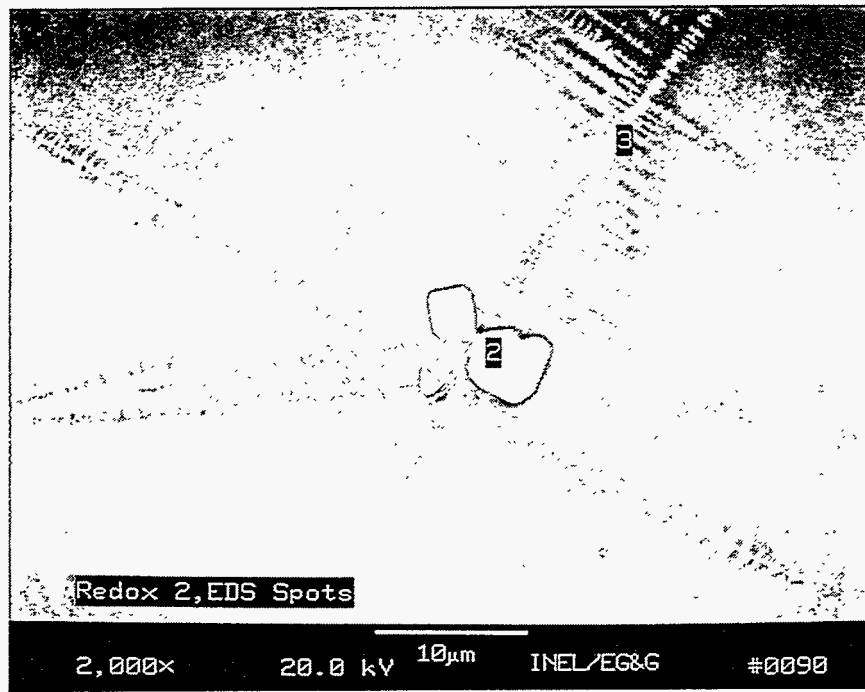
Figure 7.3



(b)



(a)



(c)

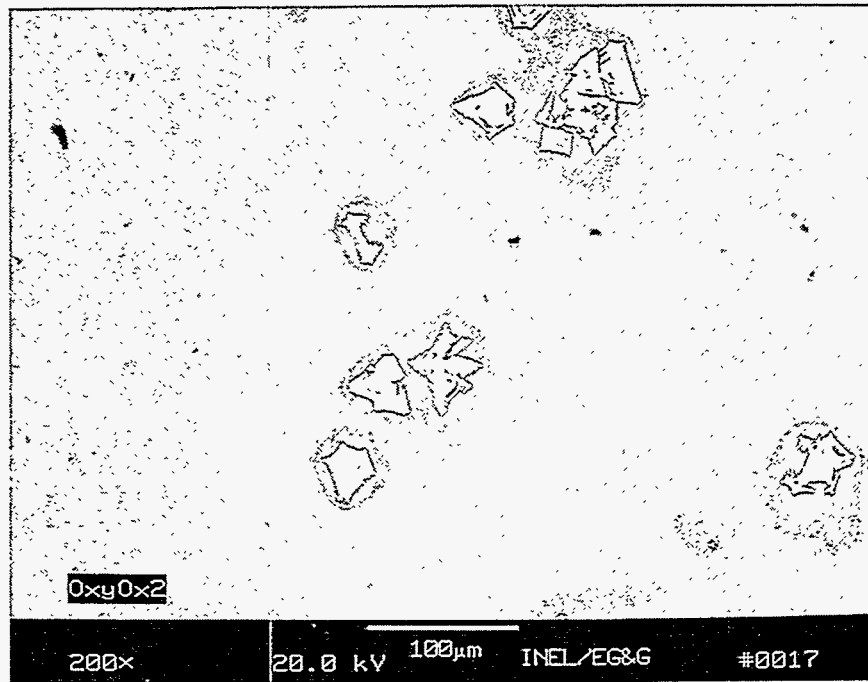
Figure 7.3 SEM micrographs for the highly reduced slags: (c) close-up of associated EDXS spots.

Table 7.4 EDXS analysis of designated spots in the highly reduced slag (RED02).

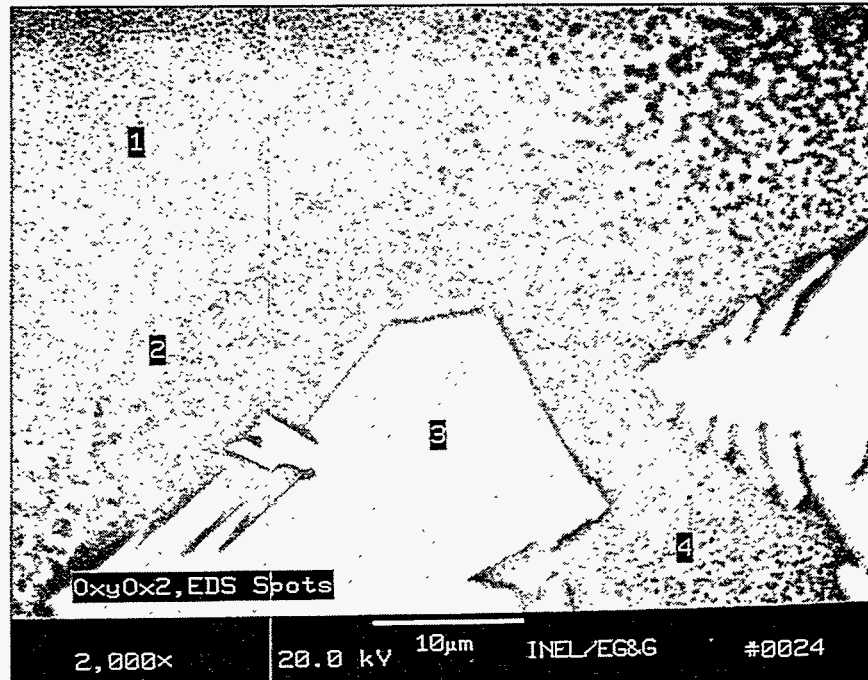
	Average	1	2*	3	4*
Na ₂ O	2.51	1.82		2.14	
MgO	2.84	3.37		2.76	
Al ₂ O ₃	10.29	10.37		9.70	
SiO ₂	54.87	55.46	0.59	44.47	0.43
K ₂ O	2.05	1.58		2.24	
CaO	7.37	8.51	0.11	1.77	
TiO ₂	5.13	4.91	0.21	5.69	
FeO	10.25	9.59	98.56	14.09	97.56
ZrO ₂	2.62	2.91		1.58	0.35
CeO ₂ or Ce ₂ O ₃	0.54	0.74			
Nd ₂ O ₃					
Sm ₂ O ₃	0.34	0.54			
Gd ₂ O ₃					
Cs ₂ O					
Cr ₂ O ₃	1.20	0.19	0.54	15.54	
ZnO					
PbO					
CdO					
Photo #	0083	0093	0090, 0093	0090, 0093	0093

* - metallic

The melts produced under oxidizing conditions appear less glassy, even though the samples were subjected to about the same cooling rate after melting was complete. The oxidized melts exhibited no metallic beads (except for some Cu that melted from the anode at the end of the heat) and considerably more crystallization. The SEM photomicrographs are shown in Figures 7.4 and 7.5, and the individual EDXS spot analyses are given in Tables 7.5 and 7.6. The spinel composition was about the same as before (chromite) and had grown much larger. Some of these spinels contained elevated levels of zinc. A substantial network of fine crystals is evident at higher magnifications which appear to be pyroxene, and this was confirmed by XRD to be augite $[\text{Ca}(\text{MgFeAl})(\text{SiAl})_2\text{O}_6]$ and/or omphacite $[\text{CaNa}(\text{MgFeAl})(\text{SiAl})_2\text{O}_6]$. The lacy network of pyroxene crystals (Figures 7.4e and 7.5b) obscures the amount of glass present. After prolonged (hours) exposure to an elevated temperature, or slower cooling, the pyroxene crystals would coalesce into a bulkier, tabular form, and it would appear that more glass was present. The feathery spinels behave in a similar manner. Growth of the pyroxene networks from individual nuclei continued until collision between adjacent growths occurs giving the appearance of grain boundaries. Lanthanides tend to become concentrated at these boundaries and precipitate, as is shown in Figures 7.4d and 7.4c. No crystals approximately conforming to the zirconolite composition could be located. Cesium was below the detection limit in the area analysis but could be found in the residual glass, and much of it was presumed to have left the melt. A large zirconia-rich area was found (Figures 7.5a and 7.5d). It was believed to result from a zircon grain from the crucible liner decomposed in the melt.

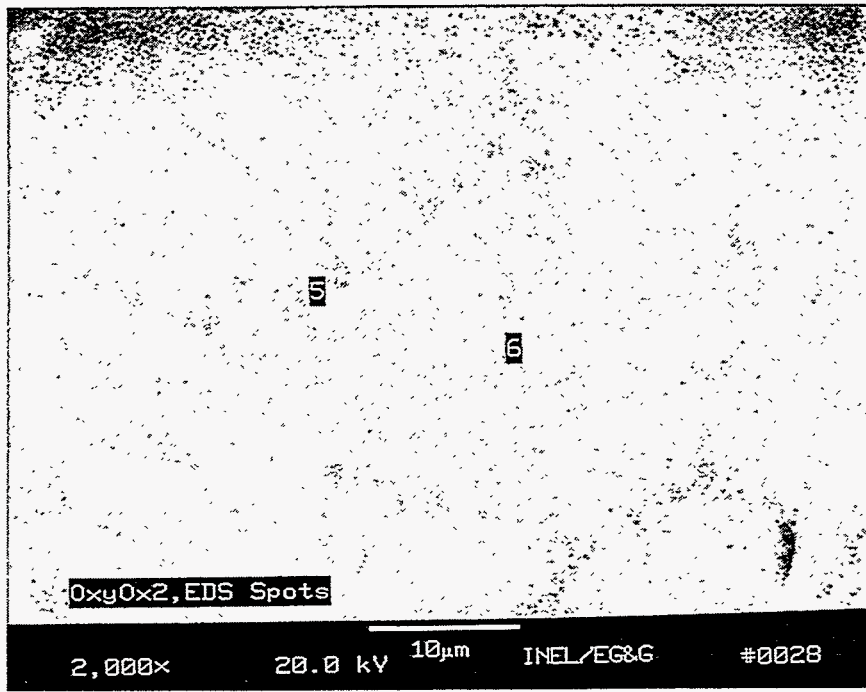


(a)



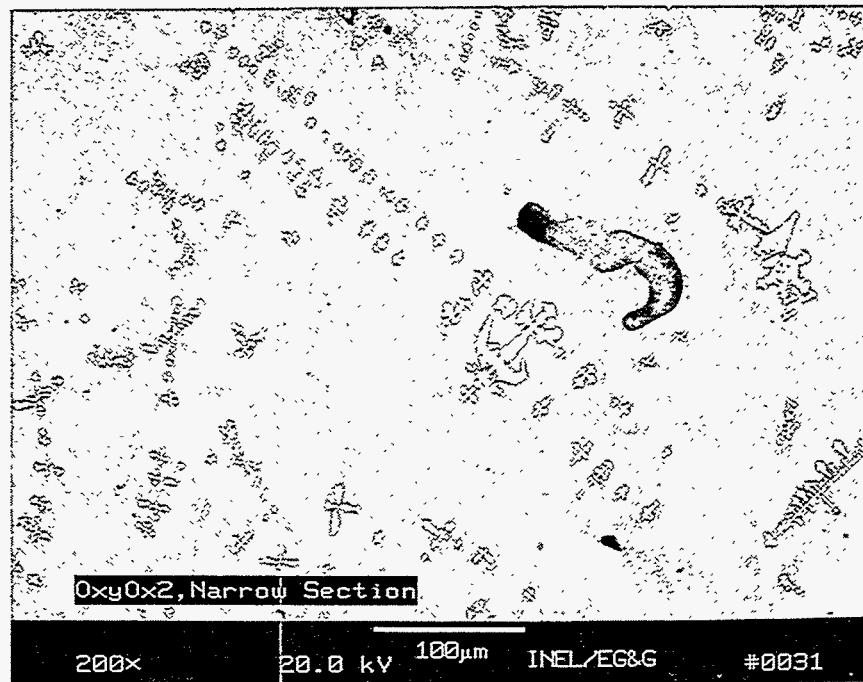
(b)

Figure 7.4 SEM micrographs for the slightly oxidized slags: (a) general area and (b) associated EDXS spots for different phases.

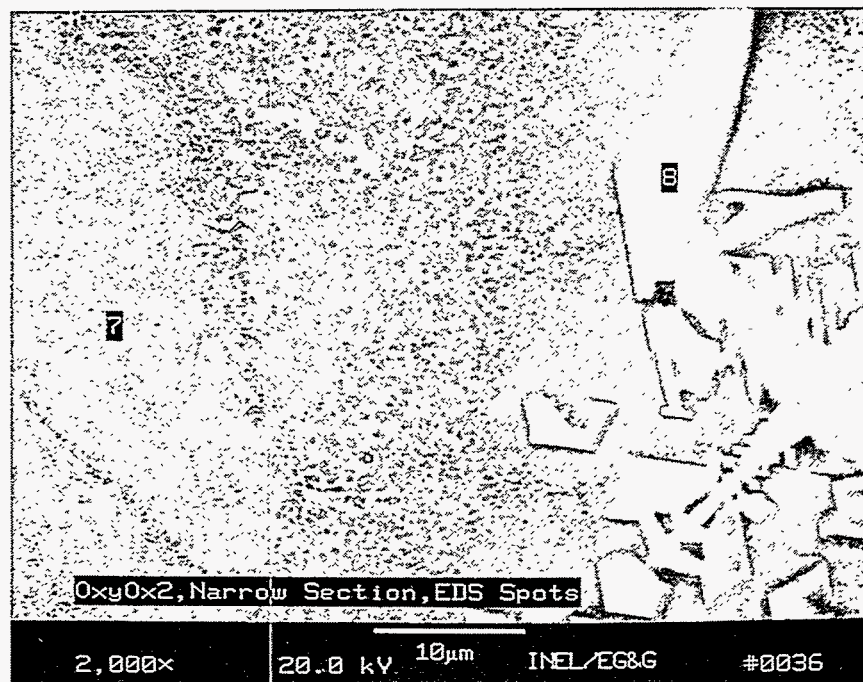


(c)

Figure 7.4 SEM micrographs for the slightly oxidized slags: (c) associated EDXS spots.



(d)



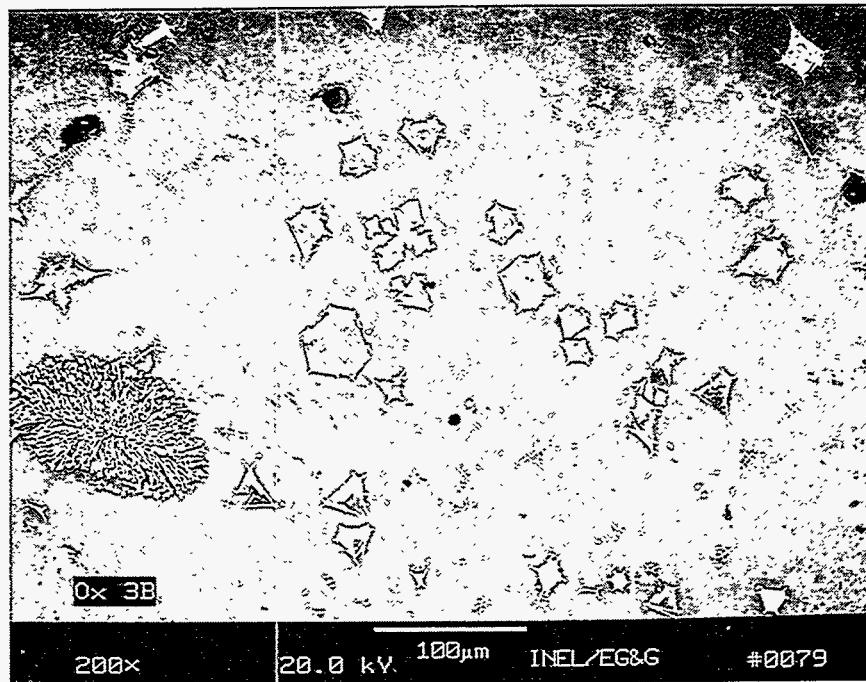
(e)

Figure 7.4 SEM micrographs for the slightly oxidized slags: (d) different general area and (e) associated EDXS spots for different phases.

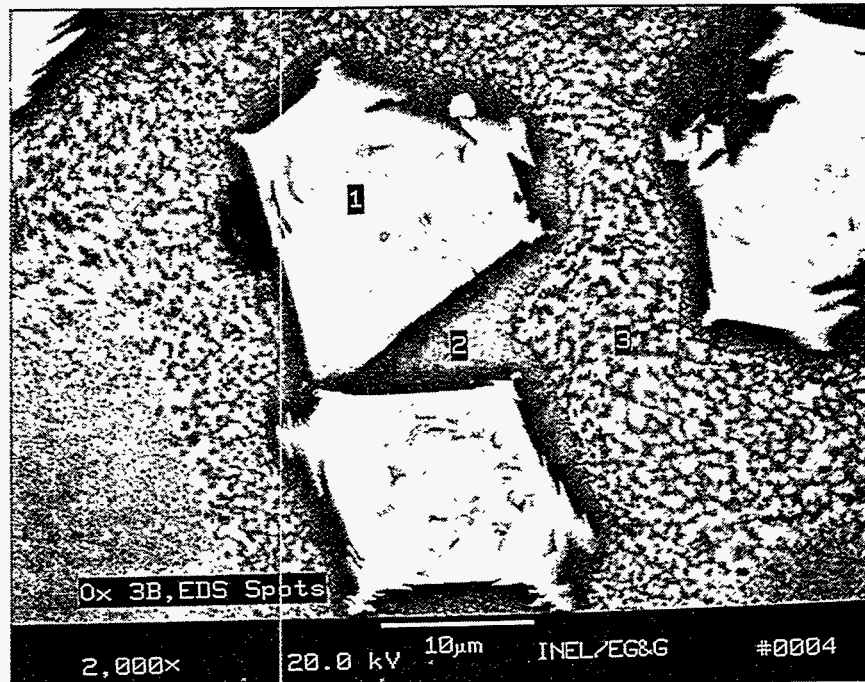
Table 7.5 EDXS analysis of designated spots for the slightly oxidized slag (OX02).

	Ave	1	2	3	4	5	6	7	8
Na ₂ O	2.28	2.08	1.42		1.64	2.11	1.96	1.77	
MgO	2.92	3.06	4.30	5.03	2.76		3.51	3.28	5.07
Al ₂ O ₃	9.96	10.07	8.34	4.87	10.83	9.71	10.08	9.84	5.89
SiO ₂	51.36	52.68	49.82	1.17	57.00	54.21	51.96	52.23	1.08
K ₂ O	1.74	1.85	1.25		2.00	1.98	1.74	1.7	
CaO	7.40	7.59	8.75		7.69	3.89	8.66	7.95	
TiO ₂	4.91	5.13	5.33	1.11	3.32	3.18	5.19	5.59	2.68
FeO	14.25	13.29	14.65	26.55	9.56	16.09	11.77	11.3	29.83
ZrO ₂	3.07	3.18	4.04		3.35	3.46	3.22	4.06	
CeO ₂	0.84	0.70	0.68		tr	1.70	0.07	0.36	
Nd ₂ O ₃			0.74	tr	0.42	1.39	0.52	0.95	
Sm ₂ O ₃	tr		0.70	tr	0.35	1.07	0.35	0.41	
Gd ₂ O ₃	tr		tr	tr	0.57	1.03	0.59	0.57	
Cs ₂ O	0.38	0.38			0.52	0.18	0.46	0.36	
Cr ₂ O ₃	0.89			60.53					54.71
ZnO				0.74					0.74
PbO									
CdO									
Photo		0017	0024	0024	0024	0024	0028	0028	0036

tr - trace

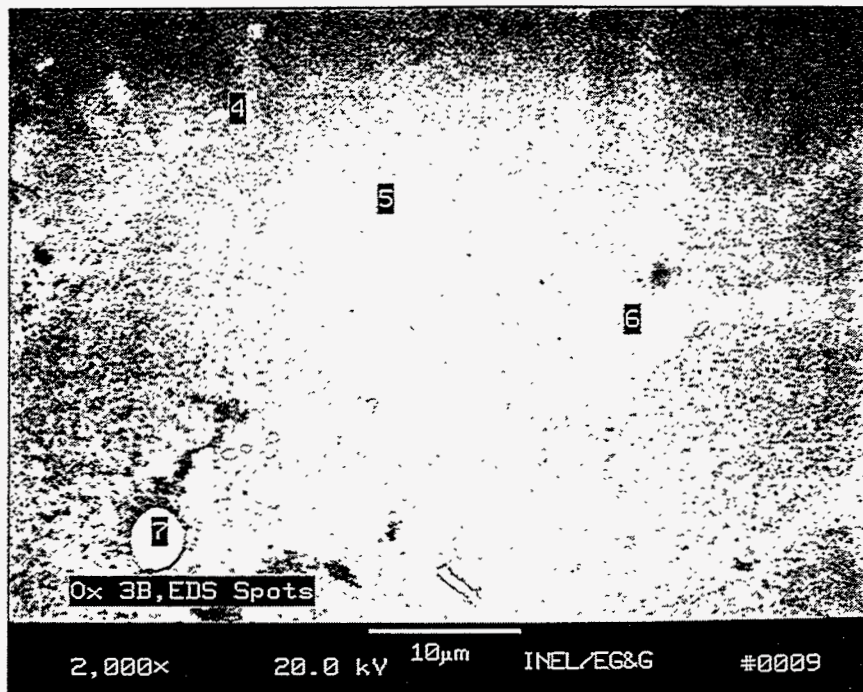


(a)

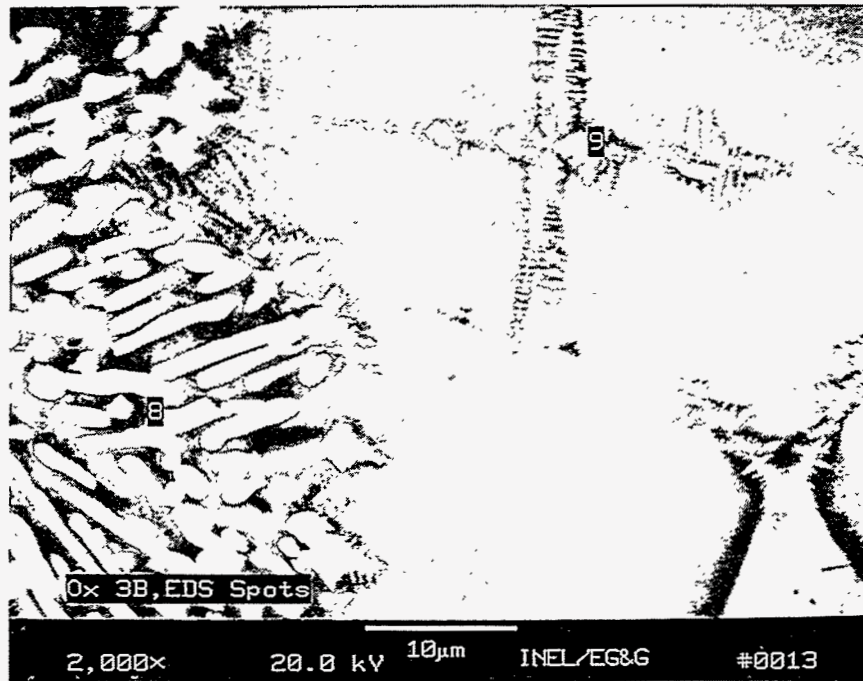


(b)

Figure 7.5 SEM micrographs for the highly oxidized slags: (a) general area and (b) associated EDXS spots for different phases.



(c)



(d)

Figure 7.5 SEM micrographs for the highly oxidized slags: (c) and (d) associated EDXS spots for different phases.

Table 7.6 EDXS analysis of designated spots in the highly oxidized slag (OX03).

	Average	1	2	3	4	5	6	7*	8	9
Na ₂ O	2.06		1.92	2.14		1.93	2.19			1.09
MgO	2.73	5.38	1.65	2.27	2.62	3.24	0.84			2.36
Al ₂ O ₃	9.03	4.02	11.6	9.88	6.47	9.38	8.84		1.04	7.66
SiO ₂	49.6	1.09	59.0	54.0	27.5	49.3	53.4	0.92	9.83	31.4
K ₂ O	1.68		2.30	2.05	0.64	1.68	1.84			1.38
CaO	8.99		6.52	7.88	3.02	10.2	7.25	0.15	0.99	1.25
TiO ₂	5.09	1.35	3.12	4.10	1.85	5.23	4.06	0.12	0.66	4.96
FeO	15.4	48.0	7.93	10.4	4.75	12.2	10.6	1.57	1.34	47.3
CuO	0.25	0.35			50.0			97.2		0.23
ZrO ₂	3.92		4.28	4.84	2.67	4.57	4.50		86.1	1.32
CeO ₂	0.57	0.70	0.27	tr	0.11	tr	2.38			
Nd ₂ O ₃	0.55			0.74	0.24	0.82	1.99			
Sm ₂ O ₃	tr			0.53	0.14	0.75	1.13			
Gd ₂ O ₃	0.17		0.34	0.53		0.44	0.98			
Cs ₂ O		0.38		0.65		0.28				0.37
Cr ₂ O ₃		37.4								
ZnO	0.25	2.52								0.69
PbO										
CdO										
Photo #	0079	0004	0004	0004	0009	0009	0009	0009	0013	0013

* - metallic

tr - trace

7.4 Discussion

The redox tests were performed as preliminary efforts to assess the ability of the laboratory arc furnace to operate under several reducing and oxidizing conditions. The furnace is small and the transients were large, yet the influence of redox conditions on microstructure was evident, even with the conditions of rapid cooling that occurred after melt termination. The reduced melts produced mostly glassy specimens, while oxidized melts developed substantially more crystalline material under similar cooling conditions. No zirconolite crystals were detected.

Table 7.7 shows overall results from the redox tests. Calculated values reflect the composition of the waste feed mix. The other columns show the general area EDX spectroscopy scans, which give the overall composition of the slags. A general comparison can be made in that the SiO_2 percentage in the slags has increased due to the absence of the HVPMs and much of the surrogate mass. This is true of other compounds such as Al_2O_3 , etc.

The disposition of the lanthanides was mixed. A significant portion of the cerium tended to remain in the glassy phases of the slag as did the samarium in the case of the reducing melts. Curiously, only trace amounts of samarium were found in the glassy matrix for the oxidizing melts, and Sm also did not appear in any crystalline phases. Neodymium and Gadolinium, which were used only in the oxidizing melts, did not appear in significant amounts in either glassy or crystalline phases, except for Nd in the glassy phase of the highly oxidized melt. Under reducing conditions, the additional surrogate, cesium, completely disappeared, while under oxidizing conditions, some of the metal remained in glassy phases of the slag.

With the exception of chromium, the HVPMs evaporated from the melt, regardless of the redox conditions. Chromium showed a strong affinity to iron in forming crystals under both reducing and oxidizing conditions, although the crystalline structures formed in reducing conditions tended to be much smaller and finer.

Table 7.7 EDX general area scan analysis for the redox tests vs. calculated waste mix composition.

	Calculated waste mix (wt%)	RED01 slag (wt%)	RED02 slag (wt%)	Calculated waste mix (wt%)	OX02 slag (wt%)	OX03B slag (wt%)
Na ₂ O	2.77	1.65	2.51	2.71	2.28	2.06
MgO	3.03	2.96	2.84	2.97	2.92	2.73
Al ₂ O ₃	8.83	11.33	10.29	8.64	9.96	9.03
SiO ₂	44.08	57.31	54.87	43.13	51.36	49.6
K ₂ O	2.25	1.92	2.05	2.20	1.74	1.68
CaO	8.40	6.82	7.37	8.22	7.40	8.99
TiO ₂	3.95	4.64	5.13	3.86	4.91	5.09
FeO	16.97	8.93	10.25	16.61	14.25	15.4
ZrO ₂	1.84	2.18	2.62	1.80	3.07	3.92
CeO ₂	0.99	0.54	0.54	0.99	0.84	0.57
Nd ₂ O ₃				0.99		0.55
Sm ₂ O ₃	0.99	0.41	0.34	0.99	tr	tr
Gd ₂ O ₃				0.99	tr	0.17
Cs ₂ O	0.99			0.99	0.38	
Cr ₂ O ₃	1.45	1.30	1.20	1.45	0.89	
ZnO	1.24			1.24		0.25
PbO	1.07			1.07		
CdO	1.14			1.14		
Photo #		0071	0083		0017	0079

8. VOLATILIZATION TESTS (FY-94)

8.1 Introduction

1

The purpose of the FY-94 HVPM tests was to determine methods to retain surrogates and HVPMs in the final waste form (IEB4/A-40). In order to analyze these methods, quantitative mass balances were needed during melter operations. An accurate mass balance was obtained by a procedure that was developed to measure all input and output materials. The arc melter system was modified to provide for complete particulate collection and thus allow accurate mass balances to be made.

8.2 Experimental Conditions

Six tests were run, using as controlled parameters: cold cap vs. non-cold cap conditions, using or not using a graphite feed tube extender, and thermally desorbing water from the simulated waste mix prior to processing in the arc melter. Table 8.1 shows the general parameters for each of the tests. The experiments began with a small amount of the IEB4/A-40 mix, usually 1.5 kg, and a carbon steel ring (about 0.4 kg) to initiate starting. Once the initial charge of material was melted, more mix was added either gradually or at faster rates in order to establish a cold cap. Average feed rates for operation are 94.7 g/min with cold cap and 54.6 g/min without cold cap. Details are given in Table 8.1. The function of the graphite feed tube extender was to limit the amount of dust and particulate generated as new material was being fed into the melt chamber. The last two tests used material that had been dried in an oven at 400°C for 2 hours then kept at above 100°C until being placed into the ceramic crucible and feeder hopper. The surrogates and HVPMs were added at this time.

All tests used IEB4/A-40 having 5 wt% each of TiO_2 and ZrO_2 and with HVPMs and surrogates in oxide form at 1 wt% each. Specific materials used were PbO (lead oxide), ZnO (zinc oxide), CdO (cadmium oxide), Cr_2O_3 (chromium oxide) as the HVPMs and Cs_2CO_3 (cesium carbonate), CeO_2 (cerium [IV] oxide), and Sm_2O_3 (samarium oxide) as surrogate radionuclides. The normal coloring of the total mix was black (due to Fe_3O_4), but for the mixes which underwent thermal desorption, the color changed to red (Fe_2O_3).

For each test about 5.0 kg of soil mixture was used. Therefore, after placing material in the crucible, as mentioned above the remaining amount would be placed in the feed hopper. The can assembly and the lid are then clamped together and cooling water flow initiated through the can assembly, electrodes, and lid. Plant air is supplied to the view port to prevent dust collection and the exhaust eductor to dilute and cool the exhaust gases.

Table 8.1 General parameters and feeding information for the FY-94 HVPM runs.

Test Name	Starting material amount (kg)	Type of run	Feed rate (g/min)	Feed duration (mins)	Amount fed (kg)
ARM082394	0.750 kg IEB4/A-40 + HVPMs + surrogates	no cold cap, no extension tube	22.6	100	2.257
ARM082694	1.500 kg IEB4/A-40 + H + S	cold cap, no extension tube	97.9	33	3.230
ARM090694	1.500 kg IEB4/A-40 + H + S	no cold cap, extension tube	56.8	52	2.950
ARM090894	1.500 kg IEB4/A-40 + H + S	cold cap, extension tube	70.3	47	3.303
ARM092094	1.500 kg IEB4/A-40 + H + S	no cold cap, extension tube, thermal desorbtion	84.6	48	4.063
ARM092294	1.683 kg IEB4/A-40 + H + S	cold cap, extension tube, thermal desorbtion	115.8	30	3.473

Typical flow rates are 1.0 slm and 50-55 slpm, respectively. All points are verified to be indicating properly, and a record file is set up. The electrodes are positioned so that they both just touch the starter ring. A video camera adapted with a pin-hole aperture is positioned over the view port, and the video equipment (camera power supply, video cassette recorder, and monitor) is energized and verified to be operating properly. As for all previous experiments, prior to arc initiation the data acquisition system is placed in the SCAN and RECORD modes. The data acquisition system is programmed to accumulate one complete data set per minute.

The power supply is then energized with the adjustment knob set at zero. An indication of voltage (~ 50 volts DC) far below open circuit voltage (~ 480 volts DC) means that a conducting path has been established between the graphite electrodes and carbon steel ring. The power is then adjusted to maintain a stable arc. The electrode arc gaps are controlled so that voltage is maintained between 50 and 250 volts DC. Typical values after initial startup are 110-200 volts DC, and 80-130 amps. This condition is maintained until the molten material covers the complete surface and then feeding commences. Cold cap vs. noncold cap conditions were accomplished by different power level adjustments and material feed rate variances. Operational data for each test are presented in Table 8.2.

Table 8.2 Data and operating conditions for the FY-94 experiments.

Test name	Date	Run time (min)	Ave temp (°C)	Ave power (°C)	Shutdown condition
ARM082394	8/23/94	109	1543	19.1	normal
ARM082694	8/26/94	64	1746	21.0	normal
ARM090694	9/06/94	75	1695	17.4	normal
ARM090894	9/08/94	64	1619	18.0	normal
ARM092094	9/20/94	89	1562	19.9	normal
ARM092294	9/22/94	56	1683	20.3	normal

Each melt started with a new filter installed and would operate until the filter loading caused a pressure drop of 5.0 inches of water, then it would be bypassed, removed, and replaced. Total off-gas loading was calculated by weighing the filter papers and determining a time averaged loading based on all the filters collected during that run. Typical amounts of time that the filter would be online ranged from 2 to 7 minutes.

8.3 Data Collection

Sample collection and classification for the FY-94 work was broken into five areas: unused feed, material recovered from the lid and head space above the melt, material recovered from exhaust lines, material recovered from the cyclone, and off-gas filter samples. Modifications were made to the off-gas system for the FY-94 work to allow for collection of particulate from these areas for mass balance calculations. A photo and a schematic of the modified off-gas system can be seen in Figures 3.4 and 3.5. The exhaust equipment consists of a piece of 1.25-inch stainless steel tubing approximately 36 inches in length and straight walled, a diffuser shaped vacuum fitting, a venturi chamber where additional air is supplied at the throat at an approximate rate of 50-60 slm, a cyclonic separator with sample container, filter box and bypass piping, and the baghouse.

Sampling of off-gas particulate is obtained in a batch operation. Typically a filter was left in place until the differential pressure across it reached 5 inches of water. It was then bypassed, isolated, and replaced with a new filter. Filters would remain online for an average of 5-6 minutes and would collect approximately 1-2 grams of particulate. Usually 4 to 5 filters were utilized during a run. The color of the deposit on the filter would vary depending on melter operating conditions.

The cyclone separator removed little particulate material from the exit gas stream. However, for most runs moisture would condense into the cyclone collection can. The quantity of moisture found here was on the order of 5-25 ml. There was no liquid found in the cyclone collection can for the last two runs where the soil was preheated to drive off moisture.

Additional particulate sample collection was done during the cleanup phase of the operation. These samples were the scrapings from under the lid (to include water cooled electrode tube walls), brushings from exhaust components minus the cyclone (which was collected separately), and the feed hopper (including feed tube). The material collected from the lid and electrode tube areas tended to be of a scaley crust most probably due to the condensation promoted by the water-cooled lid and electrodes.

The usual color of this residue was yellow to orange and red. The material collected from the exhaust components tended to be darker in color than the lid and electrode material with an appearance from gray to black. The material would collect at highest concentrations at the entrance to the exhaust line, expansion section, and upstream side of the venturi. Of the materials collected, slag (both top and bottom sections), and filter samples were aliquoted for the purpose of x-ray fluorescence (XRF) analysis. Sample aliquots were also taken on the slag, lid, and filter

materials for the purpose of energy dispersive x-ray emission (EDXS) analysis. Lastly, sample aliquots were obtained for the intent of performing moisture analysis of the various samples in house, and metals analysis of samples from slag, combined exhaust and lid and filters were contracted out. One sample of combined exhaust and lid aliquot which was sent out for wet chemistry analysis (ICP/EAS and FLAA) was spiked with 0.25 grams calcium carbonate (sample A0826EL) for quality assurance considerations.

8.4 General Mass Balance

A material mass balance of general proportions can be obtained by consideration of the various inputs and outputs of the melter system as shown in Table 8.3. The column labeled "Refractory liner" is the start weight of the liner. The regular refractory liner does not reach up to the top of the stainless steel crucible, and a refractory liner extension is used to cover the upper portion of the crucible. Small amounts of slag occasionally splash up onto this liner extension. The filters were not in continuous use during any of the runs. Therefore, some mass was lost as particulate through the bypass exhaust when filters were not in place. The amount of mass collected and time in place of each filter was recorded so that an average particulate flow in the exhaust stream can be calculated. This rate is about 0.3 g/min, but varies for each experiment. Multiplying the rate with the total time of experiment yields the total amount of particulate lost in the exhaust gas stream. This is the figure listed in the "Filters" column. In this way, particulate lost when the filters were not in use can be accounted for. The rest of the columns are self-explanatory being dust collected in the other areas of the exhaust system or materials that were added into the melt. The start weight in the column labeled "Total IEB4/A-40" includes the amount of A-40 put into the crucible before prior to starting (see Table 8.1). Since all the solids have been accounted for, the solid mass loss, listed in the last column, is therefore assumed to be made up of material lost in the conversion carbonates and hydrates as solids into gaseous CO₂ and H₂O. Except for run ARM092094 which is 17.8 wt%, this weight loss amount ranges from 10-13 wt% of the original IEB4/A-40 used during the experiment. The weight loss average for all the runs is 13.1 wt%.

Table 8.3a Mass balance information for the FY-94 HVPM experiments.

Experiment	Refractory liner (kgs)	Liner extension (kgs)	Filters (kgs)	Exhaust lines (kgs)	Lid (kgs)	Steel ring (kgs)	Cyclone (kgs)	Total IEB4/A-40 (kgs)	Solid mass loss (kgs)
ARM082394									
Start weight	7.760	4.361	.000	.000	.000	.424	.000	6.490	
End weight	10.680	4.368	.022	.018	.061	.000	.002	3.480	
Difference	2.920	.007	.022	.018	.061	-.424	.002	-3.007	-.401
ARM082694									
Start weight	7.790	4.368	.000	.000	.000	.420	.000	6.137	
End weight	12.250	4.379	.021	.025	.065	.000	.004	1.407	
Difference	4.450	.011	.021	.025	.065	-.420	.004	-4.730	-.574
ARM090694									
Start weight	7.662	4.379	.000	.000	.000	.475	.000	5.00	
End weight	11.907	4.527	.027	.034	.023	.000	.008	.547	
Difference	4.245	.148	.027	.034	.023	-.475	.008	-4.450	-.440

Table 8.3b Mass balance information for the FY-94 HVPM experiments.

Experiment	Refractory liner (kgs)	Liner extension (kgs)	Filters (kgs)	Exhaust lines (kgs)	Lid (kgs)	Steel ring (kgs)	Cyclone (kgs)	Total IEB4/A-40 (kgs)	Solid mass mismatch (kgs)
ARM090894									
Start weight	7.900	4.366	.000	.000	.000	.427	.000	5.000	
End weight	12.430	4.368	.024	.033	.039	.000	.007	0.197	
Difference	4.530	.002	.024	.033	.039	-.427	.007	-4.803	-.595
ARM092094									
Start weight	7.930	4.368	.000	.000	.000	.373	.000	5.740	
End weight	12.788	4.373	.023	.024	.035	.000	.003	0.177	
Difference	4.858	.005	.023	.024	.035	-.373	.003	-5.563	-.988
ARM092294									
Start weight	7.551	4.373	.000	.000	.000	.337	.000	5.350	
End weight	12.237	4.384	.035	.038	.056	.000	.005	0.194	
Difference	4.686	.011	.035	.038	.056	-.337	.005	-5.156	-.662

8.5 Off-Gas Particulate Analysis

Off-gas particulate evolved during operation of the melting process collects on the walls and top of the melting chamber or lid. A portion of the produced particulate is transported by the exhaust gases to filters located in the lines leading between the melt chamber and baghouse. As feed material was added to the process, the off-gas flow was diverted through these filters to collect representative samples of the evolved particulate. Over the period of one run, a number of filters were introduced to collect samples. Following termination of the run, the melt chamber was disassembled, and material deposited on the lid was removed and sampled.

Analyses for the particulates and the slags were done twice. The first analysis used XRF spectroscopy and EDX spectroscopy. The second analysis was done by an independent laboratory using ICP spectroscopy and FLAA spectroscopy.

8.5.1 EDXS and XRF Analysis of Exhaust Filter Particulate

This section details the x-ray chemical analyses obtained for the material collected on the filters and condensate collected from the chamber head. Two types of x-ray analysis methods were employed to determine the metal/elemental composition of these samples, XRF and EDX spectroscopy. These methods obtain chemical information by bombardment of the prepared sample using either x-rays in the case of XRF or electrons for EDX. The resulting x-ray emissions were analyzed relative to internal and prepared standards to obtain elemental composition. The relative error of these measurements was estimated to be approximately ± 5 to 8% of the reported value.

Table 8.4 shows the averaged results of the EDX and XRF analyses. The full data set is contained in Appendix E. The average was taken using both EDX and XRF data. In cases where only XRF or EDX data were available, the data for either the XRF or EDX cases were ignored. If zero values were part of either the EDX or XRF data, they were used in the averaging. Dashes in the table indicate that data were not taken or the concentration of the element was below detection limits for the instrument.

In all cases, the majority constituents in the filter particulate is zinc, cadmium, and lead at an levels between 15-20 wt%. Cesium was present at levels of several percent along with silicon, iron, and potassium in most cases (See Appendix E). Considering the

Table 8.4 EDXS and XRF analysis - Average concentrations for HVPMs and surrogates in exhaust filter particulate.

Element	ARM 082394 (ppm)	ARM 082694 (ppm)	ARM 090694 (ppm)	ARM 090894 (ppm)	ARM 092094 (ppm)	ARM 092294 (ppm)
Cr	-	-	3700	1840	2100	1950
Zn	187850	142075	163425	187710	217150	237830
Cd	163575	129225	223975	155100	178750	221425
Cs	72900	17450	53340	52900	19550	18125
Ce	870	578	-	-	-	-
Sm	1440	943	-	-	-	-
Pb	167900	165325	208000	138700	266000	215200

overall amounts of HVPMs and surrogates, the cold cap tests (ARM082694, ARM090894, and ARM092294) were only somewhat effective in reducing volatilization. In certain cases for specific elements, data indicate a slight increase in the volatilization in the cold cap test vs. the noncold cap test.

8.5.2 ICP Analysis of Exhaust Filter Particulate

Table 8.5 shows the averaged results of the ICP spectroscopic chemical analyses. FLAA spectroscopy was used to determine cesium concentrations only. The full data set for the ICP and FLAA analyses is contained in Appendix F. In this analysis, the filters containing particulate were prepared using microwave digestion then analyzed. Because both the filter and particulate were analyzed, a plain filter sample was also analyzed so the data from this could be subtracted from the filter plus particulate samples, yielding the elemental concentrations for the particulate only. The plain filter sample was composed primarily (98 wt%, metals basis only) of silicon with small amounts sodium, calcium, and aluminum plus trace elements.

Once again the majority constituents in the filter particulate are found to be zinc, cadmium, and lead at levels approaching between 15-20 wt%. The overall results compare reasonably well with the EDXS and XRF analysis. Cesium was present at levels of several percent, and cerium and samarium exist in amounts of only tenths and hundredths of a percent. The data in Table 8.5 suggest there is no correlation in reductions of HVPMs and surrogates in the cold cap melts, since about half the time the concentrations for specific elements increase slightly rather than decrease.

Table 8.5 ICP analysis - Average concentrations for HVPMs and surrogates in exhaust filter particulate.

Element	ARM 082394 (ppm)	ARM 082694 (ppm)	ARM 090694 (ppm)	ARM 090894 (ppm)	ARM 092094 (ppm)	ARM 092294 (ppm)
Cr	1339	2160	2062	2197	2033	1593
Zn	78972	100826	100575	142435	123782	159001
Cd	99876	127778	142407	168418	214363	197526
Cs	21413	33279	46176	45799	33776	29549
Ce	504	1077	796	1163	210	213
Sm	149	123	156	113	16	21
Pb	136296	164793	132186	146597	147130	173313

8.5.3 EDX and XRF Analysis of Melter Chamber Particulate

Table 8.6 shows the elemental composition of material removed from the cover of the arc melter chamber. Most of the elements present in the material added to the melter are present in the condensate. Major constituents are cadmium, iron, lead, and zinc. Cerium and samarium are present in measurable amounts. The HVPMs, particularly cadmium, are in higher concentrations than in the filter particulate collected downstream in the exhaust system. Samples for the last two experiments were not collected.

Table 8.6 EDX and XRF melter chamber condensate/particulate analysis.

Element	ARM082394	ARM082694	ARM090694	ARM090894
Na	0	0	0	0
Mg	0	0	0	0
Al	0	0	0	0
Si	26800	13000	7300	10900
K	16200	21000	18800	14900
Ca	26900	17000	20000	20100
Ti	23800	15000	25900	24500
Fe	146200	72600	125200	141300
Zn	155600	175600	190000	161700
Zr	27200	12300	22000	26700
Cd	313000	358400	378300	166200
Cs	18000	15600	31100	12100
Ce	7600	4600	5900	3000
Sm	9900	6700	9200	13500
Pb	230400	199500	219900	161700

8.5.4 ICP Analysis of Melter Chamber Particulate.

Data in Table 8.7 for the ICP spectroscopic analysis of HVPMS and surrogates correlates well with in Table 8.6 using EDXS and XRF analyses, in particular the somewhat higher levels of cadmium found in the chamber particulate as compared to filter particulates downstream. Data on the other elements can be found in Appendix F.

Table 8.7 ICP analysis - Average concentrations for HVPMS and surrogates for particulate collected from the melter chamber.

Element	ARM 082394 (ppm)	ARM 082694 (ppm)	ARM 090694 (ppm)	ARM 090894 (ppm)	ARM 092094 (ppm)	ARM 092294 (ppm)
Cr	1089	1345	3212	2908	3346	2329
Zn	123941	95776	108560	104802	138395	157266
Cd	262825	243015	240691	246378	279838	238345
Cs	34700	21448	47142	36836	45717	29809
Ce	4458	613	687	1308	1001	623
Sm	5972	193	421	6950	672	507
Pb	238847	285003	162706	148894	176772	178987

8.6 Slag Composition Analysis

Coincident with the XRF, EDXS, and ICP spectroscopic analyses of the particulate materials, samples of the resulting slags were also analyzed. Two samples of each melt were analyzed, one from the top portion of the melt and a second from the lower portion of the melt. The location within the melt was thought to be important in determining if mixing or stratification of the melt was occurring. Since the slag is composed of both a glass matrix and distributed distinct crystals, the applicability of XRF and EDXS for complete characterization of the exact composition of the slag is questionable. Both of these methods yield concentration

values that are averaged over an observation area. Elements that tend to segregate or congregate into localized areas can be overstated or understated by these methods. For example, zirconium tends to concentrate in large dendritic grains or crystals that spread across the melt. EDXS analyses of samples where these large crystals are exposed to detection display elevated concentrations of zirconium. These concentration values are judged high based on the original amount of oxide added and corresponding values obtained using XRF on the same and similar samples. Therefore, elements found to segregate are better defined relative to composition by using wet chemical methods (ICP and FLAA spectroscopy) than the x-ray methods (EDX and XRF) which are good indicators of elemental presence rather than precise data values when concentrations are low. EDX measurement values below 1/2 wt% may have large relative errors associated with them.

8.6.1 EDXS and XRF Slag Analysis

Slag compositions for all 1994 runs are presented in Tables 8.8 through 8.13 and are shown graphically for easy comparison in Figures 8.1 through 8.6.

Table 8.8 EDX and XRF analysis of ARM082394 slag.

Element	TOP-XRF	TOP-EDX	BOT-XRF	BOT-EDX
Na	0	9900	0	9600
Mg	26400	10300	34300	10000
Al	81200	50900	74000	51400
Si	246000	193700	276000	195000
K	19400	10700	25400	11100
Ca	38300	29900	36300	30600
Ti	24300	23900	30600	24000
Cr	0	3200	0	3200
Fe	152000	127000	126400	121000
Zn	1600	0	1100	0
Zr	15800	35500	15800	32900
Cd	8	0	0	0
Ce	483	2100	728	3400
Cs	557	2100	8800	2400
Sm	1900	1600	6900	0
Pb	2400	0	2500	0

ARM-082394 SLAG

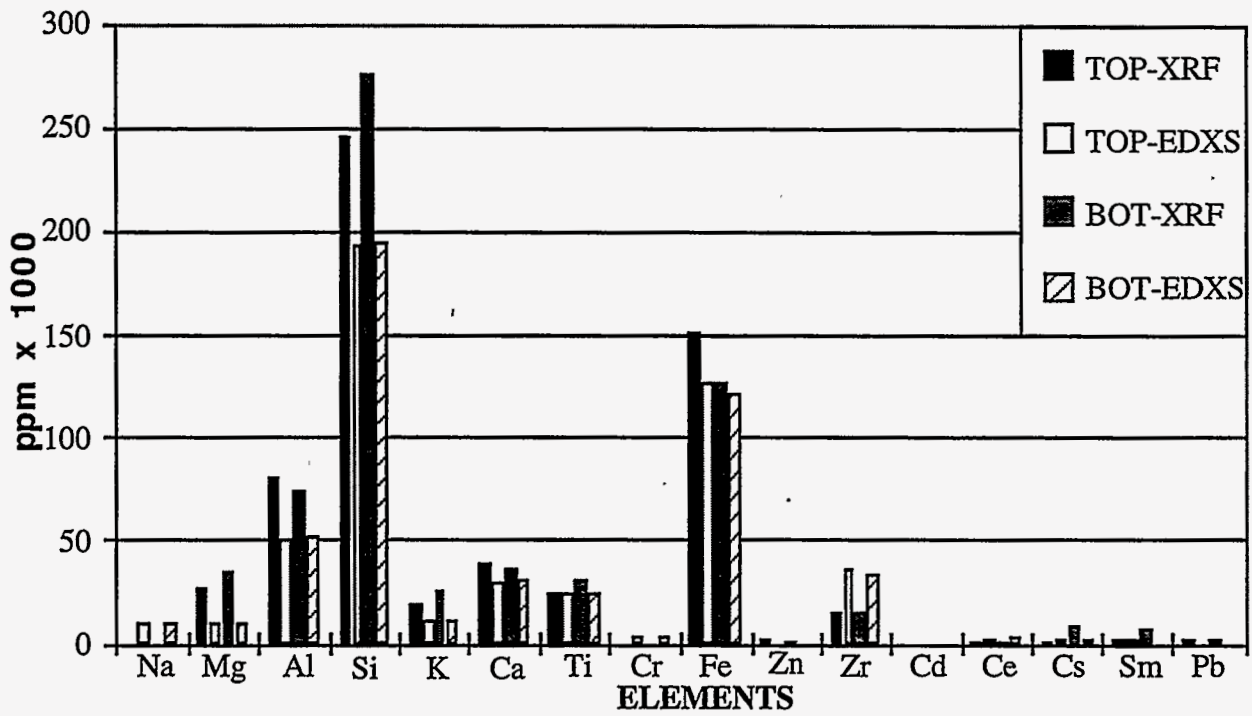


Figure 8.1 XRF and EDXS chemistry results from top and bottom samples of slag taken from run #ARM082394.

Table 8.9 EDX and XRF analysis of ARM-082694 slag.

Element	TOP-XRF	TOP-EDXS	BOT-XRF	BOT-EDXS
Na	0	12300	0	10600
Mg	28000	13100	27400	12300
Al	65100	49700	57600	47600
Si	246300	210800	218600	201600
K	22100	12200	21200	11300
Ca	37300	40200	38100	38800
Ti	29100	26300	29400	25300
Cr	0	3900	0	3700
Fe	118000	120800	129400	123500
Zn	2300	0	2100	0
Zr	15400	101500	17000	108200
Cd	215	0	79	0
Ce	1600	4900	863	3200
Cs	2300	3000	1100	3000
Sm	7100	3700	7300	2400
Pb	7000	0	6100	0

ARM-082694 SLAG

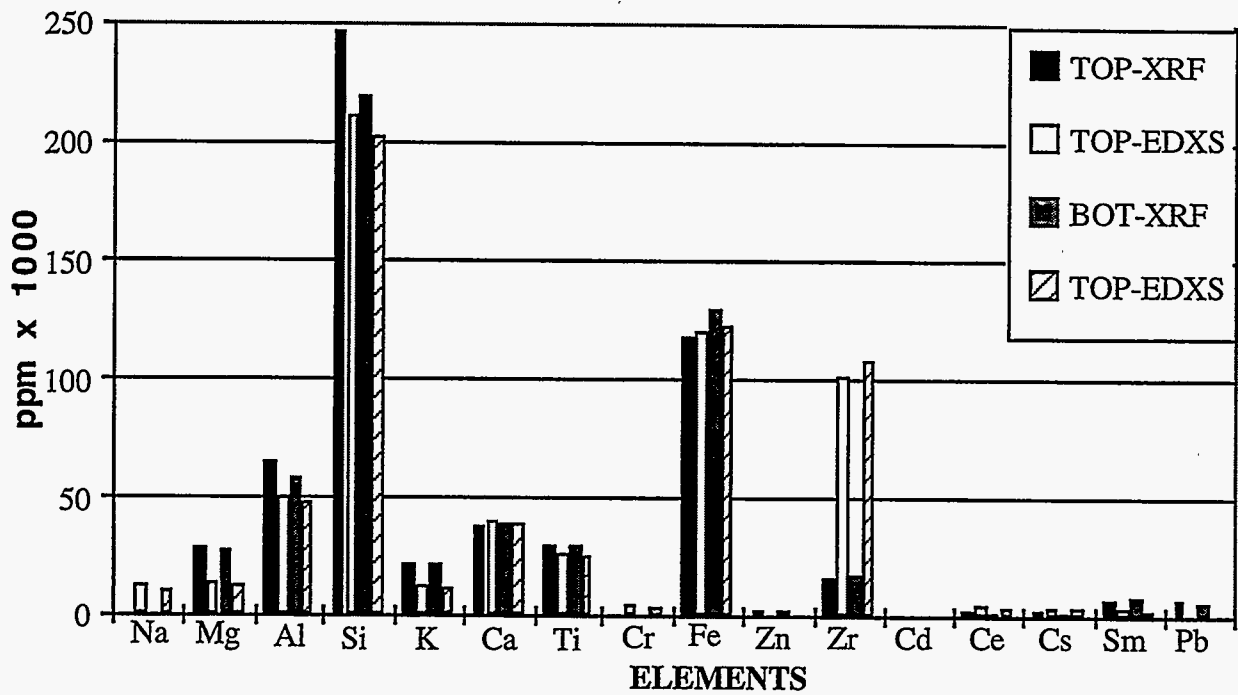


Figure 8.2 XRF and EDXS chemistry results from top and bottom samples of slag taken from run #ARM082694.

Table 8.10 EDX and XRF analysis of ARM-090694 slag.

Element	TOP-XRF	TOP-EDXS	BOT-XRF	BOT-EDXS
Na	0	13200	0	15200
Mg	32800	13000	48600	14600
Al	57600	43900	48000	45400
Si	57600	43900	222300	200000
K	22800	11200	14800	11900
Ca	45500	42600	37000	42400
Ti	34600	27000	24700	27100
Cr	0	2200	0	3100
Fe	150000	147400	126900	151800
Zn	2100	0	1700	0
Zr	14400	73100	13600	62900
Cd	45	0	32	0
Ce	1400	4300	1300	2400
Cs	1400	2100	1300	2300
Sm	6800	0	5300	1900
Pb	2500	0	2000	0

ARM-090694 SLAG

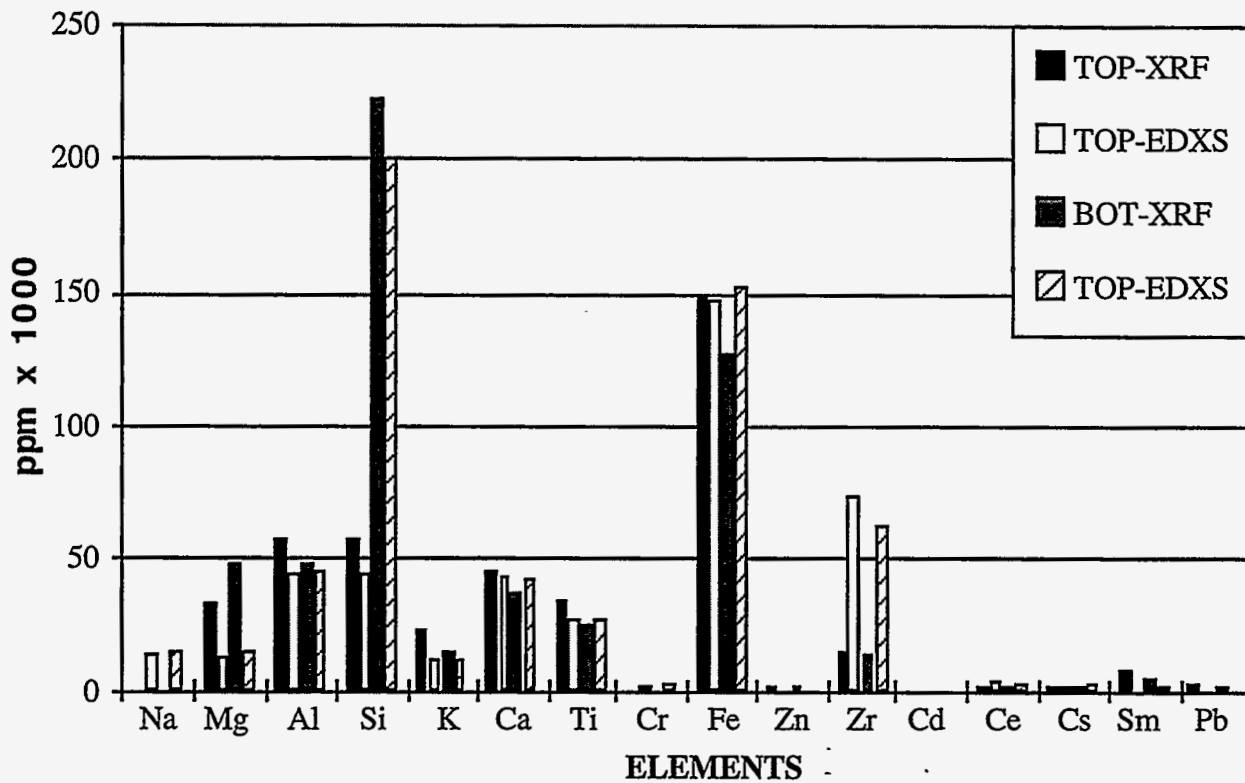


Figure 8.3 XRF and EDXS chemistry results from top and bottom samples of slag taken from run #ARM090694.

Table 8.11 EDX and XRF analysis of ARM-090894 slag.

Element	TOP-XRF	TOP-EDXS	BOT-XRF	BOT-EDXS
Na	0	14400	0	13900
Mg	26600	14900	34500	14800
Al	57200	47800	61000	47300
Si	265700	202300	263900	199300
K	20900	12700	23900	12200
Ca	41600	43400	45200	42900
Ti	30900	27500	34600	27800
Cr	0	3200	0	2100
Fe	128700	131600	143000	133200
Zn	1800	0	2000	0
Zr	16100	82300	17400	81800
Cd	19	0	20	0
Ce	1400	4700	1300	2300
Cs	1700	3400	1700	3100
Sm	6800	2900	7600	0
Pb	2700	0	2900	0

ARM-090894 SLAG

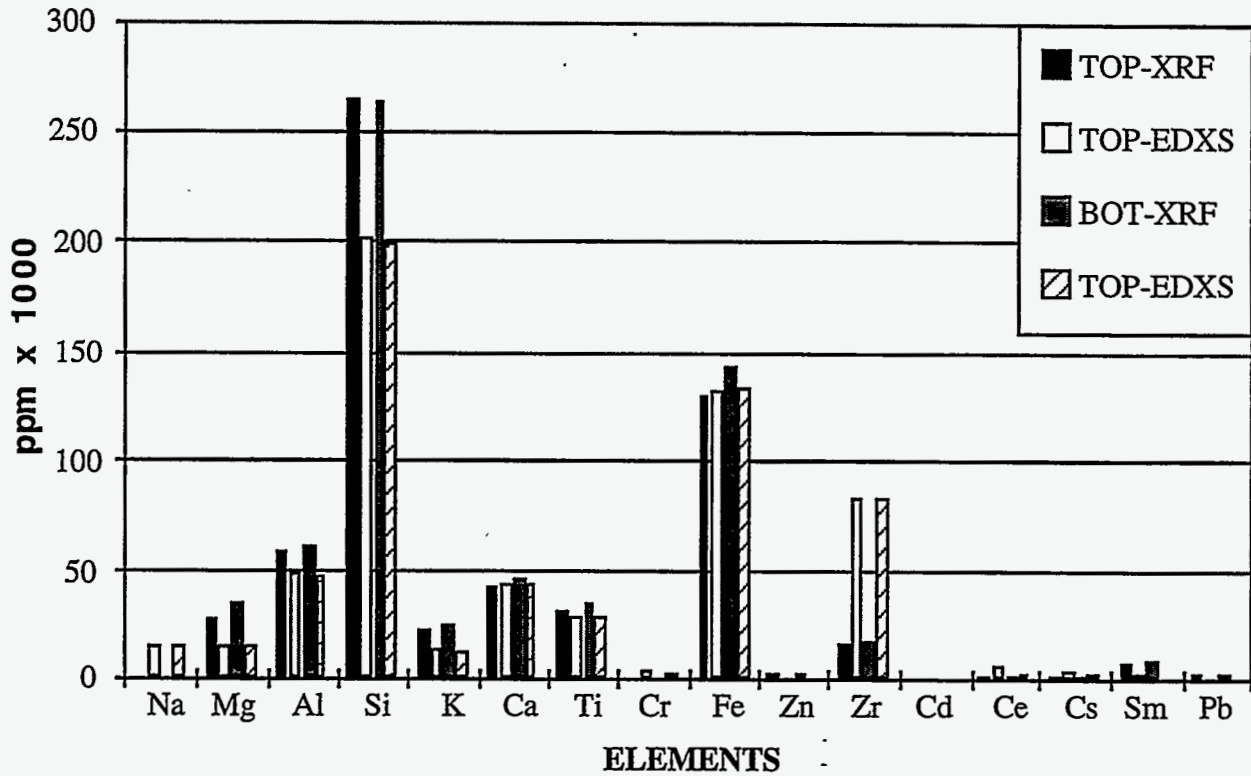


Figure 8.4 XRF and EDXS chemistry results from top and bottom samples of slag taken from run #ARM090894.

Table 8.12 EDX analysis of ARM-092094 slag.

Element	TOP-EDXS	BOT-EDXS
Na	11700	13600
Mg	14900	15300
Al	46200	48200
Si	194100	201100
K	11000	9900
Ca	46500	46600
Ti	25700	25900
Cr	1900	2200
Fe	124800	123300
Zn	0	0
Zr	84500	89000
Cd	0	0
Ce	2600	4400
Cs	2700	2200
Sm	1500	1800
Pb	0	0

ARM-092094 SLAG

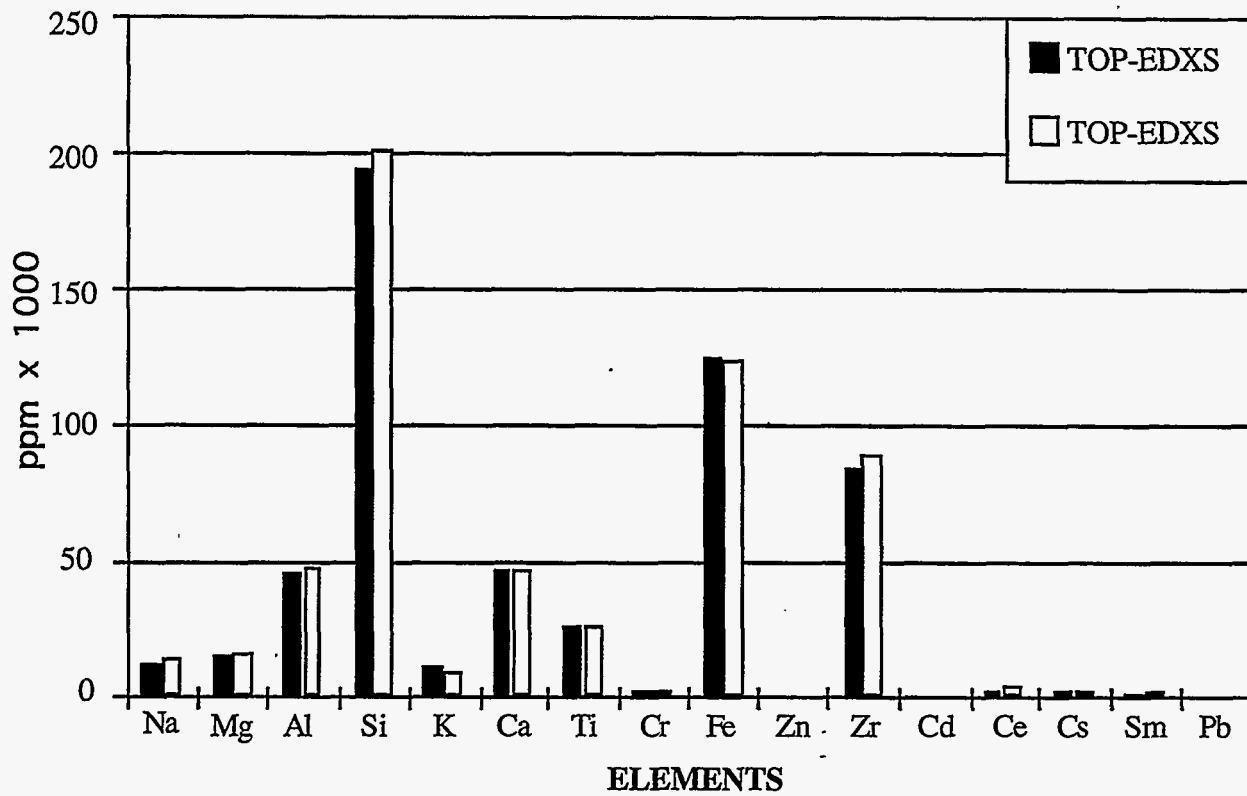


Figure 8.5 EDXS chemistry results from top and bottom samples of slag taken from run #ARM092094.

Table 8.13 EDX Analysis of ARM-092294 Slag.

Element	TOP-EDXS	BOT-EDXS
Na	10300	13900
Mg	15100	15400
Al	49500	37500
Si	212500	138000
K	13000	4700
Ca	50500	19000
Ti	28200	8000
Cr	3700	40910
Fe	109200	37500
Zn	0	0
Zr	88300	14600
Cd	0	0
Ce	3000	1000
Cs	3400	500
Sm	4100	4800
Pb	0	0

ARM-092294 SLAG

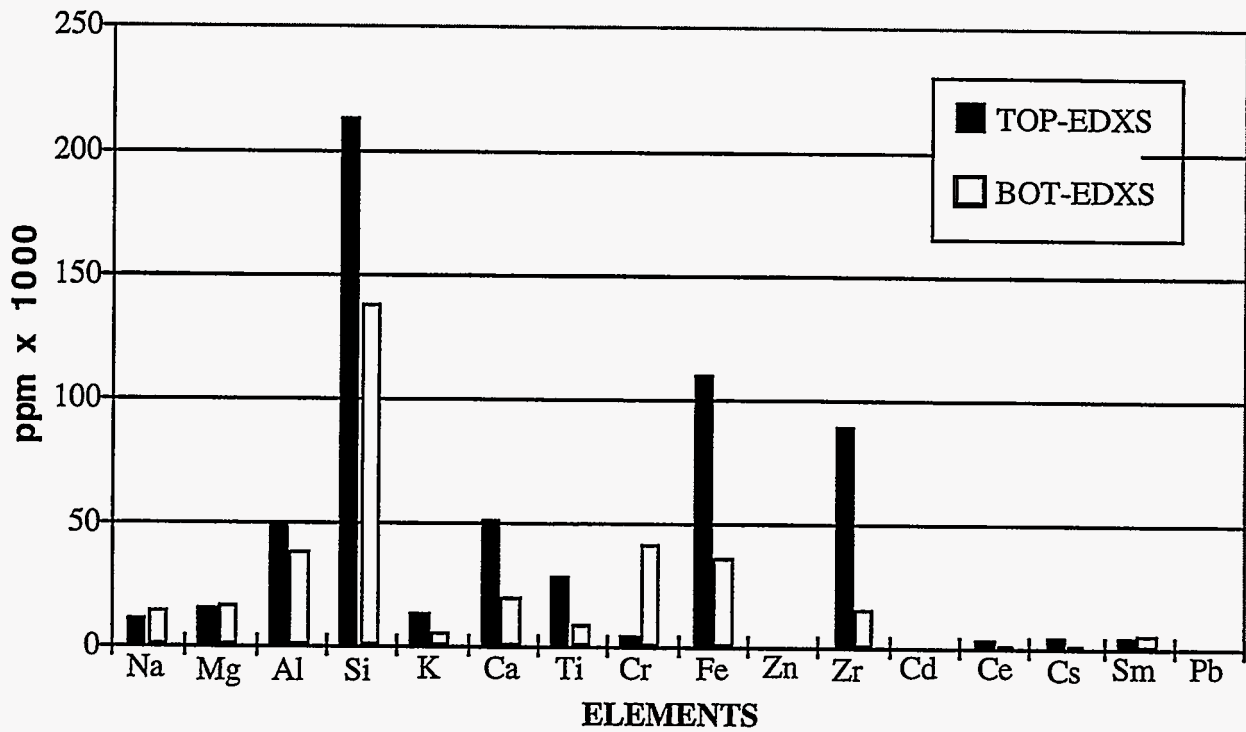


Figure 8.6 EDXS chemistry results from top and bottom samples of slag taken from run #ARM092294.

8.6.2 ICP and FLAA Slag Analysis

The ICP spectrochemical analysis of the slags for the HVPMS and surrogates for each experiment is presented in Table 8.14. FLAA spectroscopy was used only to determine cerium concentrations. Results in Table 8.14 are averaged, and the full analysis for these and the other elements can be found in Appendix F.

The ICP analysis of the slags which consists of first digesting the material to be analyzed was expected to show greater concentrations of samarium, cerium, and chromium in the slag since relatively smaller amounts of these elements were found in the particulate entrained in the off-gas as compared to the rest of HVPMS and surrogates. Data in Table 8.15, however, indicates relatively small amounts of Sm, Ce, and Cr, and is consistent with the EDXS and XRF analyses. As will be seen in section 8.7, the mass balance for these elements is very poor, with far less material accounted for than originally added to the melt. On the other hand, the volatile HVPMS (cadmium, lead, and zinc) show a marked decrease in concentration in the slag, which is commensurate with the high concentrations found in the off-gas particulates.

Table 8.14 ICP analysis - Average concentrations for HVPMS and surrogates in the slag.

Element	ARM 082394 (ppm)	ARM 082694 (ppm)	ARM 090694 (ppm)	ARM 090894 (ppm)	ARM 092094 (ppm)	ARM 092294 (ppm)
Cr	3557	3301	1599	2258	3257	3404
Zn	2113	8976	6076	2165	3097	1002
Cd	1832	1086	222	111	1289	91
Cs	5082	2732	3216	5060	4325	5319
Ce	2514	1139	1251	2038	1145	1020
Sm	1154	167	794	1041	331	659
Pb	2808	6128	2126	2385	3181	870

8.7 Detailed Mass Balance for HVPMS and Surrogates

With the concentrations of HVPMS and surrogates in the slag and particulates identified, a detailed mass balance for each element can be formulated. As a first step, Table 8.15 gives the elemental composition of the starting material, IEB4/A-40 with HVPMS and surrogates added. Using this table, the total amount (grams) of any element can be calculated by knowing the total amount of IEB4/A-40 used in the melt. Since the chemical analyses indicate only the metals amounts and not oxide forms, Table 8.15 also contains the metals basis wt% and parts per million for each metals constituent.

Table 8.16 contains the necessary information to complete the mass balances. The information is similar to that contained in Table 8.3, but has been rearranged and grouped differently. Column two contains the total amount of IEB4/A-40 added during the experiment. The total mass (column three Table 8.16) is simply the sum of IEB4/A-40 mass plus the mass of the iron starting ring. The total solids mass measured after the experiment is the sum of the next three columns, which includes the slag mass and the particulate collected within the arc melter system. The chamber mass (column 5) is the sum of masses listed under liner extension and lid in Table 8.3. This is total particulate collected in the melt chamber just above the slag. The remaining particulates collected in the exhaust system equal the sum of material collected in the exhaust lines, filters, and cyclone.

8.7.1 Detailed Mass Balances for HVPMS

Using the information on concentrations of HVPMS in the slag and particulates found in Sections 8.5 and 8.6, and the information in Table 8.16 listing the mass amounts of slag and particulates, a detailed mass balance can be calculated. Table 8.17 lists the wt% of each constituent HVPM found in the slag and particulates as determined by EDX and XRF analysis and in the next column the mass amount of that constituent. In the second to the last column, the masses are added together yielding the total amount of each HVPM found in the slag and particulates. This can be compared with the total mass amount of each HVPM originally introduced into the IEB4/A-40. EDX or XRF spectroscopic analyses were not performed for ARM092094 and ARM092294. While the mass balance for chromium cannot be calculated since the particulates were not analyzed for that element, the results for the remaining HVPMS in general do not account for all the HVPMS. Averaging over results of the four tests, lead shows the best mass balance at 89%, while zinc and cadmium average only 76% and 64%, respectively.

Table 8.15 IEB4/A-40, HVPMs, and surrogates composition for the FY-94 tests.

Oxide component	Calculated oxide values (wt%)	Calculated oxide values (ppm)	Metals basis values (wt%)	Metals basis values (ppm)
Na ₂ O	2.678	26780	1.987	19870
MgO	2.930	29300	1.767	17670
Al ₂ O ₃	8.537	85370	4.520	45200
SiO ₂	42.603	426030	19.881	198810
K ₂ O	2.176	21760	1.806	18060
CaO	8.119	81190	5.803	58030
TiO ₂	4.902	49020	2.939	29390
Cr ₂ O ₃	1.000	10000	0.684	6840
Fe ₂ O ₃	16.405	164050	11.747	11747
ZnO	1.000	10000	0.803	8030
ZrO ₂	4.650	46500	3.442	34420
CdO	1.000	10000	0.875	8750
Cs ₂ CO ₃	1.000	10000	0.820	8200
CeO ₂	1.000	10000	0.814	8140
Sm ₂ O ₃	1.000	10000	0.862	8620
PbO	1.000	10000	0.928	9280

IEB4/A-40 COMPOSITION

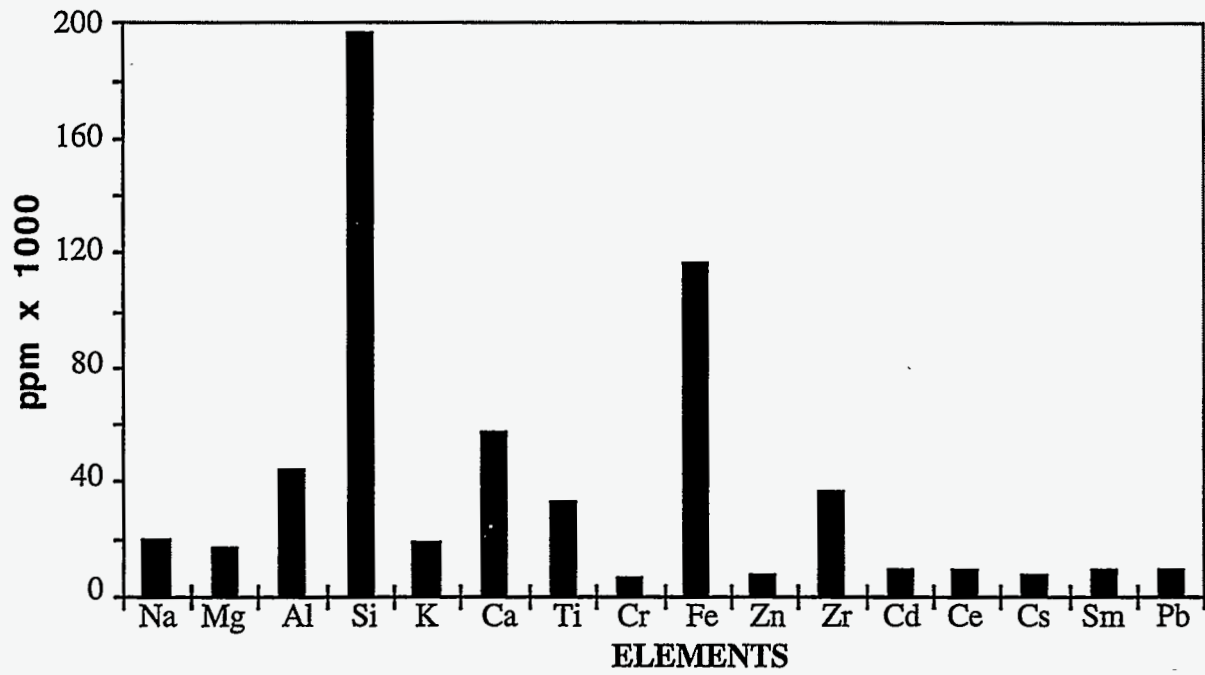


Figure 8.7 Calculated composition of the starting IEB4/A-40 waste-soil mixture.

Table 8.16 Mass balance information for solid materials in the arc melter system.

Experiment	IEB4/A-40 mass (kg)	Total mass (kg)	Slag mass (kg)	Chamber mass (kg)	Exhaust mass (kg)	Diff (kg)
ARM082394	3.007	3.431	2.920	0.068	0.042	0.401
ARM082694	4.730	5.150	4.450	0.076	0.050	0.574
ARM090694	4.450	4.925	4.245	0.033	0.069	0.440
ARM090894	4.803	5.230	4.530	0.041	0.064	0.595
ARM092094	5.563	5.936	4.858	0.040	0.050	0.988
ARM092294	5.156	5.493	4.686	0.067	0.078	0.662

Slag and particulate samples were also analyzed using ICP spectroscopy by an independent source. Table 8.18 contains the results for the HVPMS. These results are similar to those of the EDX and XRF analysis in that generally the amounts of each element found in the slag and particulates are lower than the amount initially introduced, although in some instances the amount is greater. The amount of chromium found in the slag and particulates is consistently much lower than the amount introduced. Over the six experiments, the average mass balance for chromium is just 40%. The other HVPMS show much better recovery, averaging 83% for zinc, 67% for cadmium and 79% for lead, however, there are extreme fluctuations in the data. For instance for lead, the mass balance for ARM082694 is 134%, while the mass balance for ARM092094 is only 57%.

8.7.2 Detailed Mass Balances for Radionuclide Surrogates.

The mass balance closure for the surrogate elements is more worrisome than for the HVPMS. Table 8.19 shows both the EDX and ICP analytical results for ARM082394. Both data sets are extremely consistent, and the data in Table 8.19 are representative of any of the other experiments. The mass balance closure for cesium is close to 60%, which is similar to the HVPMS (Cs is also very volatile). The closure for cerium and samarium is only within the range of 20-30%, even less than that of chromium. It is notable that for the surrogate elements, there is consistency between the x-ray analytical methods (EDX and XRF) and the wet chemical analysis (ICP and FLAA).

Table 8.17a HVPM mass balance using EDXS and XRF spectroscopic analysis.

Element	Slag (wt%)	Slag mass (g)	Chamber particulate mass (wt%)	Chamber particulate mass (g)	Exhaust filter particulate (wt%)	Filter particulate mass (g)	Total mass (g)	Introduced mass (g)
ARM082394								
Cr	0.32	11.7	-		-			25.7
Zn	0.14	5.1	15.56	13.3	18.79	7.9	23.6	30.2
Cd	0.00	0.0	31.30	27.2	16.36	6.9	28.2	32.9
Pb	0.25	9.2	23.04	15.2	16.79	7.1	32.0	34.9
ARM082694								
Cr	0.38	22.6	-		-			42.6
Zn	0.22	13.1	17.56	13.3	14.21	7.1	33.5	50.0
Cd	0.02	1.2	35.84	27.2	12.92	6.5	34.9	54.5
Pb	0.66	39.3	19.95	15.2	16.53	8.3	62.8	57.8
ARM090694								
Cr	0.27	15.9	-		0.38	22.6		40.7
Zn	0.19	11.2	19.00	6.3	16.34	11.3	28.8	47.8
Cd	0.00	0.0	37.83	12.5	22.40	15.5	28.0	52.1
Pb	0.23	13.5	21.99	7.3	20.80	14.4	35.2	55.2

Table 8.17b HVPM mass balance using EDXS and XRF spectroscopic analysis.

Element	Slag (wt%)	Slag mass (g)	Chamber particulate mass (wt%)	Chamber particulate Mass (g)	Exhaust filter particulate (wt%)	Filter particulate mass (g)	Total Mass (g)	Introduced Mass (g)
ARM090894								
Cr	0.27	16.3	-		0.18	10.7		43.1
Zn	0.19	11.5	16.17	6.6	18.77	12.0	30.1	31.0
Cd	0.00	0.0	16.62	6.8	15.51	9.9	16.7	32.0
Pb	0.28	16.9	16.17	6.6	13.87	8.9	32.4	34.9

Table 8.18a HVPM mass balance using ICP spectroscopic analysis.

Element	Slag (wt%)	Slag Mass (g)	Chamber Particulate (wt%)	Chamber Particulate Mass (g)	Exhaust Filter Particulate (wt%)	Filter Particulate Mass (g)	Total Mass (g)	Introduced Mass (g)
ARM082394								
Cr	0.36	10.4	0.11	0.1	0.13	0.1	10.6	20.6
Zn	0.21	6.2	12.39	8.4	7.90	3.3	17.9	24.1
Cd	0.18	5.3	26.28	17.9	9.99	4.2	27.4	26.3
Pb	0.28	8.2	23.88	16.2	13.63	5.7	30.1	27.9
ARM082694								
Cr	0.33	14.7	0.13	0.1	0.22	0.1	14.9	32.4
Zn	0.90	38.6	9.58	7.3	10.08	5.0	50.9	38.0
Cd	0.11	4.8	24.32	18.5	12.78	6.4	29.7	41.4
Pb	0.61	27.3	28.50	21.7	16.48	8.3	57.3	43.9
ARM090694								
Cr	0.16	6.8	0.32	0.1	0.21	0.1	7.0	30.4
Zn	0.61	25.8	10.82	3.6	10.06	6.9	36.3	35.7
Cd	0.02	0.9	24.07	7.9	14.24	9.8	18.6	38.9
Pb	0.21	9.0	16.27	5.4	13.22	9.1	23.5	41.3

Table 8.18b HVPM mass balance using ICP spectroscopic analysis.

Element	Slag (wt%)	Slag Mass (g)	Chamber Particulate (wt%)	Chamber Particulate Mass (g)	Exhaust Filter Particulate (wt%)	Filter Particulate Mass (g)	Total Mass (g)	Introduced Mass (g)
ARM090894								
Cr	0.23	10.3	0.29	0.1	0.22	0.1	10.5	32.8
Zn	0.22	9.8	10.48	4.3	14.24	9.1	23.2	38.6
Cd	0.01	0.5	24.64	10.1	16.84	10.8	21.4	42.0
Pb	0.24	10.8	14.89	6.1	14.66	9.4	26.3	44.6
ARM092094								
Cr	0.33	15.8	0.33	0.1	0.20	0.1	16.0	38.1
Zn	0.31	15.0	13.84	5.5	12.38	6.2	26.7	44.7
Cd	0.13	6.3	27.98	11.2	21.44	10.7	28.2	48.7
Pb	0.32	14.9	17.68	7.1	14.71	7.4	29.4	51.6
ARM092294								
Cr	0.34	16.0	0.23	0.2	0.16	0.1	16.3	35.2
Zn	0.10	4.7	15.73	10.5	15.90	12.4	27.8	41.4
Cd	0.01	0.4	23.83	16.0	19.75	15.4	31.8	45.1
Pb	0.08	4.1	17.90	12.0	17.33	13.5	29.6	47.8

Table 8.19 Surrogate mass balance for ARM082394.

Element	Slag (wt%)	Slag Mass (g)	Chamber Particulate (wt%)	Chamber Particulate Mass (g)	Exhaust Filter Particulate (wt%)	Filter Particulate Mass (g)	Total Mass (g)	Introduced Mass (g)
ARM082394 - EDX & XRF								
Cs	0.35	12.8	1.80	1.2	7.29	3.1	17.1	24.7
Ce	0.17	6.3	0.76	0.5	0.09	0.1	6.9	24.5
Sm	0.26	9.5	0.99	0.8	0.14	0.1	10.4	25.9
ARM082394 - ICP & FLAA								
Cs	0.51	14.8	3.47	2.4	2.14	1.0	18.2	24.7
Ce	0.25	7.3	0.45	0.3	0.05	0.0	7.6	24.5
Sm	0.12	4.5	0.60	0.4	0.02	0.0	4.9	25.9

8-35

8.8 Discussion

The mass balance closures for both the HVPM and surrogate elements are low. Reasons for this are not entirely clear, particularly since separate analytical methods were employed and are generally consistent with each other. The largest possibility for error is in the slag analysis since the concentrations of the subject elements are quite low (less than 1 wt%). The relative error for low-concentration measurements is probably higher than for high-concentration measurements. This is compounded by the fact that the slag constitutes by far the largest mass amount of melter residues. Therefore, even modest errors in the slag concentrations could cause large deviations in the mass balance closure. There are other possible reasons. The varied mass closure results of lead (57% to 134%) might suggest the partitioning of elements within the slag. This condition could arise due to different processing conditions within the melt. This possibility, however, was taken into account and samples were taken from different parts of the melt such as from the top and bottom regions. An additional possibility is that the surrogates, which are not expected to volatilize, may have selectively partitioned into the refractory liner. Liners for the FY-94 work were an HP-CAST ZR-AL composed of SiO_2 - 27%, Al_2O_3 - 16%, ZrO_2 - 54% and CaO - 3%.

9. CONCLUSIONS AND RECOMMENDATIONS

The INEL small DC arc melter has proven to be a useful tool in supporting the efforts of several initiatives to remediate mixed low-level wastes at the INEL. These initiatives include the Buried Waste Integration Demonstration (BWID) Program, Private Sector Participation Initiative (PSPI) Program, and Integrated Waste Processing Facility (IWPF) Program. These programs took advantage of the capabilities of the INEL small arc melter to investigate the effects of various processing conditions in a DC arc melter on the properties of thermally treated mixed low-level waste.

9.1 Arc Melter System and Operations

An arc-melter facility having undergone a series of modifications has conducted volatilization and redox studies on simulated wastes containing toxic and high vapor pressure metals, as well as TRU surrogates. Operational observations reveal that there is more volatile and particulate emission from the melt chamber when the HVPMS and TRU are present in the simulated waste mix than when they are not. Obviously, the HVPMS contribute most to this increased particulate loading in the exhaust gases. Entrainment of particulate from the waste mix is increased when feeding material into a melt that has already been established. The small size of the pulverized feed particles contribute to this type of emission problem. This increase in particulate loading made it difficult for the operator to view the inside the melt chamber with the video monitor and adjust the position of the electrodes to account for the receding of the melt-feed interface and electrode loss.

Monitoring energy balance data (energy input vs. energy output as a function of time) revealed important insights into the ability of the arc melter to process material under various conditions. Crucible inserts provided better insulation from the water-cooled stainless steel crucible than coating the crucible with thin layers of mortar. This resulted in more heat being supplied to the simulated waste mixtures in a shorter time. For instance, in open melt conditions, six kilograms of material could be melted in 45 minutes using an insert vs. 1 hour otherwise. Establishment of a cold cap would prevent energy from being radiated away from the melt surface. This captured radiation energy would accelerate melting of the cold cap surface material and in some cases increase the overall temperature of the melt. The energy balance data revealed useful information about melting rates and material feeding rates in addition to maintenance problems.

Coatings on the carbon electrodes had a modest effect on increasing their lifetime and thereby increasing the time available for processing. Non-coated electrodes would erode along

the entire length of the electrode showing progressively increased erosion closer to the tip. Coated electrodes eroded only at the tip, with the coatings protecting the upper portions from oxidation. Plasma-sprayed coatings of ceramic oxides, alumina, and zirconia were used in FY-93, and plasma-sprayed silicon and painted coatings of silicon carbide were used in FY-94.

Slag temperature measurements proved to be problematic. Type C thermocouples encased in alumina sheaths lasted only minutes depending on the slag temperature. A water-cooled TC probe with an alumina sheath and a graphite extension tube coated with silicon carbide proved to be most effective for extended temperature measurements. The graphite extension tube must be long enough so as to not be affected by the water-cooled section of the probe.

Below are lessons learned in operating the present arc melter system:

1. For the initial heating period, two 80 kW power supplies set for 400 VOC are required to provide stability to account for potentially large shifts in current and voltage. After operation has stabilized, one power supply may be turned off.
2. Operation at low temperatures (<1400°C) and low power with the compositions studied is not conducive to stable operation and should be avoided.
3. Temperatures in excess of 2000°C can be easily obtained. The melt temperature may require monitoring with feedback control to maintain the desired set point.
4. When adding feed at low power and with manual control, it may be necessary to increase the power so that the cold, nonconducting feed does not significantly alter the operating conditions and cause the arc to extinguish. For this system, 100 A or more is recommended.
5. Solidified slag from previous experiments melts more easily and can be operated at higher currents than the initial simulated-waste/soil mixture.
6. Exhaust lines must be cleaned out after each test to ensure that plugging will not occur.
7. The cold trap must be kept at the appropriate temperature range so that ice will not form but at the same time, it must sufficiently cool the exhaust gas. Water and ice, rather than liquid nitrogen, provided an adequate amount of cooling.

9.2 Effects of Redox Conditions

The redox experiments conducted in FY-94 tested the extremes in reducing or oxidizing conditions and their effect on melt chemistry and crystallization. Reducing conditions for two melts were achieved by using different levels of carbon blended into the melt mix. In the case of these two melts, that was one-half of the stoichiometric amount of carbon needed to reduce iron oxides to metals and twice the stoichiometric amount. Two levels of oxidation were maintained by introducing air under the surface of the melt with a water-cooled air lance.

An overall generalization of the difference between slag material processed under reducing and oxidizing conditions is that the reduced melts produced mostly glassy slag while the oxidized melts developed substantially more crystalline structure even though the cooling rates were very similar. The highly oxidizing condition resulted in the highest volume fraction of crystalline phases. This may be an important factor to consider in the formulation of a final waste form. Some Cs appears to be interstitially bound to a chromite phase. No zirconolite was observed in any of these experiments. In part this may be due to unfavorable chemistry conditions and to rapid slag cooling that did not allow enough time for nucleation and growth to occur.

Redox conditions had little influence on the disposition of the HVPs. With the exception of chromium, the HVPs evaporated from the melt in both reducing and oxidizing environments. Chromium showed a strong tendency to form crystals in conjunction with iron, although the crystalline structures formed in reducing conditions tended to be much smaller and finer. The surrogates did not tend to collect preferentially in the crystalline phases as was hoped. This may be due primarily to relatively fast slag cooling rates once the melter is turned off.

Of the surrogates, only cerium demonstrated an ability to remain in the slag in significant amounts, retaining about half of the original amount in the simulated waste mix. The cerium was found in the glassy phases of the slag. In general, the rest of the surrogates tended to be volatilized although there were exceptions. For instance, cesium showed modest retention under oxidizing conditions but was completely volatilized in the reducing environment.

9.3 Volatilization in a DC Arc Melter

There were two experimental campaigns conducted during FY-93 and FY-94 to specifically try and quantify the volatilization of HVPMs and radionuclide surrogates under open melt and cold cap conditions. The first test series in FY-93 collected exhaust gases while feed material containing the HVPMs and surrogates was introduced into the melt with the auger feeder. The exhaust gas particulates were collected by an exhaust gas analyzer. After analysis by an independent laboratory, volatilization rates in units of milligrams per hour were calculated for the elements of interest.

Examination of the data showed only the slightest correlation for reduction in volatilization in the cold cap melts vs. the open melts. This conclusion, however, may only point to the need for a thicker cold cap layer. Only in the case chromium of was there a clear indication of reduced volatilization in the cold cap experiments. Results for the other elements show only a slight reduction in volatilization in most cases during cold cap conditions, but there are many instances in which the opposite is true.

Measured volatilization rates can be expected to be system dependent since the geometry, temperature profiles, exhaust gas flow rates, etc., which will affect volatilization will be unique for each melter system. Primary factors affecting volatilization are the amount and surface area of the slag, concentration of the volatile material in the slag, and slag temperature. In general, volatilization rates for the INEL small arc melter show the expected correlation between temperature and volatilization, i.e. higher rates for higher slag temperatures, although there are some exceptions. Lack of a strict correlation can likely be attributed to uncertainties in slag temperature and unknown HVPM and surrogate concentrations during exhaust sampling. In order to obtain reliable volatilization rate data for any processing system, detailed slag temperature must be taken along with slag samples to determine volatile element concentrations.

Volatilization testing was continued in FY-94, again under open melt and cold cap conditions. In these experiments, the arc melter exhaust system was modified to streamline the task of obtaining a global mass balance. Masses of the slag (including metal if any), particulates in the melter chamber, and particulate in the exhaust system were collected and measured. In order to do elemental masses balances, the slag and particulates were analyzed using energy dispersive x-ray spectroscopy and x-ray fluorescence spectroscopy. Additionally, the slag and particulates were analyzed using inductively coupled plasma-atomic emission absorption spectroscopy. All of these analytical methods produced similar results.

A general mass balance comparing the amount of starting material with the amount of material after processing revealed an average mass loss of 10.7 wt%. This is a typical amount expected to be lost from carbonated and hydrated compounds in the starting material which will be released as carbon dioxide and water vapor during processing. A more complete mass balance would include measurement of the exhaust gas flow rate and input air flow rate rather than assuming the deficit mass was part of the off-gas. While measurement and analysis of exhaust gas flows is necessary to obtain a complete mass balance, in practical terms, it is somewhat complex and expensive. Also, since conservation of total mass must hold, measurements of only solid masses may be considered adequate for the scope and requirements of this project.

The elemental mass balance for the HVPMS revealed that the majority of zinc, cadmium, and lead ended up in particulates in the melt chamber and exhaust system while chromium tended to remain in the slag. The elemental mass balances in general did not account for the metal amounts originally introduced, particularly for chromium having a mass balance closure of just 35%. Mass balances for the other toxic metals on average were 80% for lead, 73% for zinc, and 67% for cadmium. Cesium tended to partition half into the slag and half into the off-gas particulates. The mass balance closure for cesium was just 60%. Partitioning behavior of the surrogate elements, cerium and samarium, is uncertain due the very poor mass balance results ranging from 20-30%. These elements are expected to remain in the slag, and indeed while the relative mass amounts found in the slag are much higher (about 10 times) than for the off-gas particulates, the poor mass balance closure leaves open the question about the ultimate fate of the surrogate elements.

A reason for the poor mass balances may be the result of two factors. First, the mass of the slag is substantially larger than that of the particulates. Therefore a small discrepancy in the measured concentrations of HVPMS and surrogates could cause large discrepancies in the overall mass balance for an element. Second, the widely varying mass closure results suggest the possibility of elemental partitioning to different parts of the slag. Although this possibility was taken into account by taking samples from the top and bottom parts of the melt, elements may have been concentrated in regions of the slag that were not sampled. Based on these possibilities, more samples need to be analyzed to determine average concentrations of an element in the slag.

An additional reason for the poor mass balance in the case of the surrogates may be the presence of the refractory liners. It is unknown whether the refractory liners could selectively react with components of the melt, particularly the surrogates, since this possibility was not investigated. Further work to explore this possibility should be funded, since, in an actual processing setting, selective migration of radionuclides would be entirely unwanted.

9.4 Conclusions

The volatilization experiments conducted in FY-93 and FY-94 provided valuable information on partitioning of toxic heavy metals and radionuclides via surrogate elements in a high temperature arc melter processing system. During the course of the experiments many improvements to the data gathering and analysis procedures were made and areas where further improvements could be made were identified. As a minimum, data collection must include measurement of solid mass amounts distributed during processing and elemental analysis of specific areas where solids have accumulated within the processing system. Exhaust gas mass amounts and elemental analysis can be done if budget constraints allow and if the scope of a project require. This may be dictated for preproduction systems where EPA and other environmental regulations will necessitate off-gas measurements to ensure compliance of that system and future production systems. Off-gas measurements will allow total mass balance measurements to made but are not necessary to determine solid mass partitioning within the melter and air pollution control systems.

It is suspected that the standardless EDXS analysis used for elemental analysis tends to slightly overestimate the amounts of titanium, iron and zirconium. This can be seen particularly in the FY-93 volatilization tests where titanium and zirconium were used to normalize calculated compositions for comparison to EDXs data. For this reason it is recommended that for future work the SEM/EDXS equipment be calibrated with a specimen of known concentrations of these elements.

Measurement of volatilization rates for any specific processing system require good temperature and volatile element concentration measurements of the slag. Although individual processing systems will affect volatilization due to geometry, surface area of the melt, energy input mechanism, etc., slag temperature and volatile element concentration are the primary factors affecting volatilization. Future testing must include radioactive bench scale testing where these considerations are taken into account. Also modelling of the partitioning mechanisms within specific processing systems may prove to be an important aspect in gaining knowledge for control of volatilization during radioactive waste processing.

The overall results of these experiments show that provisions must be made for the air pollution control system of any high temperature radioactive processing system containing toxic metals to deal with them since the majority of these metals volatilized. Approximately half or more of any cadmium, zinc, lead and cesium will be volatilized or entrained and end up in the off-gas system. In addition some radionuclide elements (based on results from the surrogate elements) will also end up in the off-gas system. Particulates containing these elements must either be rerouted back to the melter or treated as a separate secondary waste stream.

10. REFERENCES

1. J. L. Mayberry et al., *Preliminary Systems Design Study Assessment Report*, EGG-WTD-9594, EG&G Idaho, Inc., June 1991.
2. F. Feizollahi and W. J. Quapp, *Integrated Thermal Treatment System Study - Phase 2 Results*, INEL-95/0129, Lockheed Idaho Technologies Company, February 1996.
3. F. Feizollahi et al., *Preliminary Stored Waste Systems Design Study for Low-Level TRU Waste Treatment Assessment Report*, EGG-WTD-10254, June 1992.
4. J. E. Flinn et. al., *Annual Report on the TRU Waste Form Studies with Special Reference to Iron-Enriched Basalt: 1980*, EGG-FM-5366, EG&G, Idaho, Inc., June 1981.
5. J. M. Welch, C. W. Sill, and J. E. Flinn, *Leach Tests of Simulated Low-Level Transuranic Waste Forms Containing Transuranic Elements*, EGG-FM-6153, EG&G Idaho, Inc., January 1983.
6. G. A. Reiman, J. D. Grandy, and T. L. Eddy, *Survey of INEL Research on the Iron-Enriched Waste Form*, EGG-WTD-10056, EG&G Idaho, Inc., January 1992.
7. P. C. Kong and G. A. Reiman, *Improving Iron-Enriched Basalt with Additions of ZrO_2 and TiO_2* , EGG-MS-10642, EG&G Idaho, Inc., June 1993.
8. G. A. Reimann and P. C. Kong, "Iron-Enriched Basalt Waste Form Improved with TiO_2 and ZrO_2 ", *Actinide Processing*, (Proc.), p. 275, B. Mishra and W. A. Averill (eds.), The Metallurgical Society, Warrendale, PA, March 1994.
9. J. M. Welch, R. L. Miller, and J. E. Flinn, *Fuel and Core Storage and Disposal Development: FY-82 Immobilization of Three-Mile Island Core Debris*, EGG-FM-6059, EG&G Idaho, Inc., June 1983.
10. J. M. Welch, R. L. Miller, and J. E. Flinn, "Immobilization of Three-Mile Island Core Debris," *2nd Int. Symp. Ceramics in Nuclear Waste Management, Chicago, April 1983*.
11. J. G. Conley, P. V. Kelsey, and D. V. Miley, "Investigation of the Properties of Iron-Enriched Basalt with TiO_2 and ZrO_2 Addition," *American Ceramic Society 85th Annual Meeting, 1983*.

12. T. L. Eddy, P. C. Kong, B. D. Raivo, and G. L. Anderson, *Thermal Processing System Concepts and Considerations for RWMC Buried Waste*, EGG-WTD-10058, EG&G Idaho, Inc., February 1992.
13. P. C. Kong, J. D. Grandy, A. D. Watkins, T. L. Eddy, and G. L. Anderson, *Bench-Scale Arc Melter for R&D in Thermal Treatment of Mixed Wastes*, EGG-MS-10646, EG&G Idaho, Inc., May 1993.
14. T. L. Eddy, et. al., *Modified Bench-Scale Arc Melter for Waste Processing*, EG&G Idaho, Inc., EGG-MS-10941, March 1994.
15. D. R. Lide (ed.), *CRC Handbook of Chemistry and Physics*, 75th Edition, Section 4, CRC Press, Boca Raton, 1994.

Appendix A

LDRD FY-94 Annual Report

Project Title: Sensing Techniques for Thermal Treatment of Mixed Waste

Project Leader: N.M. Carlson

PHONE 6-6302

II. FY 1994 ACCOMPLISHMENTS: What did you accomplish and how does this compare with your project plan? How did you demonstrate the viability of the idea?

Electrical signals from the arc melter were monitored on three separate arc melter runs. During these runs a Hall effect probe was used to measure the AC transient current in the electrodes at various times and under various conditions during each run. Because of safety considerations, the voltage across the electrodes was not monitored. One run included a start with a steel bar for which baseline current data was obtained.

The current signal correlated with the state of operation of the arc melter, to the extent that the state was known from visual observation or from parameter settings. Obvious qualitative differences were observed in the current signal among start up, steady-state operation, and transient events, such as arc extinction and starting or stopping feed into the melter. These qualitative differences could be used to determine the state of the melter in real time, thus providing a basis for automatic control. However, better, independent, correlated observations of the state of the melter are required to confirm the few correlations observed in the three runs. One easy way to accomplish this would be to use the weld vision system to observe the interior of the reactor, as was proposed in the renewal of this LDRD.

Mounts for acoustic sensors were designed and constructed and the data acquisition system was modified to obtain acoustical data. Due to the limitation of only being able to monitor three arc melter runs, no acoustical data was acquired.

LABORATORY DIRECTED RESEARCH AND DEVELOPMENT

FY-1994 ANNUAL REPORT

Project Number: 8714

Project Title: Sensing Techniques for Thermal Treatment of Mixed
Waste

Project Leader: N.M. Carlson

PHONE 6-6302

Date Initiated: April, 1994

Prior Year Costs: \$0

FY-1994 Costs: \$12K

Appendix B

Melter Off Gas Sampling Procedures

Melter Off Gas Sampling Procedure

- 1) Level and zero the Method 5 (M-5) box manometer.
- 2) Record local atmospheric parameters and sample identification information on the data sheet.
- 3) Place the crushed ice/water mixture in the sample train assembly box.
- 4) Perform the first pretest leak check
 - a. Fully open the M-5 bypass valve and close the M-5 coarse valve.
 - b. Start the pump and operate for a 15 minute warm-up time, prior to leak checking the sample train.
 - c. Connect the sample train assembly to the pump and place a stopper in the first impinger inlet (will be connected to the in the following step).
 - d. Open the M-5 coarse valve to mid-position.
 - e. Slowly close the bypass valve until a 15 in. Hg vacuum is obtained. To not reopen the bypass valve, since the impinger water may be drawn out.
 - f. Note the leak rate measured by the dry gas meter (DGM). Failure is defined as leakage above 0.02 cfm or above 4% of the average sampling rate. If the leakage is excessive, check the tightness of the fittings along the sampling flowpath.
 - g. After a successful leak test, slowly break the vacuum upstream of the impinger assembly.
 - h. Return the M-5 bypass valve to the fully open position and the coarse valve to the fully cooled position.
 - i. Record the pretest leak rate on the data sheet.
- 5) Perform the second pretest leak check
 - a. Check/close the sampling valve.
 - b. Connect the sample train assembly to the melter through the swaglock fitting.
 - c. Repeat steps d through i in 3) above.
- 6) Record the initial DGM reading.

- 7) When the melter is fully operational, observe the melter air inlet flowrate on the melter digital flow meter.
- 8) Collect a sample as follows
 - a. Open the M-5 bypass valve and the coarse valve.
 - b. Open the melter sampling valve, then close the melter baghouse valve.
Caution: Some reverse flow, initiated by the baghouse vacuum, may occur. Watch the sampling rate, dH on the M-5 manometer during this process.
 - c. Record the start time.
 - d. Slowly close the bypass valve until the desired manometer level differential is obtained, or until the inlet flow rate on the digital meter noted in step 6) is matched with the flowrate prior to sampling.
 - e. Adjust the M-5 bypass valve during sampling as necessary to maintain the desired flowrate.
 - f. Record complete sets of data at least once each 5 minutes during the sampling period.
 - g. Ensure the air temperature exiting the sample train assemble does not exceed 68 F. Add ice to sample train assembly box as necessary to maintain exit air temperature.
 - h. To conclude the sampling, open the melter baghouse valve, the close the M-5 coarse valve.
 - i. Record the sampling stop time.
 - j. Close the melter sampling valve. Note: A slight vacuum will exist between the sample train assemble and the melter sampling valve.
 - k. Record the final set of data corresponding to the stop time.
- 9) Perform the post test leak check
 - a. Fully open the M-5 bypass valve and close the M-5 coarse valve.
 - b. Open the coarse valve to the mid-position.
 - c. Slowly close the bypass valve until a vacuum is reached that is greater than the maximum value obtained during the sample run.
 - d. Note the leak rate measured by the DGM. Failure criteria are the same as before. Excessive leakage requires either adjustment of flow volume data or voiding the run.
 - e. After a successful leak test, slowly break vacuum upstream of the sample train assembly.
 - f. Shut off the pump.
- 10) Disconnect the filter/impinger assembly and cap off the melter end of the assembly. Transfer the assembly to the designated area for sample recovery.

Appendix C

Composition and Normalization Calculation Worksheets

For all HVPM runs and CC01 & CC02						
	IEB4/A-80	IEB4A-40	IEB/A-40+H+S	Alkali Mix		
	(8wt%ti,4wt%zr)	(4wt%ti,2wt%zr)	(9wt%h+s)			
	(wt%)	(wt%)	(wt%)	(wt%)		
SiO2	53.15	47.94	43.63	23.97		
Al2O3	10.56	9.59	8.73	4.79		
Fe2O3						
Fe3O4	8.27	18.33	16.68	9.17		
CaO	8.71	9.12	8.30	4.56		
MgO	2.46	3.29	2.99	1.65		
Na2O	1.94	3.01	2.74	1.50		
NaOH				33.33		
K2O	2.46	2.44	2.22	1.22		
KOH				16.67		
TiO2	8.44	4.28	3.90	2.14		
ZrO2	4.00	2.00	1.82	1.00		
Pb			1.00			
Cd			1.00			
Zn			1.00			
Cr			1.00			
CeO2			1.00			
Sm2O3			1.00			
Gd2O3			1.00			
Nd2O3			1.00			
CsCO3			1.00			
Total	100.00	100.00	100.00	100.00		
IEB4/A-80 is 10 wt% TiO2 and 5wt% ZrO2 by soil mass (80%).			By total wt% this is 8 and 4			
IEB4/A-40 is 10 wt% TiO2 and 5wt% ZrO2 by soil mass (40%).			By total wt% this is 4 and 2			

C-3

C-5

	HVPM-02	plus	HVPM-02 Final Composition	HVPM-03	plus	HVPM-03 Final Compositi
	(6 kg IEB4/A-80)	(1 kg IEB4/A-40+H+S)	(6 kg IEB4/A-80)	(1 kg IEB4/A-40+H+S)	(6 kg IEB4/A-80)	(1 kg IEB4/A-40+H+S)
	(grams)	(grams)	(grams)	(grams)	(grams)	(grams)
SiO2	3189.12	436.25	3625.37	3189.12	436.25	3625.37
Al2O3	633.6	87.25	720.85	633.60	87.25	720.85
Fe2O3					0.00	0.00
Fe3O4	496.32	166.80	663.12	496.32	166.80	663.12
CaO	522.72	82.97	605.69	522.72	82.97	605.69
MgO	147.84	29.94	177.78	147.84	29.94	177.78
Na2O	116.16	27.37	143.53	116.16	27.37	143.53
NaOH					0.00	0.00
K2O	147.84	22.24	170.08	147.84	22.24	170.08
KOH		0.00	0.00		0.00	0.00
TiO2	506.4	38.97	545.37	506.40	38.97	545.37
ZrO2	240	18.20	258.20	240.00	18.20	258.20
Pb		10.00	10.00		10.00	10.00
Cd		10.00	10.00		10.00	10.00
Zn		10.00	10.00		10.00	10.00
Cr		10.00	10.00		10.00	10.00
CeO2		10.00	10.00		10.00	10.00
Sm2O3		10.00	10.00		10.00	10.00
Gd2O3		10.00	10.00		10.00	10.00
Nd2O3		10.00	10.00		10.00	10.00
CsCO3		10.00	10.00		10.00	10.00
Total	6000	1000	7000	6000	1000	7000

	HVPM-04 (restart of 03) (grams)	plus (0.7 kg alkali mix) (grams)	HVPM-04 Final Composition (grams)
SiO2	3625.37	167.79	3793.16
Al2O3	720.85	33.56	754.41
Fe2O3			0.00
Fe3O4	663.12	64.16	727.28
CaO	605.69	31.91	637.61
MgO	177.78	11.52	189.29
Na2O	143.53	10.53	154.06
NaOH		233.33	233.33
K2O	170.08	8.55	178.63
KOH		116.67	116.67
TiO2	545.37	14.99	560.35
ZrO2	258.20	7.00	265.20
Pb	10.00		10.00
Cd	10.00		10.00
Zn	10.00		10.00
Cr	10.00		10.00
CeO2	10.00		10.00
Sm2O3	10.00		10.00
Gd2O3	10.00		10.00
Nd2O3	10.00		10.00
CsCO3	10.00		10.00
Total	7000	700	7700

	HVPM-05 (restart of 04) (grams)	plus (0.5 kg IEB4/A-40) (grams)	plus (2 kg IEB4/A40+H+S) (grams)	plus (0.87 kg Alkali mix) (grams)	HVPM-05 Final Composition (grams)
SiO2	3793.16	239.70	872.51	208.54	5113.91
Al2O3	754.41	47.94	174.50	41.71	1018.56
Fe2O3	0.00			0.00	0.00
Fe3O4	727.28	91.65	333.61	79.74	1232.27
CaO	637.61	45.59	165.95	39.66	888.81
MgO	189.29	16.45	59.88	14.31	279.93
Na2O	154.06	15.04	54.75	13.08	236.93
NaOH	233.33			290.00	523.33
K2O	178.63	12.22	44.48	10.63	245.97
KOH	116.67			145.00	261.67
TiO2	560.35	21.41	77.93	18.63	678.32
ZrO2	265.20	10.00	36.40	8.70	320.30
Pb	10.00		20.00		30.00
Cd	10.00		20.00		30.00
Zn	10.00		20.00		30.00
Cr	10.00		20.00		30.00
CeO2	10.00		20.00		30.00
Sm2O3	10.00		20.00		30.00
Gd2O3	10.00		20.00		30.00
Nd2O3	10.00		20.00		30.00
CsCO3	10.00		20.00		30.00
Total	7700	500	2000	870	11070

C-7

	HVPM-06	plus	plus	plus	HVPM-06
	(restart of 05)	(0.5 kg IEB4/A-40)	(2 kg IEB4/A40+H+S)	(2 kg IEB4/A-40)	Final
	(grams)	(grams)	(grams)	(grams)	Composition
SiO2	5113.91	239.70	872.51	958.80	7184.92
Al2O3	1018.56	47.94	174.50	191.76	1432.76
Fe2O3					0.00
Fe3O4	1232.27	91.65	333.61	366.60	2024.13
CaO	888.81	45.59	165.95	182.36	1282.71
MgO	279.93	16.45	59.88	65.80	422.06
Na2O	236.93	15.04	54.75	60.16	366.88
NaOH	523.33				523.33
K2O	245.97	12.22	44.48	48.88	351.55
KOH	261.67				261.67
TiO2	678.32	21.41	77.93	85.64	863.30
ZrO2	320.30	10.00	36.40	40.00	406.70
Pb	30.00		20.00		50.00
Cd	30.00		20.00		50.00
Zn	30.00		20.00		50.00
Cr	30.00		20.00		50.00
CeO2	30.00		20.00		50.00
Sm2O3	30.00		20.00		50.00
Gd2O3	30.00		20.00		50.00
Nd2O3	30.00		20.00		50.00
CsCO3	30.00		20.00		50.00
Total	11070	500	2000	2000	15570

	CC-05	plus	CC-05
	(6 kg IEB4/A-80)	(4.031 kg IEB4/A40+H+S)	Final
	(grams)	(grams)	Composition
			(grams)
SiO2	3189.12	1683.71	4872.83
Al2O3	633.60	336.74	970.34
Fe2O3			
Fe3O4	496.32	643.77	1140.09
CaO	522.72	320.23	842.95
MgO	147.84	115.55	263.39
Na2O	116.16	105.64	221.80
NaOH			
K2O	147.84	85.84	233.68
KOH			
TiO2	506.40	193.31	699.71
ZrO2	240.00	183.41	423.41
Pb		40.31	40.31
Cd		40.31	40.31
Zn		40.31	40.31
Cr		40.31	40.31
CeO2		40.31	40.31
Sm2O3		40.31	40.31
Gd2O3		40.31	40.31
Nd2O3		40.31	40.31
CsCO3		40.31	40.31
Total	6000.00	4031.00	10031.00

C-12

C-17

					3.105929	2.802298				
HVPM05					correct	correct	slag		(Ti basis)	(Zr basis)
		metals	oxide	with	with		chemical		amount	amount
		basis	basis	titanium	zirconium		analysis		retained	retained
	m/o ratio	(ppm)	(ppm)	(ppm)	(ppm)		(ppm)		%	%
SiO2	0.467	215736	246225	670060	604556		262000		39	43
Al2O3	0.529	48674	43337	151177	136398		52900		35	39
Fe2O3	0.699	77810	33506	241672	218047		97600		40	45
CaO	0.715	57407	22883	178303	160872		70800		40	44
MgO	0.603	15248	10039	47360	42730		19200		41	45
Na2O	0.742	50959	17719	158274	142801		22700		14	16
K2O	0.830	38062	7796	118216	106660		26400		22	25
TiO2	0.599	36704	24571	114000	102856		114000		100	111
ZrO2	0.740	21411	7523	66502	60001		60000		90	100
Pb	1.000	2710	0	8417	7594		524		6	7
Cd	1.000	2710	0	8417	7594		210		2	3
Zn	1.000	2710	0	8417	7594		1420		17	19
Cr	1.000	2710	0	8417	7594		3130		37	41
CeO2	0.814	2206	504	6852	6182		2960		43	48
Sm2O3	0.862	2336	374	7256	6546		2700		37	41
Gd2O3	0.868	2352	358	7306	6592		2880		39	44
Nd2O3	0.857	2322	388	7213	6508		2880		40	44
Cs2CO3	0.816	2211	499	6868	6197		2310		34	37
Totals		584279	415721	1814729	1637324	Total	744614			

C-21

					2.904599	3.016803				
CC-01					correct	correct		slag	(Ti basis)	(Zr basis)
			metals	oxide	with	with		chemical	amount	amount
			basis	basis	titanium	zirconium		analysis	retained	retained
	m/o factor		(ppm)	(ppm)	(ppm)	(ppm)		(ppm)	%	%
SiO2	0.467		224147	255825	651057	676207		231000	35	34
Al2O3	0.529		50616	45067	147020	152700		54400	37	36
Fe2O3	0.699		91029	39199	264403	274617		186000	70	68
CaO	0.715		60854	24256	176755	183583		71400	40	39
MgO	0.603		16706	10999	48524	50399		17900	37	36
Na2O	0.742		17755	6174	51572	53565		2500	5	5
K2O	0.830		19408	3975	56372	58550		21500	38	37
TiO2	0.599		35461	23739	102999	106978		103000	100	96
ZrO2	0.740		20651	7256	59983	62300		62300	104	100
Pb	1.000		5209	0	15131	15715		1940	13	12
Cd	1.000		5209	0	15131	15715		805	5	5
Zn	1.000		5209	0	15131	15715		3240	21	21
Cr	1.000		5209	0	15131	15715		5790	38	37
CeO2	0.814		4240	969	12317	12792		3960	32	31
Sm2O3	0.862		4490	719	13043	13547		3700	28	27
Gd2O3	0.868		4522	688	13134	13641		3840	29	28
Nd2O3	0.857		4464	745	12967	13468		4020	31	30
Cs2CO3	0.816		4251	959	12347	12824		4030	33	31
			579432	420568	1683017	1748032	Total	781325		
			Total (ppm)	1000000						

Appendix D

Volatilization Rate Calculations

IRC ARC MELTER
MULTIPLE METALS/PARTICLE EMISSIONS

Page 1 of 3

PLANT:	INEL	OPERATORS:	HILLARY, GOTSCH
FACILITY:	IRC	ENTERED BY:	D. M. GINOSAR
SAMPLE LOCATION:	IRC MELTER OUTLET	CHECKED BY:	

09/20/93
IRCRUN1

ENTERED DATA	SYMBOL	UNITS	DATA	DATA	DATA	AVERAGE
RUN NUMBER	---	---	2	3	5	---
TEST DATE			06/23/93	06/24/93	07/01/93	
TEMPERATURES:						
STACK AVERAGE	Cs	deg C	252.2	325.3	257.9	
METER INLET	Fmi	deg F	79.3	77.8	78.5	
METER OUTLET	Fmo	deg F	76.9	74.7	76.1	
METER AVERAGE	Fm	deg F	78.1	76.3	77.3	
PRESSURES:						
BAROMETRIC	Pbar	in Hg	25.36	25.43	25.24	
dH (AVERAGE)	dH	in H2O	0.24	1.04	0.28	
GAS SAMPLE VOLUME	Vm	cu ft	9.687	10.01	10.14	
METER CALIBRATION FACTOR	Y	---	1	1	1	
SAMPLING TIME (TOTAL)	min	min	30	17	30	
STACK GAS CONTENT:						
OXYGEN	Co2	%	21	21	21	
CARBON DIOXIDE	Cco2	%	0	0	0	
WATER COLLECTED	Wlc	gm	73.2	61.59	52.2	
FILTER CATCH	Wf	mg	2370	1171	1849	
METALS CATCH:						
VOL OF ANALYZED SAMPLE	Vl	L	0.25	0.25	0.25	
CADMIUM	CCd	ug/l	947,000	449,000	666,000	
CERIUM	CCe	ug/l	6,230	5,690	4,240	
CESIUM	CCs	ug/l	164,000	73,900	124,000	
CHROMIUM (TOTAL)	CCr	ug/l	3,260	2,260	8,620	
GADOLINIUM	CGd	ug/l	10,100	10,700	5,490	
LEAD	CPb	ug/l	1,360,000	473,000	713,000	
NEODYMIUM	CNd	ug/l	9,240	12,200	5,580	
SAMARIUM	CSm	ug/l	6,980	7,560	5,120	
ZINC	CZn	ug/l	991,000	581,000	574,000	

MULTIPLE METALS/PARTICLE EMISSIONS

PLANT: INEL

09/20/93
IRCRUN1

CALCULATED DATA	SYMBOL	UNITS	DATA	DATA	DATA	AVERAGE
RUN NUMBER	—	—	2	3	5	—
TEST DATE			06/23/93	06/24/93	07/01/93	
TEMPERATURES: STACK AVERAGE, [Cs*1.8+492] METER INLET, [Fmi+460] METER OUTLET, [Fmo+460] METER AVERAGE, [Fm+460]	Ts Tmi Tmo Tm	deg R deg R deg R deg R	946 539 537 538	1078 538 535 536	956 539 536 537	
GAS SAMPLE VOLUME (STP) [17.64*Y*(Vm/Tm)* (Pbar+dH/13.6)]	VmStd	cu ft	8.059	8.399	8.409	
WATER VAPOR VOLUME [0.04647*Wlc]	VwStd	cu ft	3.40	2.86	2.43	
GAS MOISTURE FRACTION [VwStd/(VmStd+VwStd)]	Bws	—	0.2968	0.2542	0.2239	
GAS MOLECULAR WEIGHT DRY STACK GAS [0.32(Co2,m)+0.44(Cco2,m)+ 0.28(100-(Co2,m)-(Cco2,m))] WET STACK GAS [Md(1-Bws)+18.0*Bws]	Md Mw	g/g-mol g/g-mol	28.84 25.62	28.84 26.08	28.84 26.41	
STACK GAS FLOWRATE, (DStd) VmStd/min	Qsd Qsdm	dscfm dscmm	0.269 0.00761	0.494 0.01399	0.280 0.00794	
PARTICLE MATTER PASSING THRU IMPINGERS CONCENTRATION (DRY, STD) [0.01543*Wf/VmStd] MASS FLOW [(Qst*Wf/VmStd)*1.323e-4]	Ct Ctm Ms Msm	gr/dscf g/dscm lb/hr g/hr	4.537 10.38 0.01045 4.74	2.151 4.92 0.00911 4.13	3.393 7.76 0.00815 3.70	
METAL CONCENTRATIONS: (DRY STP) (1.543E-5)*VI*C/VmStd						
CADMIUM	Ct,Cd Ctm,Cd	gr/dscf g/dscm	4.53E-01 1.04E+00	2.06E-01 4.72E-01	3.06E-01 6.99E-01	
CERIUM	Ct,Ce Ctm,Ce	gr/dscf g/dscm	2.98E-03 6.82E-03	3.39E-02 7.77E-02	5.69E-02 1.30E-01	
CESIUM	Ct,Cs Ctm,Cs	gr/dscf g/dscm	7.85E-02 1.80E-01	3.39E-02 7.77E-02	5.69E-02 1.30E-01	
CHROMIUM (TOTAL)	Ct,Cr Ctm,Cr	gr/dscf g/dscm	1.56E-03 3.57E-03	1.04E-03 2.38E-03	3.95E-03 9.05E-03	
GADOLINIUM	Ct,Gd Ctm,Gd	gr/dscf g/dscm	4.83E-03 1.11E-02	4.91E-03 1.12E-02	2.52E-03 5.76E-03	
LEAD	Ct,Pb Ctm,Pb	gr/dscf g/dscm	6.51E-01 1.49E+00	2.17E-01 4.97E-01	3.27E-01 7.48E-01	
NEODYMIUM	Ct,Nd Ctm,Nd	gr/dscf g/dscm	4.42E-03 1.01E-02	5.60E-03 1.28E-02	2.56E-03 5.86E-03	
SAMARIUM	Ct,Sm Ctm,Sm	gr/dscf g/dscm	3.34E-03 7.65E-03	3.47E-03 7.95E-03	2.35E-03 5.37E-03	
ZINC	Ct,Zn Ctm,Zn	gr/dscf g/dscm	4.74E-01 1.09E+00	2.67E-01 6.11E-01	2.63E-01 6.03E-01	

MULTIPLE METALS/PARTICLE EMISSIONS

PLANT: INEL

09/20/93
IRCRUN1

CALCULATED DATA	SYMBOL	UNITS	DATA	DATA	DATA	AVERAGE
RUN NUMBER	---	---	2	3	5	---
TEST DATE			06/23/93	06/24/93	07/01/93	
METAL MASS FLOWS: (DRY, STP) [(1.323E-7)*V1*C*Qsd/VmStd]						
CADMIUM	M,Cd	lb/hr kg/hr	1.04E-03 4.74E-04	8.74E-04 3.96E-04	7.34E-04 3.33E-04	
CERIUM	M,Ce	lb/hr kg/hr	6.87E-06 3.12E-06	1.11E-05 5.02E-06	4.67E-06 2.12E-06	
CESIUM	M,Cs	lb/hr kg/hr	1.81E-04 8.20E-05	1.44E-04 6.52E-05	1.37E-04 6.20E-05	
CHROMIUM (TOTAL)	M,Cr	lb/hr kg/hr	3.59E-06 1.63E-06	4.40E-06 1.99E-06	9.50E-06 4.31E-06	
GADOLINIUM	M,Gd	lb/hr kg/hr	1.11E-05 5.05E-06	2.08E-05 9.44E-06	6.05E-06 2.75E-06	
LEAD	M,Pb	lb/hr kg/hr	1.50E-03 6.80E-04	9.20E-04 4.17E-04	7.86E-04 3.57E-04	
NEODYMIUM	M,Nd	lb/hr kg/hr	1.02E-05 4.62E-06	2.37E-05 1.08E-05	6.15E-06 2.79E-06	
SAMARIUM	M,Sm	lb/hr kg/hr	7.70E-06 3.49E-06	1.47E-05 6.67E-06	5.64E-06 2.56E-06	
ZINC	M,Zn	lb/hr kg/hr	1.09E-03 4.96E-04	1.13E-03 5.13E-04	6.33E-04 2.87E-04	

IRC ARC MELTER
MULTIPLE METALS/PARTICLE EMISSIONS

Page 1 of 3

PLANT:
FACILITY:
SAMPLE LOCATION:

INEL
IRC
IRC MELTER OUTLET

OPERATORS:
ENTERED BY:
CHECKED BY:

HILLARY, GOTSCH
D. M. GINOSAR

09/20/93
IRCRUN2

ENTERED DATA	SYMBOL	UNITS	DATA	DATA	DATA	AVERAGE
RUN NUMBER	---	---	6	6		---
TEST DATE			07/02/93	07/02/93		
TEMPERATURES:						
STACK AVERAGE	Cs	deg C	193.0	149.9		171.5
METER INLET	Fmi	deg F	77.0	79.5		78.3
METER OUTLET	Fmo	deg F	75.0	78.3		76.7
METER AVERAGE	Fm	deg F	76.0	78.9		77.5
PRESSURES:						
BAROMETRIC	Pbar	in Hg	25.19	25.19		25.2
dH (AVERAGE)	dH	in H2O	0.33	0.19		0.3
GAS SAMPLE VOLUME	Vm	cu ft	4	2.4		3.2
METER CALIBRATION FACTOR	Y	---	1	1		1.0
SAMPLING TIME (TOTAL)	min	min	11	9		10.0
STACK GAS CONTENT:						
OXYGEN	Co2	%	21	21		21.0
CARBON DIOXIDE	Cco2	%	0	0		
WATER COLLECTED	Wlc	gm	10.81	1.9		6.4
FILTER CATCH	Wf	mg	729	248		488.2
METALS CATCH:						
VOL OF ANALYZED SAMPLE	VI	L	0.25	0.25		0.25
CADMIUM	CCd	ug/l	206,000	191,000		198,500
CERIUM	CCe	ug/l	1,410	500		955
CESIUM	CCs	ug/l	99,000	12,000		55,500
CHROMIUM (TOTAL)	CCr	ug/l	12,300	8,880		10,590
GADOLINIUM	CGd	ug/l	1,850	500		1,175
LEAD	CPb	ug/l	162,000	25,500		93,750
NEODYMIUM	CNd	ug/l	1,790	500		1,145
SAMARIUM	Csm	ug/l	1,770	500		1,135
ZINC	CZn	ug/l	338,000	32,000		185,000

MULTIPLE METALS/PARTICLE EMISSIONS

PLANT: INEL

09/20/93
IRCRUN2

CALCULATED DATA	SYMBOL	UNITS	DATA	DATA	DATA	AVERAGE
RUN NUMBER	---	---	6	6		---
TEST DATE			07/02/93	07/02/93		
TEMPERATURES: STACK AVERAGE, [Cs*1.8+492] METER INLET, [Fmi+460] METER OUTLET, [Fmo+460] METER AVERAGE, [Fm+460]	Ts Tmi Tmo Tm	deg R deg R deg R deg R	839 537 535 536	762 540 538 539		801 538 537 537
GAS SAMPLE VOLUME (STP) [17.64*Y*(Vm/Tm)* (Pbar+dH/13.6)]	VmStd	cu ft	3.319	1.980		2.648
WATER VAPOR VOLUME [0.04647*Wlc]	VwStd	cu ft	0.50	0.09		0.30
GAS MOISTURE FRACTION [VwStd/(VmStd+VwStd)]	Bws	---	0.1314	0.0427		0.1003
GAS MOLECULAR WEIGHT DRY STACK GAS [0.32(Co2,m)+0.44(Cco2,m)+ 0.28(100-(Co2,m)-(Cco2,m))] WET STACK GAS [Md(1-Bws)+18.0*Bws]	Md Mw	g/g-mol g/g-mol	28.84 27.42	28.84 28.38		28.84 27.75
STACK GAS FLOWRATE, (DStd) VmStd/min	Qsd Qsdm	dscfm dscmm	0.302 0.00855	0.220 0.00623		0.265 0.00750
PARTICLE MATTER PASSING THRU IMPINGERS CONCENTRATION (DRY, STD) [0.01543*W/VmStd] MASS FLOW [(Qst*W/VmStd)*1.323e-4]	Ct Ctm Ms Msm	g/dscf g/dscm lb/hr g/hr	3.387 7.75 0.00876 3.97	1.931 4.42 0.00364 1.65		2.845 6.51 0.00646 2.93
METAL CONCENTRATIONS: (DRY STP) (1.543E-5)*VI*C/VmStd						
CADMIUM	Ct,Cd Ctm,Cd	g/dscf g/dscm	2.39E-01 5.48E-01	3.72E-01 8.52E-01		2.89E-01 6.62E-01
CERIUM	Ct,Ce Ctm,Ce	g/dscf g/dscm	1.64E-03 3.75E-03	2.34E-02 5.35E-02		8.09E-02 1.85E-01
CESIUM	Ct,Cs Ctm,Cs	g/dscf g/dscm	1.15E-01 2.63E-01	2.34E-02 5.35E-02		8.09E-02 1.850E-01
CHROMIUM (TOTAL)	Ct,Cr Ctm,Cr	g/dscf g/dscm	1.43E-02 3.27E-02	1.73E-02 3.96E-02		1.54E-02 3.531E-02
GADOLINIUM	Ct,Gd Ctm,Gd	g/dscf g/dscm	2.15E-03 4.92E-03	9.74E-04 2.23E-03		1.71E-03 3.917E-03
LEAD	Ct,Pb Ctm,Pb	g/dscf g/dscm	1.88E-01 4.31E-01	4.97E-02 1.14E-01		1.37E-01 3.13E-01
NEODYMIUM	Ct,Nd Ctm,Nd	g/dscf g/dscm	2.08E-03 4.76E-03	9.74E-04 2.23E-03		1.67E-03 3.817E-03
SAMARIUM	Ct,Sm Ctm,Sm	g/dscf g/dscm	2.06E-03 4.71E-03	9.74E-04 2.23E-03		1.65E-03 3.784E-03
ZINC	Ct,Zn Ctm,Zn	g/dscf g/dscm	3.93E-01 8.99E-01	6.23E-02 1.43E-01		2.70E-01 6.168E-01

MULTIPLE METALS/PARTICLE EMISSIONS

PLANT: INEL

09/20/93
IRCRUN2

CALCULATED DATA	SYMBOL	UNITS	DATA	DATA	DATA	AVERAGE
RUN NUMBER	--	--	6	6		--
TEST DATE			07/02/93	07/02/93		
METAL MASS FLOWS: (DRY, STP) [(1.323E-7)*VI*C*Qsd/VmStd]						
CADMIUM	M,Cd	lb/hr kg/hr	6.19E-04 2.81E-04	7.02E-04 3.18E-04		6.57E-04 2.978E-04
CERIUM	M,Ce	lb/hr kg/hr	4.24E-06 1.92E-06	1.84E-06 8.33E-07		3.16E-06 1.433E-06
CESIUM	M,Cs	lb/hr kg/hr	2.98E-04 1.35E-04	4.41E-05 2.00E-05		1.84E-04 8.327E-05
CHROMIUM (TOTAL)	M,Cr	lb/hr kg/hr	3.70E-05 1.68E-05	3.26E-05 1.48E-05		3.50E-05 1.59E-05
GADOLINIUM	M,Gd	lb/hr kg/hr	5.56E-06 2.52E-06	1.84E-06 8.33E-07		3.89E-06 1.76E-06
LEAD	M,Pb	lb/hr kg/hr	4.87E-04 2.21E-04	9.37E-05 4.25E-05		3.10E-04 1.41E-04
NEODYMIUM	M,Nd	lb/hr kg/hr	5.38E-06 2.44E-06	1.84E-06 8.33E-07		3.79E-06 1.718E-06
SAMARIUM	M,Sm	lb/hr kg/hr	5.32E-06 2.41E-06	1.84E-06 8.33E-07		3.75E-06 1.703E-06
ZINC	M,Zn	lb/hr kg/hr	1.02E-03 4.61E-04	1.18E-04 5.33E-05		6.12E-04 2.776E-04

IRC ARC MELTER
MULTIPLE METALS/PARTICLE EMISSIONS

Page 1 of 3

PLANT:
FACILITY:
SAMPLE LOCATION:

INEL
IRC
IRC MELTER OUTLET

OPERATORS:
ENTERED BY:
CHECKED BY:

HILLARY, GOTSCH
D. M. GINOSAR

09/20/93
IRCRUN3

ENTERED DATA	SYMBOL	UNITS	DATA	DATA	DATA	AVERAGE
RUN NUMBER	--	--	7	8	9	--
TEST DATE			07/09/93	07/13/93	07/14/93	
TEMPERATURES:						
STACK AVERAGE	Cs	deg C	209.8	57.0	108.0	
METER INLET	Fmi	deg F	82.2	76.5	78.8	
METER OUTLET	Fmo	deg F	79.3	74.3	77.5	
METER AVERAGE	Fm	deg F	80.8	75.4	78.1	
PRESSURES:						
BAROMETRIC	Pbar	in Hg	25.28	25.36	25.32	
dH (AVERAGE)	dH	in H2O	0.94	0.48	0.19	
GAS SAMPLE VOLUME	Vm	cu ft	8.97	9.685	4.23	
METER CALIBRATION FACTOR	Y	--	1	1	1	
SAMPLING TIME (TOTAL)	min	min	15	22	12	
STACK GAS CONTENT:						
OXYGEN	Co2	%	21	21	21	
CARBON DIOXIDE	Cco2	%	0	0	0	
WATER COLLECTED	Wlc	gm	87.42	12.38	37.6	
FILTER CATCH	Wf	mg	607	154	300	
METALS CATCH:						
VOL OF ANALYZED SAMPLE	VI	L	0.25	0.25	0.25	
CADMIUM	CCd	ug/l	2,700,000	816,000	1,110,000	
CERIUM	CCe	ug/l	2,880	3,180	1,030	
CESIUM	CCs	ug/l	113,000	4,890	16,500	
CHROMIUM (TOTAL)	CCr	ug/l	1,140	500	500	
GADOLINIUM	CGd	ug/l	45,500	10,400	10,100	
LEAD	CPb	ug/l	2,230,000	11,700	564,000	
NEODYMIUM	CNd	ug/l	43,600	7,280	11,100	
SAMARIUM	Csm	ug/l	42,100	9,190	8,630	
ZINC	CZn	ug/l	1,330,000	107,000	210,000	

MULTIPLE METALS/PARTICLE EMISSIONS

PLANT: INEL

09/20/93
IRCRUN3

CALCULATED DATA	SYMBOL	UNITS	DATA	DATA	DATA	AVERAGE
RUN NUMBER	--	--	7	8	9	--
TEST DATE			07/09/93	07/13/93	07/14/93	
TEMPERATURES: STACK AVERAGE, [Cs*1.8+492] METER INLET, [Fmi+460] METER OUTLET, [Fmo+460] METER AVERAGE, [Fm+460]	Ts Tmi Tmo Tm	deg R deg R deg R deg R	870 542 539 541	595 537 534 535	686 539 538	
GAS SAMPLE VOLUME (STP) [17.64*Y*(Vm/Tm)* (Pbar+dH/13.6)]	VmStd	cu ft	7.417	8.104	3.513	
WATER VAPOR VOLUME [0.04647*Wlc]	VwStd	cu ft	4.06	0.58	1.75	
GAS MOISTURE FRACTION [VwStd/(VmStd+VwStd)]	Bws	--	0.3539	0.0663	0.3322	
GAS MOLECULAR WEIGHT DRY STACK GAS [0.32(Co2,m)+0.44(Cco2,m)+ 0.28(100-(Co2,m)-(Cco2,m))] WET STACK GAS [Md(1-Bws)+18.0*Bws]	Md Mw	g/g-mol g/g-mol	28.84 25.00	28.84 28.12	28.84 25.24	
STACK GAS FLOWRATE, (DStd) VmStd/min	Qsd Qsdm	dscfm dscmm	0.494 0.01400	0.368 0.01043	0.293 0.00829	
PARTICLE MATTER PASSING THRU IMPINGERS CONCENTRATION (DRY, STD) [0.01543*Wf/VmStd] MASS FLOW [(Qst*Wf/VmStd)*1.323e-4]	Ct Ctm Ms Msm	gr/dscf g/dscm lb/hr g/hr	1.262 2.89 0.00535 2.43	0.293 0.67 0.00092 0.42	1.315 3.01 0.00330 1.50	
METAL CONCENTRATIONS: (DRY STP) (1.543E-5)*VI*C/VmStd						
CADMIUM	Ct,Cd Ctm,Cd	gr/dscf g/dscm	1.40E+00 3.21E+00	3.88E-01 8.89E-01	1.22E+00 2.79E+00	
CERIUM	Ct,Ce Ctm,Ce	gr/dscf g/dscm	1.50E-03 3.43E-03	2.33E-03 5.33E-03	1.81E-02 4.15E-02	
CESIUM	Ct,Cs Ctm,Cs	gr/dscf g/dscm	5.88E-02 1.34E-01	2.33E-03 5.33E-03	1.81E-02 4.15E-02	
CHROMIUM (TOTAL)	Ct,Cr Ctm,Cr	gr/dscf g/dscm	5.93E-04 1.36E-03	2.38E-04 5.45E-04	5.49E-04 1.26E-03	
GADOLINIUM	Ct,Gd Ctm,Gd	gr/dscf g/dscm	2.37E-02 5.42E-02	4.95E-03 1.13E-02	1.11E-02 2.54E-02	
LEAD	Ct,Pb Ctm,P	gr/dscf g/dscm	1.16E+00 2.65E+00	5.57E-03 1.27E-02	6.19E-01 1.42E+00	
NEODYMIUM	Ct,Nd Ctm,Nd	gr/dscf g/dscm	2.27E-02 5.19E-02	3.47E-03 7.93E-03	1.22E-02 2.79E-02	
SAMARIUM	Ct,Sm Ctm,Sm	gr/dscf g/dscm	2.19E-02 5.01E-02	4.37E-03 1.00E-02	9.48E-03 2.17E-02	
ZINC	Ct,Zn Ctm,Zn	gr/dscf g/dscm	6.92E-01 1.58E+00	5.09E-02 1.17E-01	2.31E-01 5.28E-01	

MULTIPLE METALS/PARTICLE EMISSIONS

PLANT: INEL

09/20/93
IRCRUN3

CALCULATED DATA	SYMBOL	UNITS	DATA	DATA	DATA	AVERAGE
RUN NUMBER	—	—	7	8	9	—
TEST DATE			07/09/93	07/13/93	07/14/93	
METAL MASS FLOWS: (DRY, STP) [(1.323E-7)*V1*C*Qsd/VmStd]						
CADMIUM	M,Cd	lb/hr kg/hr	5.95E-03 2.70E-03	1.23E-03 5.56E-04	3.06E-03 1.39E-03	
CERIUM	M,Ce	lb/hr kg/hr	6.35E-06 2.88E-06	4.78E-06 2.17E-06	2.84E-06 1.29E-06	
CESIUM	M,Cs	lb/hr kg/hr	2.49E-04 1.13E-04	7.35E-06 3.33E-06	4.55E-05 2.06E-05	
CHROMIUM (TOTAL)	M,Cr	lb/hr kg/hr	2.51E-06 1.14E-06	7.52E-07 3.41E-07	1.38E-06 6.25E-07	
GADOLINIUM	M,Gd	lb/hr kg/hr	1.00E-04 4.55E-05	1.56E-05 7.09E-06	2.78E-05 1.26E-05	
LEAD	M,Pb	lb/hr kg/hr	4.92E-03 2.23E-03	1.76E-05 7.98E-06	1.55E-03 7.05E-04	
NEODYMIUM	M,Nd	lb/hr kg/hr	9.61E-05 4.36E-05	1.09E-05 4.96E-06	3.06E-05 1.39E-05	
SAMARIUM	M,Sm	lb/hr kg/hr	9.28E-05 4.21E-05	1.38E-05 6.27E-06	2.38E-05 1.08E-05	
ZINC	M,Zn	lb/hr kg/hr	2.93E-03 1.33E-03	1.61E-04 7.30E-05	5.79E-04 2.63E-04	

IRC ARC MELTER
MULTIPLE METALS/PARTICLE EMISSIONS

PLANT: INEL
FACILITY: IRC
SAMPLE LOCATION: IRC MELTER OUTLET

OPERATORS:
ENTERED BY:
CHECKED BY:

GOTSCH
D. M. GINOSAR

09/20/93
IRCRUN4

ENTERED DATA	SYMBOL	UNITS	DATA	DATA	DATA	AVERAGE
RUN NUMBER	---	---	10			---
TEST DATE			07/16/93			
TEMPERATURES:						
STACK AVERAGE	Cs	deg C	107.3			
METER INLET	Fmi	deg F	77.5			
METER OUTLET	Fmo	deg F	76.0			
METER AVERAGE	Fm	deg F	76.8			
PRESSURES:						
BAROMETRIC	Pbar	in Hg	25.38			
dH (AVERAGE)	dH	in H2O	0.29			
GAS SAMPLE VOLUME	Vm	cu ft	7.545			
METER CALIBRATION FACTOR	Y	---	1			
SAMPLING TIME (TOTAL)	min	min	21			
STACK GAS CONTENT:						
OXYGEN	Co2	%	21			
CARBON DIOXIDE	Cco2	%	0			
WATER COLLECTED	Wlc	gm	126.9			
FILTER CATCH	WF	mg	414			
METALS CATCH:						
VOL OF ANALYZED SAMPLE	Vl	L	0.25			
CADMIUM	CCd	ug/l	1,580,000			
CERIUM	CCe	ug/l	5,920			
CESIUM	CCs	ug/l	65,500			
CHROMIUM (TOTAL)	CCr	ug/l	500			
GADOLINIUM	CGd	ug/l	94,400			
LEAD	CPb	ug/l	141,000			
NEODYMIUM	CNd	ug/l	114,000			
SAMARIUM	CSm	ug/l	91,300			
ZINC	CZn	ug/l	176,000			

MULTIPLE METALS/PARTICLE EMISSIONS

PLANT: INEL

09/20/93
IRCRUN4

CALCULATED DATA	SYMBOL	UNITS	DATA	DATA	DATA	AVERAGE
RUN NUMBER	--	--	10			--
TEST DATE			07/16/93			
TEMPERATURES: STACK AVERAGE, [Cs*1.8+492] METER INLET, [Fmi+460] METER OUTLET, [Fmo+460] METER AVERAGE, [Fm+460]	Ts Tmi Tmo Tm	deg R deg R deg R deg R	685 538 536 537			
GAS SAMPLE VOLUME (STP) [17.64*Y*(Vm/Tm)* (Pbar+dH/13.6)]	VmStd	cu ft	6.298			
WATER VAPOR VOLUME [0.04647*Wic]	VwStd	cu ft	5.90			
GAS MOISTURE FRACTION [VwStd/(VmStd+VwStd)]	Bws	--	0.4836			
GAS MOLECULAR WEIGHT DRY STACK GAS [0.32(Co2,m)+0.44(Cco2,m)+ 0.28(100-(Co2,m)-(Cco2,m))] WET STACK GAS [Md(1-Bws)+18.0*Bws]	Md Mw	g/g-mol g/g-mol	28.84 23.60			
STACK GAS FLOWRATE, (DStd) VmStd/min	Qsd Qsdm	dscfm dscmm	0.300 0.00849			
PARTICLE MATTER PASSING THRU IMPINGERS CONCENTRATION (DRY, STD) [0.01543*Wf/VmStd] MASS FLOW [(Qst*Wf/VmStd)*1.323e-4]	Ct Ctm Ms Msm	gr/dscf g/dscm lb/hr g/hr	1.013 2.32 0.00261 1.18			
METAL CONCENTRATIONS: (DRY STP) (1.543E-5)*VI*C/VmStd						
CADMIUM	Ct,Cd Ctm,Cd	gr/dscf g/dscm	9.68E-01 2.21E+00			
CERIUM	Ct,Ce Ctm,Ce	gr/dscf g/dscm	3.63E-03 8.30E-03			
CESIUM	Ct,Cs Ctm,Cs	gr/dscf g/dscm	4.01E-02 9.18E-02			
CHROMIUM (TOTAL)	Ct,Cr Ctm,Cr	gr/dscf g/dscm	3.06E-04 7.01E-04			
GADOLINIUM	Ct,Gd Ctm,Gd	gr/dscf g/dscm	5.78E-02 1.32E-01			
LEAD	Ct,Pb Ctm,P	gr/dscf g/dscm	8.64E-02 1.98E-01			
NEODYMIUM	Ct,Nd Ctm,Nd	gr/dscf g/dscm	6.98E-02 1.60E-01			
SAMARIUM	Ct,Sm Ctm,Sm	gr/dscf g/dscm	5.59E-02 1.28E-01			
ZINC	Ct,Zn Ctm,Zn	gr/dscf g/dscm	1.08E-01 2.47E-01			

MULTIPLE METALS/PARTICLE EMISSIONS

PLANT: INEL

09/20/93
IRCRUN4

CALCULATED DATA	SYMBOL	UNITS	DATA	DATA	DATA	AVERAGE
RUN NUMBER	--	--	10			--
TEST DATE			07/16/93			
METAL MASS FLOWS: (DRY, STP) $[(1.323E-7) \cdot VI \cdot C \cdot Q_{sd} / V_{mStd}]$						
CADMIUM	M,Cd	lb/hr	2.49E-03			
		kg/hr	1.13E-03			
CERIUM	M,Ce	lb/hr	9.32E-06			
		kg/hr	4.23E-06			
CESIUM	M,Cs	lb/hr	1.03E-04			
		kg/hr	4.68E-05			
CHROMIUM (TOTAL)	M,Cr	lb/hr	7.88E-07			
		kg/hr	3.57E-07			
GADOLINIUM	M,Gd	lb/hr	1.49E-04			
		kg/hr	6.74E-05			
LEAD	M,Pb	lb/hr	2.22E-04			
		kg/hr	1.01E-04			
NEODYMIUM	M,Nd	lb/hr	1.80E-04			
		kg/hr	8.14E-05			
SAMARIUM	M,Sm	lb/hr	1.44E-04			
		kg/hr	6.52E-05			
ZINC	M,Zn	lb/hr	2.77E-04			
		kg/hr	1.26E-04			

Appendix E

EDXS and XRF Data

-

Filter Particulate Analysis - ARM082394.

Element	XRF 4.1	XRF 5.1	EDXS #1	EDXS #3
Mg	0	0	0	0
Al	0	0	0	2900
Si	38300	84300	35500	139000
K	15900	18000	0	37300
Ca	2800	4600	0	2900
Ti	3000	5700	0	5400
Fe	45600	75900	16100	39100
Zn	204300	156300	129800	261000
Zr	611	1900	0	0
Cd	237000	78000	240200	99100
Cs	12700	13800	18100	28300
Ce	442	1300	0	0
Sm	785	2100	0	0
Pb	232100	18400	261600	159500

Filter Particulate Analysis - ARM082694.

Element	XRF 4.1	XRF 5.1	EDXS #1	EDXS #3
Mg	0	0	0	2600
Al	0	0	0	3400
Si	33800	111300	40200	109500
K	11200	32300	34300	29800
Ca	1500	12600	0	7900
Ti	2600	3000	0	9800
Fe	22400	27900	22600	52800
Zn	179700	150300	153300	85000
Zr	741	654	0	0
Cd	157600	33200	216700	109400
Cs	14700	3000	27100	25000
Ce	381	775	0	0
Sm	786	1100	0	0
Pb	174700	146000	191600	149000

Filter Particulate Analysis - ARM090694.

Element	XRF 4.1	XRF 5.1	EDXS F1	EDXS F2	EDXS F3	EDXS F4	EDXS F5	EDXS F6
Al	0	0	0	0	0	0	6700	0
Si	41600	29900	27900	22200	25900	20200	23300	66100
K	41600	32600	21400	77600	35900	41300	41200	52000
Ca	1100	4000	1800	600	0	0	1900	2300
Cr	3100	4300	0	0	0	0	0	0
Fe	59300	33100	298000	13000	14200	618400	36000	23200
Zn	173000	173500	205900	146400	143100	175200	126700	163600
Zr	755	978	0	7000	1700	3100	6300	0
Cd	216000	222900	203500	246700	241600	241600	244000	175500
Cs	17300	23300	29600	73300	81900	58300	82400	60600
Pb	199100	215100	216000	230400	229100	196200	237200	140900

Filter Particulate Analysis - ARM090894

Element	XRF 4.1	XRF 5.1	EDXS F1	EDXS F2	EDXS F3	EDXS F4	EDXS F5
Al	0	0	0	0	0	0	6700
Si	27800	55800	51100	48600	85900	105900	54200
K	13200	7900	39000	40400	55500	60700	54200
Ca	1100	2200	600	4900	1000	4300	2900
Cr	0	0	900	5000	1400	1000	900
Fe	35900	19800	38300	67200	40000	27600	28200
Zn	190100	200600	212700	145300	211600	123400	230300
Zr	656	1100	0	0	0	0	0
Cd	218200	61800	220000	289500	187600	57800	50800
Cs	14700	22600	34200	33100	72700	81000	112000
Pb	178700	145200	196100	124000	108000	86400	132500

Filter Particulate Analysis - ARM092094.

Element	EDXS-F1	EDXS-F2
Al	0	0
Si	36900	24700
K	17700	31500
Ca	0	900
Cr	800	3400
Fe	16100	12500
Zn	238800	195500
Zr	0	0
Cd	157800	199700
Cs	12100	27000
Pb	277300	254700

Filter Particulate Analysis - ARM092294.

Element	EDXS-F1	EDXS-F3	EDXS-F4	EDXS-F5
Al	0	1000	0	900
Si	3200	28900	34700	68300
K	23600	30700	37800	32300
Ca	0	2400	1300	2000
Cr	0	0	5200	2600
Fe	5000	12500	21500	29600
Zn	292400	242900	165100	250900
Zr	0	0	0	0
Cd	208700	231000	281700	164300
Cs	19700	13800	21800	17200
Pb	244500	199800	196500	220000

Melter Chamber Condensate/Particulate Analysis.

Element	ARM082394	ARM082694	ARM090694	ARM090894
Na	0	0	0	0
Mg	0	0	0	0
Al	0	0	0	0
Si	26800	13000	7300	10900
K	16200	21000	18800	14900
Ca	26900	17000	20000	20100
Ti	23800	15000	25900	24500
Fe	146200	72600	125200	141300
Zn	155600	175600	190000	161700
Zr	27200	12300	22000	26700
Cd	313000	358400	378300	166200
Cs	18000	15600	31100	12100
Ce	7600	4600	5900	3000
Sm	9900	6700	9200	13500
Pb	230400	199500	219900	161700

ARM082394 Slag Analysis.

Element	TOP-XRF	TOP-EDXS	BOT-XRF	BOT-EDXS
Na	0	9900	0	9600
Mg	26400	10300	34300	10000
Al	81200	50900	74000	51400
Si	246000	193700	276000	195000
K	19400	10700	25400	11100
Ca	38300	29900	36300	30600
Ti	24300	23900	30600	24000
Cr	0	3200	0	3200
Fe	152000	127000	126400	121000
Zn	1600	0	1100	0
Zr	15800	35500	15800	32900
Cd	8	0	0	0
Ce	483	2100	728	3400
Cs	557	2100	8800	2400
Sm	1900	1600	6900	0
Pb	2400	0	2500	0

ARM-082694 Slag Analysis.

Element	TOP-XRF	TOP-EDXS	BOT-XRF	BOT-EDXS
Na	0	12300	0	10600
Mg	28000	13100	27400	12300
Al	65100	49700	57600	47600
Si	246300	210800	218600	201600
K	22100	12200	21200	11300
Ca	37300	40200	38100	38800
Ti	29100	26300	29400	25300
Cr	0	3900	0	3700
Fe	118000	120800	129400	123500
Zn	2300	0	2100	0
Zr	15400	101500	17000	108200
Cd	215	0	79	0
Ce	1600	4900	863	3200
Cs	2300	3000	1100	3000
Sm	7100	3700	7300	2400
Pb	7000	0	6100	0

ARM-090694 Slag Analysis.

Element	TOP-XRF	TOP-EDXS	BOT-XRF	BOT-EDXS
Na	0	13200	0	15200
Mg	32800	13000	48600	14600
Al	57600	43900	48000	45400
Si	57600	43900	222300	200000
K	22800	11200	14800	11900
Ca	45500	42600	37000	42400
Ti	34600	27000	24700	27100
Cr	0	2200	0	3100
Fe	150000	147400	126900	151800
Zn	2100	0	1700	0
Zr	14400	73100	13600	62900
Cd	45	0	32	0
Ce	1400	4300	1300	2400
Cs	1400	2100	1300	2300
Sm	6800	0	5300	1900
Pb	2500	0	2000	0

ARM-090894 Slag Analysis.

Element	TOP-XRF	TOP-EDXS	BOT-XRF	BOT-EDXS
Na	0	14400	0	13900
Mg	26600	14900	34500	14800
Al	57200	47800	61000	47300
Si	265700	202300	263900	199300
K	20900	12700	23900	12200
Ca	41600	43400	45200	42900
Ti	30900	27500	34600	27800
Cr	0	3200	0	2100
Fe	128700	131600	143000	133200
Zn	1800	0	2000	0
Zr	16100	82300	17400	81800
Cd	19	0	20	0
Ce	1400	4700	1300	2300
Cs	1700	3400	1700	3100
Sm	6800	2900	7600	0
Pb	2700	0	2900	0

ARM-092094 Slag Analysis.

Element	TOP-EDXS	BOT-EDXS
Na	11700	13600
Mg	14900	15300
Al	46200	48200
Si	194100	201100
K	11000	9900
Ca	46500	46600
Ti	25700	25900
Cr	1900	2200
Fe	124800	123300
Zn	0	0
Zr	84500	89000
Cd	0	0
Ce	2600	4400
Cs	2700	2200
Sm	1500	1800
Pb	0	0

ARM-092294 Slag Analysis.

Element	TOP-EDXS	BOT-EDXS
Na	10300	13900
Mg	15100	15400
Al	49500	37500
Si	212500	138000
K	13000	4700
Ca	50500	19000
Ti	28200	8000
Cr	3700	40910
Fe	109200	37500
Zn	0	0
Zr	88300	14600
Cd	0	0
Ce	3000	1000
Cs	3400	500
Sm	4100	4800
Pb	0	0

Appendix F

ICP and FLAA Data

Lockheed Martin Idaho Technologies								
Experiment Name - ARM082394								
Date conducted - Aug 23, 1994								
Analysis - Triangle Labs								
Project # - 33627A								
Filter Samples								
		A0823F12	A0823F12 L	A0823F22	A0823F22 DA	A0823F32	A0823F42	
analyte		total ug	total ug	total ug	total ug	total ug	total ug	total ug
Al		4250	10000	4000	4420	3990	3240	
Ca		6260	7160	5020	5150	6160	5710	
Cd		194400	200000	81200	82400	78200	75500	
Ce		772	828	171	938	523	378	
Cr		1370	1410	1010	1110	2230	2480	
Cs		25000	25000	22600	22600	37600	20400	
Fe		50000	51700	29400	29500	44700	27200	
K		15300	26700	14500	14200	29200	17000	
Mg		2550	3140	2610	2760	2900	2040	
Na		32100	40400	24900	25100	51500	35500	
Ni		67	74	44	45	112	87	
P		3780	4280	3730	3780	8280	6150	
Pb		237500	242900	93300	94500	161300	141300	
Si		1030700	1356000	804700	821700	1107900	995700	
Ti		1740	1860	2210	2250	2860	3070	
Zn		124700	127900	64500	65400	82200	98100	
Sm		140	200	366	381	171	40	
Total mass (ug)		1730629	2099552	1154261	1176234	1619826	1433895	

F-2

Lockheed Martin Idaho Technologies			
Experiment Name - ARM082394			
Date conducted - Aug 23, 1994			
Analysis - Triangle Labs			
Project # - 33627B			
Slag and Particulate Samples			
		A0823SG1	A0823EL
analyte		(mg/Kg)	(mg/Kg)
Al		20200	10600
Ca		11700	22600
Cd		1370	311300
Ce		1880	5280
Cr		2660	1290
Cs		3800	41100
Fe		96200	79900
K		8460	22800
Mg		4100	10100
Na		6430	32100
Ni		41	66
P		291	2760
Pb		2100	282900
Si		221500	7670
Ti		22800	3630
Zn		1580	146800
Sm		834	7020
Total		405946	987916

Particulate						
	A0823EL				NORM	NORM
	METALS			OXIDES	OXIDES	METALS
analyte	(mg/Kg)		m/o ratio	(mg/kg)	(mg/Kg)	(mg/kg)
Al	10600	Al2O3	0.529	20038	16918	8949
Ca	22600	CaO	0.715	31608	26686	19081
Cd	311300	CdO	0.875	355771	300371	262825
Ce	5280	CeO2	0.814	6486	5476	4458
Cr	1290	Cr2O3	0.684	1886	1592	1089
Cs	41100	Cs2O	0.943	43584	36797	34700
Fe	79900	Fe2O3	0.699	114306	96507	67458
K	22800	K2O	0.83	27470	23192	19250
Mg	10100	MgO	0.603	16750	14141	8527
Na	32100	Na2O	0.742	43261	36525	27101
Ni	66	NiO	0.786	84	71	56
P	2760	P2O3	0.563	4902	4139	2330
Pb	282900	PbO	0.928	304849	257379	238847
Si	7670	SiO2	0.467	16424	13866	6476
Ti	3630	TiO2	0.599	6060	5116	3065
Zn	146800	ZnO	0.803	182814	154347	123941
Sm	7020	Sm2O3	0.862	8144	6876	5927
Totals	987916			1184439	1000000	834079

6-1

Lockheed Martin Idaho Technologies							
Experiment Name - ARM082694							
Date conducted - Aug 26, 1994							
Analysis - Triangle Labs							
Project # - 33627A							
Filter Samples							
							blank filter
		A0826F12	A0826F22	A0826F32	A0826F42		A1013F123
analyte		total ug	total ug	total ug	total ug		blank filter
Al		5560	4190	4600	2470		1920
Ca		8000	6540	10100	4830		3120
Cd		315600	99500	125600	32200		84
Ce		779	1630	2350	83		4
Cr		2930	2790	3670	341		13
Cs		64000	34800	43200	7600		120
Fe		60200	35500	56100	4220		130
K		29800	18400	24700	5380		859
Mg		3350	3920	5330	1160		663
Na		52200	27400	37000	12500		11200
Ni		245	55	60	58		23
P		10100	5880	8810	2350		437
Pb		420000	136000	149700	32900		43
Si		941400	829700	1050500	952300		741400
Ti		2600	4740	8600	388		13
Zn		212600	90300	129700	19500		76
Sm		40	185	574	40		40
Total mass (ug)		2129404	1301530	1660594	1078320		760145

F-11

Filters	TOTAL				TOTAL	A082694						
	METALS				OXIDES	OXIDES						
analyte	(ug)		m/o ratio		(ug)	(wt%)						
Al	9140	Al2O3	0.529		17278	0.39						
Ca	16990	CaO	0.715		23762	0.53						
Cd	572564	CdO	0.875		654359	14.60						
Ce	4826	CeO2	0.814		5929	0.13						
Cr	9679	Cr2O3	0.684		14151	0.32						
Cs	149120	Cs2O	0.943		158134	3.53						
Fe	155500	Fe2O3	0.699		222461	4.96						
K	74844	K2O	0.83		90173	2.01						
Mg	11108	MgO	0.603		18421	0.41						
Na	84300	Na2O	0.742		113612	2.54						
Ni	326	NiO	0.786		415	0.01						
P	25392	P2O3	0.563		45101	1.01						
Pb	738428	PbO	0.928		795720	17.76						
Si	808300	SiO2	0.467		1730835	38.63						
Ti	16276	TiO2	0.599		27172	0.61						
Zn	451796	ZnO	0.803		562635	12.56						
Sm	679	Sm2O3	0.862		788	0.02						
	3129268				4480945	100.00						
										note: ignore ZrO2 mass contributions to filter particulate		
Average HVPM Concentrations					Average Surrogate Concentration							
	ppm			ppm								
Cd	127778		Ce	1077								
Cr	2160		Cs	33279								
Pb	164793		Sm	123								
Zn	100826											

Lockheed Martin Idaho Technologies		Experiment Name - ARM082694		Date conducted - Aug 26, 1994		Analysis - Triangle Labs		Project # - 33627B		Slag and Particulate Samples		analyte	
		A0826SG1		A0826EL								mg/kg	
Al	11100	7470											
Ca	5840	42100											
Cd	1030	428300											
Ce	1080	1080											
Cr	3130	2370											
Cs	2590	37800											
Fe	85900	66900											
K	8960	19000											
Mg	1440	6790											
Na	4240	21400											
Ni	110	48											
P	450	5680											
Pb	5810	502300											
Si	329200	97200											
Ti	26600	15700											
Zn	8510	168800											
Sm	158	340											
Total	496148	1423278											

F-13

Slag																		
	A0826SG1					NORM	NORM											
	METALS				OXIDES	OXIDES	METALS											
analyte	(mg/Kg)		m/o ratio	(mg/Kg)	(mg/Kg)	(mg/Kg)	(mg/Kg)											
Al	11100	Al2O3	0.529	20983	22132	11708												
Ca	5840	CaO	0.715	8168	8615	6160												
Cd	1030	CdO	0.875	1177	1242	1086												
Ce	1080	CeO2	0.814	1327	1399	1139												
Cr	3130	Cr2O3	0.684	4576	4827	3301												
Cs	2590	Cs2O	0.943	2747	2897	2732												
Fe	85900	Fe2O3	0.699	122890	129620	90604												
K	8960	K2O	0.83	10795	11386	9451												
Mg	1440	MgO	0.603	2388	2519	1519												
Na	4240	Na2O	0.742	5714	6027	4472												
Ni	110	NiO	0.786	140	148	116												
P	450	P2O3	0.563	799	843	475												
Pb	5810	PbO	0.928	6261	6604	6128												
Si	329200	SiO2	0.467	704925	743531	347229												
Ti	26600	TiO2	0.599	44407	46839	28057												
Zn	8510	ZnO	0.803	10598	11178	8976												
Sm	158	Sm2O3	0.862	183	193	167												
Totals	496148			948078	1000000	523320												

Lockheed Martin Idaho Technologies						
Experiment Name - ARM090694						
Date conducted - Sep 06, 1994						
Analysis - Triangle Labs						
Project # - 33627A						
Filter Samples						
		A0906F12	A0906F32	A0906F42	A0906F42 L	A0906F62
analyte		total ug	total ug	total ug	total ug	total ug
Al		4440	3970	4030	10300	4560
Ca		6020	5180	4200	6000	6070
Cd		214200	150700	133900	135200	134900
Ce		585	335	143	700	2040
Cr		2890	1470	967	1010	3640
Cs		33600	49200	63200	56000	52400
Fe		69200	11600	12600	13300	30500
K		15100	19500	29400	36700	25000
Mg		2410	1890	1450	3000	2940
Na		26500	24900	33700	31500	34900
Ni		105	54	49	11	62
P		4620	3150	4620	4650	6280
Pb		168500	122600	145400	146700	158100
Si		1009300	1006200	829300	1037000	946100
Ti		2300	1380	527	546	3230
Zn		136400	88100	111700	112700	124000
Sm		80	40	40	200	549
Total mass (ug)		1696250	1490269	1375226	1595517	1535271

F-15

F-18

Filters											
					TOTAL			TOTAL	A090694		
A0906F62 DA	A0906F72				METALS			OXIDES	OXIDES		
total ug	total ug				(ug)		m/o ratio	(ug)	(wt%)		
2970	2960			Al	23630	Al2O3	0.529	44669	0.58		
3060	1650			Ca	16580	CaO	0.715	23189	0.30		
137216	189616			Cd	1095312	CdO	0.875	1251785	16.28		
2126	210			Ce	6119	CeO2	0.814	7517	0.10		
3677	2267			Cr	15856	Cr2O3	0.684	23181	0.30		
53480	47880			Cs	355160	Cs2O	0.943	376628	4.90		
31070	15170			Fe	182790	Fe2O3	0.699	261502	3.40		
23841	21441			K	166687	K2O	0.83	200828	2.61		
2367	1017			Mg	11759	MgO	0.603	19501	0.25		
24300	19900			Na	139700	Na2O	0.742	188275	2.45		
38	32			Ni	236	NiO	0.786	300	0.00		
5843	5593			P	32571	P2O3	0.563	57853	0.75		
160657	114957			Pb	1016699	PbO	0.928	1095581	14.24		
193400	159500			Si	1473800	SiO2	0.467	3155889	41.03		
3277	790			Ti	11985	TiO2	0.599	20008	0.26		
125724	75324			Zn	773568	ZnO	0.803	963347	12.52		
492	0			Sm	1201	Sm2O3	0.862	1393	0.02		
773538	658307				5323653			7691446	100.00		
							note: ignore ZrO2 mass contributions to filter particulate				
Average HVPM Concentration				Average Surrogate Concentration							
<u>ppm</u>				<u>ppm</u>							
Cd	142407			Ce	796						
Cr	2062			Cs	46176						
Pb	132186			Sm	156						
Zn	100575										

F-20

Slag												
	A0906SG1				OXIDES	NORM OXIDES	NORM METALS					
analyte	(mg/Kg)		m/o ratio	(mg/Kg)	(mg/Kg)	(mg/Kg)	(mg/Kg)					
Al	18300	Al ₂ O ₃	0.529	34594	30908	16350						
Ca	19400	CaO	0.715	27133	24242	17333						
Cd	249	CdO	0.875	285	254	222						
Ce	1400	CeO ₂	0.814	1720	1537	1251						
Cr	1790	Cr ₂ O ₃	0.684	2617	2338	1599						
Cs	3600	Cs ₂ O	0.943	3818	3411	3216						
Fe	131700	Fe ₂ O ₃	0.699	188412	168340	117670						
K	10000	K ₂ O	0.83	12048	10765	8935						
Mg	5920	MgO	0.603	9818	8772	5289						
Na	8820	Na ₂ O	0.742	11887	10620	7880						
Ni	366	NiO	0.786	466	416	327						
P	431	P ₂ O ₃	0.563	766	684	385						
Pb	2380	PbO	0.928	2565	2291	2126						
Si	356800	SiO ₂	0.467	764026	682633	318789						
Ti	29700	TiO ₂	0.599	49583	44301	26536						
Zn	6800	ZnO	0.803	8468	7566	6076						
Sm	889	Sm ₂ O ₃	0.862	1031	921	794						
Totals	598545			1119234	1000000	534781						

Lockheed Martin Idaho Technologies								
Experiment Name - ARM090894								
Date conducted - Sep 08, 1994								
Analysis - Triangle Labs								
Project # - 33627A								
Filter Samples								
							blank filter	
	A0908F12	A0908F22	A0908F32	A0908F52			A1013F123	
analyte	total ug	total ug	total ug	total ug			total ug	
Al	5830	5900	4810	6840			1920	
Ca	6060	7280	5500	6740			3120	
Cd	285400	279100	169000	113800			84	
Ce	991	2020	2520	336			4	
Cr	2520	3020	4260	1300			13	
Cs	41200	46400	52800	90400			120	
Fe	78900	42000	41100	23900			130	
K	18000	19600	22600	38700			859	
Mg	2960	4110	3500	3710			663	
Na	36100	38200	30800	53200			11200	
Ni	1270	62	61	87			23	
P	5920	5660	6620	10500			437	
Pb	259300	174400	90400	213300			43	
Si	946100	926400	776200	988200			741400	
Ti	2200	4210	3990	973			13	
Zn	197100	160300	125100	234100			76	
Sm	195	237	214	83			40	
Total mass (ug)	1890046	1718899	1339475	1786169			760145	

F-22

Lockheed Martin Idaho Technologies				
Experiment Name - ARM090894				
Date conducted - Sep 08, 1994				
Analysis - Triangle Labs				
Project # - 33627B				
Slag and Particulate Samples				
	A0908SG1	A0908SG1 DA	A0908EL	
analyte	mg/Kg	mg/Kg	mg/Kg	
Al	20900	20800	8080	
Ca	22700	22600	21500	
Cd	96	90	397300	
Ce	1760	1760	2110	
Cr	1950	1950	4690	
Cs	4370	4370	59400	
Fe	122300	121700	168500	
K	11000	11100	24100	
Mg	5980	5960	10900	
Na	8760	8690	27300	
Ni	23	23	119	
P	508	528	6020	
Pb	2060	2040	240100	
Si	238800	241200	81900	
Ti	32800	32600	35400	
Zn	1870	1850	16900	
Sm	899	1040	1120	
Total	476776	478301	1105439	

F-25

Lockheed Martin Idaho Technologies								
Experiment Name - ARM092094								
Date conducted - Sep 20, 1994								
Analysis - Triangle Labs								
Project # - 33627A								
Filter Samples								
								blank filter
		A0920F12	A0920F22	A0920F32	A0920F52			A1013F123
analyte		total ug	total ug	total ug	total ug			total ug
Al		5470	5980	6020	5870			1920
Ca		4820	6040	5940	5900			3120
Cd		413600	306300	359500	337000			84
Ce		143	467	333	462			4
Cr		2130	3370	2910	5070			13
Cs		40800	51600	65600	65600			120
Fe		11600	28000	26800	15500			130
K		14300	19600	27500	24000			859
Mg		1910	2430	2510	2350			663
Na		32300	53000	51800	48300			11200
Ni		42	53	58	69			23
P		7000	8790	13000	19800			437
Pb		239600	253500	240700	238300			43
Si		951100	1045700	973700	982700			741400
Ti		376	1220	1090	1140			13
Zn		205700	211200	210800	190300			76
Sm		40	40	77	111			40
Total mass (ug)		1930931	1997290	1988338	1942472			760145

F-29

Lockheed Martin Idaho Technologies				
Experiment Name - ARM092094				
Date conducted - Sep 20, 1994				
Analysis - Triangle Labs				
Project # - 33627B				
Slag and Particulate Samples				
		A0920SG1	A0920SG2	A0920EL
analyte		mg/Kg	mg/Kg	mg/Kg
Al		10200	9470	5920
Ca		7410	6520	1120
Cd		724	795	449900
Ce		643	437	1610
Cr		1830	2320	5380
Cs		2430	2250	73500
Fe		69700	76800	103100
K		6590	6780	22400
Mg		2150	1870	7520
Na		3830	3470	30600
Ni		16	22	100
P		458	421	9930
Pb		1790	1850	284200
Si		172800	179800	62300
Ti		20200	21100	17400
Zn		1740	2480	222500
Sm		186	131	1080
Total		302697	316516	1298560

F-32

Slag						
	A0920SG2				NORM	NORM
	METALS			OXIDES	OXIDES	METALS
analyte	(mg/Kg)		m/o ratio	(mg/Kg)	(mg/Kg)	(mg/Kg)
Al	9470	Al2O3	0.529	17902	30533	16152
Ca	6520	CaO	0.715	9119	15553	11120
Cd	795	CdO	0.875	909	1550	1356
Ce	437	CeO2	0.814	537	916	745
Cr	2320	Cr2O3	0.684	3392	5785	3957
Cs	2250	Cs2O	0.943	2386	4070	3838
Fe	76800	Fe2O3	0.699	109871	187395	130989
K	6780	K2O	0.83	8169	13932	11564
Mg	1870	MgO	0.603	3101	5289	3189
Na	3470	Na2O	0.742	4677	7976	5918
Ni	22	NiO	0.786	28	48	38
P	421	P2O3	0.563	748	1275	718
Pb	1850	PbO	0.928	1994	3400	3155
Si	179800	SiO2	0.467	385011	656671	306665
Ti	21100	TiO2	0.599	35225	60080	35988
Zn	2480	ZnO	0.803	3088	5268	4230
Sm	131	Sm2O3	0.862	152	259	223
Totals	316516			586307	1000000	539847

F-34

Chamber Particulate							
	A0920EL					NORM	NORM
	METALS			OXIDES	OXIDES	METALS	
analyte	(mg/Kg)		m/o ratio	(mg/Kg)	(mg/Kg)	(mg/Kg)	
Al	5920	Al2O3	0.529	11191	6961	3682	
Ca	1120	CaO	0.715	1566	974	697	
Cd	449900	CdO	0.875	514171	319815	279838	
Ce	1610	CeO2	0.814	1978	1230	1001	
Cr	5380	Cr2O3	0.684	7865	4892	3346	
Cs	73500	Cs2O	0.943	77943	48480	45717	
Fe	103100	Fe2O3	0.699	147496	91743	64128	
K	22400	K2O	0.83	26988	16787	13933	
Mg	7520	MgO	0.603	12471	7757	4677	
Na	30600	Na2O	0.742	41240	25651	19033	
Ni	100	NiO	0.786	127	79	62	
P	9930	P2O3	0.563	17638	10971	6176	
Pb	284200	PbO	0.928	306250	190488	176772	
Si	62300	SiO2	0.467	133405	82978	38751	
Ti	17400	TiO2	0.599	29048	18068	10823	
Zn	222500	ZnO	0.803	277086	172347	138395	
Sm	1080	Sm2O3	0.862	1253	779	672	
Totals	1298560			1607717	1000000	807704	

Lockheed Martin Idaho Technologies							
Experiment Name - ARM092294							
Date conducted - Sep 22, 1994							
Analysis - Triangle Labs							
Project # - 33627A							
Filter Samples							
							blank filter
		A0922F12	A0922F32	A0922F42	A0922F52	A1013F123	
analyte		total ug	total ug	total ug	total ug	total ug	
Al		4900	5130	4550	5140	1920	
Ca		4810	6670	4450	5960	3120	
Cd		367800	381700	302400	113700	84	
Ce		405	365	261	244	4	
Cr		2010	2820	2870	1750	13	
Cs		48400	58400	50000	18000	120	
Fe		26100	19500	15400	24300	130	
K		11200	21200	19500	10600	859	
Mg		1860	2490	1980	1810	663	
Na		43200	46800	35700	35200	11200	
Ni		61	60	69	56	23	
P		81400	10900	10300	8260	437	
Pb		337900	265200	196500	223000	43	
Si		918900	1032700	745900	969900	741400	
Ti		686	1570	879	925	13	
Zn		281600	246400	166300	244000	76	
Sm		40	105	95	46	40	
Total mass (ug)		2131272	2102010	1557154	1662891	760145	

F-36

Filters	TOTAL				TOTAL	A092294						
	METALS				OXIDES	OXIDES						
analyte	(ug)		m/o ratio	(ug)	(wt%)							
Al	12040	Al2O3	0.529	22760	0.39							
Ca	9410	CaO	0.715	13161	0.22							
Cd	1165264	CdO	0.875	1331730	22.57							
Ce	1259	CeO	0.814	1547	0.03							
Cr	9398	Cr2O3	0.684	13740	0.23							
Cs	174320	Cs2O	0.943	184857	3.13							
Fe	84780	Fe2O3	0.699	121288	2.06							
K	59064	K2O	0.83	71161	1.21							
Mg	5488	MgO	0.603	9101	0.15							
Na	116100	Na2O	0.742	156469	2.65							
Ni	154	NiO	0.786	196	0.00							
P	109112	P2O3	0.563	193805	3.29							
Pb	1022428	PbO	0.928	1101754	18.68							
Si	701800	SiO2	0.467	1502784	25.47							
Ti	4008	TiO2	0.599	6691	0.11							
Zn	937996	ZnO	0.803	1168115	19.80							
Sm	126	Sm2O3	0.862	146	0.00							
	4412747			5899304	100.00							
Average HVPM Concentrations						Average Surrogate Concentrations						
	ppm					ppm						
Cd	197526					Ce	213					
Cr	1593					Cs	29549					
Pb	173313					Sm	21					
Zn	159001											

F-38

Chamber Particulate													
	A0922EL					NORM	NORM						
	METALS			OXIDES	OXIDES	METALS							
analyte	(mg/Kg)		m/o ratio	(mg/Kg)	(mg/Kg)	(mg/Kg)							
Al	7950	Al2O3	0.529	15028	9803	5186							
Ca	11700	CaO	0.715	16364	10674	7632							
Cd	365400	CdO	0.875	417600	272394	238345							
Ce	955	CeO	0.814	1173	765	623							
Cr	3570	Cr2O3	0.684	5219	3404	2329							
Cs	45700	Cs2O	0.943	48462	31611	29809							
Fe	119100	Fe2O3	0.699	170386	111140	77687							
K	21400	K2O	0.83	25783	16818	13959							
Mg	5430	MgO	0.603	9005	5874	3542							
Na	30800	Na2O	0.742	41509	27076	20090							
Ni	76	NiO	0.786	97	63	50							
P	9880	P2O3	0.563	17549	11447	6445							
Pb	274400	PbO	0.928	295690	192874	178987							
Si	63200	SiO2	0.467	135332	88275	41224							
Ti	19600	TiO2	0.599	32721	21344	12785							
Zn	241100	ZnO	0.803	300249	195848	157266							
Sm	778	Sm2O3	0.862	903	589	507							
Total	1221039			1533071	1000000	796466							

F-42